University of Alberta

The Development of a Micro-Total Analysis System For Gene Detection and Quantitation Using Cycling Probe Technology with Capillary Zone Electrophoresis.

By

Mohammed Youssouf Badal

A thesis submitted to the Faculty of Graduate Studies and Research in partial fulfillment of the requirements for the degree of **Doctor of Philosophy**

Department of Chemistry

Edmonton, Alberta

Spring 2001

National Library of Canada
Acquisitions and Bibliographic Services
395 Wellington Street
Ottawa ON K1A 0N4
Canada

Bibliothèque nationale du Canada
Acquisitions et services bibliographiques
395, rue Wellington
Ottawa ON K1A 0N4
Canada

Your file Votre référence

Our file Notre référence

The author has granted a non-exclusive licence allowing the National Library of Canada to reproduce, loan, distribute or sell copies of this thesis in microform, paper or electronic formats.

The author retains ownership of the copyright in this thesis. Neither the thesis nor substantial extracts from it may be printed or otherwise reproduced without the author's permission.

L'auteur a accordé une licence non exclusive permettant à la Bibliothèque nationale du Canada de reproduire, prêter, distribuer ou vendre des copies de cette thèse sous la forme de microfiche/film, de reproduction sur papier ou sur format électronique.

L'auteur conserve la propriété du droit d'auteur qui protège cette thèse. Ni la thèse ni des extraits substantiels de celle-ci ne doivent être imprimés ou autrement reproduits sans son autorisation.

0-612-60272-9

Canada

University of Alberta

Library Release Form

Name of Author: Mohammed Youssouf Badal

Degree: Doctor of Philosophy

Title of Thesis: The Development of a Micro-Total Ana.'sis System For Gene Detection and Quantitation Using Cycling Probe Technology with Capillary Zone Electrophoresis.

Year this Degree Granted: 2001

Permission is hereby granted to the University of Alberta Library to reproduce single copies of this thesis and to lend or sell such copies for private, scholarly or scientific purposes only.

The author reserves all other publication and other rights in association with the copyright in the thesis, and except as the herein before provided, neither the thesis nor any substantial portion thereof may be printed or otherwise reproduced in any material form whatever without the author's prior written permission.

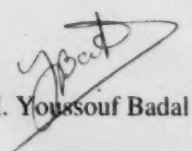

M. Youssouf Badal

2B- 8916 112 St
Edmonton, AB
Canada, T6G 2C5

February 2001

University of Alberta

Faculty of Graduate Studies and Research

The undersigned certify that they have read, and recommend to the Faculty of Graduate Studies and Research for acceptance, a thesis entitled "**The Development of a Micro-Total Analysis System for Gene Detection and Quantitation using Cycling Probe Technology with Capillary Zone Electrophoresis**" submitted by **Mohammed Youssouf Badal** in partial fulfillment of the requirements for the degree of **Doctor of Philosophy**.

Supervisor: Dr. D. Jed Harrison

Dr. Frederick F. Cantwell

Dr. Mark T. McDermott

Dr. Rik R. Tykwinski

Dr. Martin J. Somerville

External Examiner: Dr. Ulrich J. Krull

Date: Feb 9th, 2001

To my dear father, Late W. A. BADAL,
whose support, love and inspiration has made
this dream come true.
You will be missed .....

Thesis Abstract

The goal of the thesis was to develop a μ-TAS for DNA analysis using cycling probe technology (CPT) as a DNA amplification reaction and using capillary zone electrophoresis CZE as separation technique.

Chapter 2 describes a method to modify the surface of channel walls in the chip and subsequently perform capillary zone electrophoresis. Experiments were done to study the electroosmotic flow (EOF) behavior of the poly(dimethylsiloxane) PDMS coated capillaries in the presence of charged and neutral surfactants. The results showed it is possible to fine tune the EOF by adjusting the surfactant concentration. Subsequently, the use of the coating in the CPT project was not pursued. However, we concluded that the coating could be useful in protein separation.

In Chapter 3 and 4 we describe a micro-chip device, named GOCPTTT, that was capable of performing enzyme mediated signal amplification of a target DNA sequence, followed by separation and analysis of the reaction products for quantitation. CPT utilizes signal amplification through the cleavage of a 5' end-labeled fluorescein DNA-RNA-DNA probe when hybridized to a target DNA and subsequent enzyme action (RNase H). This thesis work shows how the technique was developed on microfluidic devices, which provide a powerful means of integrating sample preparation or reaction steps with separation. The samples used in the study were from methicillin resistant *Staphylococcus aureus* (Chapter 3) and *Erwinia herbicola* (Chapter 4). These bacteria are representative of a typical clinical assay, and a simulant of pathogens in the environment, respectively. The probe, enzyme and target were electrokinetically mixed on-chip, incubated under isothermal conditions (60 °C) in a reaction zone (integrated on the device), then mobilized for separation on-chip. The cleaved and intact probes were separated using gel-free, open tubular CZE with the help of a 3' end-labeled biotin moiety on the probe. The ratio of accumulated cleaved probe to intact probe identifies the amount of target present. Amplification of five orders of magnitude was achieved, with a detection limit of about 0.1 attomoles of target DNA and a quantitative response across a wide range of target DNA concentrations. This work shows that each of these steps may be integrated together on a single chip, and it establishes quantitative performance for the on-chip devices.

Acknowledgements

Special gratitude to my research supervisor, Prof D. Jed Harrison. He introduced me to this exciting field of microfluidics and provided me with valuable guidance and support throughout the course of my research. I am very thankful for his patience in reading my thesis and making it in its present form. Also, not to forget the scientific knowledge I have gathered from all the conferences I have attended thanks to Prof D. Jed Harrison.

My sincere thanks go to the Harrison's group who really made my stay as a graduate student very enjoyable in the chemistry department. Special thanks to my friend Thompson Tang for introducing me to the field of cycling probe technology. Thank you to Dr. Hossein Salimi-Mossavi for his technical and personal advice when I started my graduate work. Thank you to Dr. Fahima Ouchen for teaching me microfabrication at the student microfab. I wish to express to my gratitude to Mrs. Arlene Figley for reading my thesis and making grammatical corrections.

My appreciation also extend to the technical support staff in this chemistry department especially to those of the glass, electronic and machine shops. Thank you to Dr. William E. Lee and Douglas. E. Bader from the Defence Research Establishment at Suffield, Terina Dickingson-Laing from C.W. Bios Inc., and Dr. Faouzi Bekkaoui from ID Biomedical for providing DNA samples and also for valuable discussion and suggestions for this research. My thanks also go to the members of my candidacy and defence committee in the persons of Dr. Frederick Cantwell, Dr. Norman Dovichi, Dr. Mark Mcdermott, Dr. Rik Tykwinski, Dr. Martin Somerville and Dr. Ulrich Krull.

Special thanks to my country mates from Mauritius, Soleiman and Asvina for their personal support. I thank Dr. Ahmad Khodabocus, Senior lecturer at the University of Mauritius, for his support and encouragement. Thank you to my family, My late father, Waheb, my mother, Rosida, and my two brothers Rezah and Nazim for their support, love and inspiration. And most importantly thank you God for giving the courage and patience to persevere during the course of my research.

Table of Contents

CHAPTER 1: Introduction

		Page
1.1	**Miniaturization**	**1**
1.1.2	Micro (or Miniaturized) Total Analysis Systems	1
1.1.2.1	Microfluidics and "lab on a chip"	2
1.1.3	Focus of Chapter One	3
1.2	**Mode of Capillary Electrophoresis**	**3**
1.2.1	Capillary Zone Electrophoresis	3
1.2.2	Micellar Electrokinetic Capillary Chromatography	3
1.2.3	Capillary Gel Electrophoresis	4
1.2.4	Capillary Isoelectric Focusing	5
1.2.5	Capillary Isotachophoresis	5
1.3	**Theory of Capillary Electrophoresis**	**6**
1.3.1	Double Layer Theory	6
1.3.2	Generation of Electroosmotic Flow	8
1.3.3	Fundamentals of CE	9
1.3.4	Efficiency of Separation	11
1.3.5	Characterization of Electroosmotic Flow	12
1.3.6	Resolution Between Two Peaks	14
1.4	**Surface Modification in Capillary Electrophoresis**	**15**
1.4.4	Importance of Coating	15
1.4.2	Different Coating Procedures	16
1.4.2.1	Covalent Bonding	16
1.4.2.2	Adsorption Methods	17
1.5	**The Development of Micro-Total Analysis Systems**	**18**
1.5.1	μTAS for Gene Analysis	20
1.5.2	Mixing	26
1.6	**Basic DNA Concepts**	**30**
1.6.1	Deoxyribonucleic Acid (DNA) Structure	30
1.6.2	Properties of RNA	32
1.6.3	Denaturation and Renaturation of DNA	32
1.6.3.1	Renaturation	32
1.6.4	Identification of Microorganisms or Bacteria by Conventional Methods	33
1.6.5	Polymerase Chain Reaction	33
1.6.6	Cycling Probe Technology	34
1.6.6.1	DNA-RNA Hybrid Recognition by Rnase H	36
1.6.6.2	Application of CPT Published to Date	37
1.6.7	Physical Artifacts in DNA and RNA	38
1.6.7.1	Hairpin Loop Formation	38
1.6.7.2	Primer-Dimer	38
1.7	**Scope of the Thesis**	**39**
1.8	**References**	**40**

CHAPTER 2: Electroosmotic Flow Study on Poly(dimethylsiloxane) Coated Capillaries

		Page
2.1	**Introduction**	**48**
2.2	**Experimental**	**52**
2.2.1	Instrumentation	52
2.2.2	Reagents	52
2.2.3	Coating of Capillaries	53
2.2.4	Protein Separation	54
2.2.5	EOF Measurement	55
2.3	**Results and Discussion**	**55**
2.3.1	Coating Evaluation	55
2.3.2	Effect of pH on the EOF in Coated Capillaries	59
2.3.3	Effect of SDS on the EOF	60
2.3.4	Effect of CTAB on the EOF	63
2.3.5	Effect of pH on the study in the Presence of Charged Surfactants	69
2.4	**2.4 Conclusion**	**70**
2.5	**2.5 References**	**71**

CHAPTER 3: Methicilin Resistant *Staphylococcus aureus* DNA Assay Using Cycling Probe Technology with Capillary Zone Electrophoresis on a Chip

3.1	**Introduction**	**75**
3.2	**Experimental**	**80**
3.2.1	CPT Components and Conditions	80
3.2.2	**Device Design and Fabrication**	80
3.2.3	Method of Fabricating the Drilled Cover Plates	81
3.2.4	Method of Fabricating the Etched Plates	82
3.2.5	Cold Bonding the Substrate with the Cover Plate to Make the Microfluidic Device	83
3.2.6	Thermal Bonding of the Substrates	83
3.2.7	Device Layouts	84
3.2.8	Channel Derivatization	84
3.2.9	Instrumentation Set-up and Optimization to do CE on Chip	84
3.2.10	Signal Optimization	87
3.2.11	Instrumentation Set-up and Optimization for On-chip Cycling and Separation	89
3.2.12	LIF Detection Using an Inverted Confocal Microscope	90
3.2.13	Instrumentation Alignment for Optimum Fluorescent Signal	91
3.2.14	On-chip Cycling and Separation	92
3.3	**Results and Discussion**	**95**
3.3.1	Cycling Probe Technology and Capillary Electrophoresis	95
3.3.2	On-Chip Mixing, Reaction, Separation and LIF Detection Using the GOCPTTT Device	104
3.3.2.1	Temperature Control On-chip	106
3.3.2.2	On-chip CPT process: Mixing, Reaction and Separation	107
3.3.2.2.1	Diffusional Mixing	108
3.3.2.2.2	CZE Separation	111
3.3.2.2.3	Calibration with On-chip CPT Reaction	115
3.4	**Conclusion**	**119**
3.5	**References**	**120**

CHAPTER 4: A μ-TAS for Detection of Pathogens in the Environment Using Cycling Probe Technology for DNA Amplification

		Page
4.1	**Introduction**	124
4.2	**Experimental**	126
4.2.1	Materials and Methods	126
4.2.1.1	Target DNA	126
4.2.1.2	CPT Reagents	126
4.2.1.3	Chemical Reagents	127
4.2.2	Devices	127
4.2.3	Channel Derivatization	128
4.2.4	Instrumentation	128
4.2.5	On-chip Cycling and Separation	128
4.3	**Results and Discussion**	**131**
4.3.1	Earlier Work	131
4.3.2	Development of CPT Probes to Detect for *Erwinia herbicola* Target DNA	131
4.3.3	Assessment of CPT Probes	133
4.3.4	CPT Assay for *Erwinia herbicola* On-chip Format	135
4.3.4.1	Calibration	138
4.3.4.2	On-chip Reaction Using 15 min Incubation Time	141
4.4	**Conclusion**	141
4.5	**References**	142

CHAPTER 5: Conclusion And Future Suggestions

5.1	**Conclusion from thesis work**	**146**
5.2	Surface Modification and Suggestions for Further Work with Preliminary Data	148
5.2.1	Surface Modification	148
5.2.2	Epoxy Coating	149
5.2.2.1	Epoxy Coating Procedure	149
5.2.2.2	Separation of a Synthetic Mixture of DNA Fragment and the MRSA Probe	149
5.2.3	Conclusion	150
5.3	**Future design**	**150**
5.3.1	A New Chip and New Set-up	150
5.3.2	Ruggedness and Portability	151
5.4	**Final Conclusion**	**154**
5.5	**References**	**154**

List of Tables

		page
Chapter 2		
Table 2.1	The electroosmotic mobility at different pH values	55
Table 2.2	pI values of different proteins	59
Table 2.3	μ_{eo} of bare capillaries at different SDS concentrations at pH 6.3	61
Chapter 3		
Table 3.1	Voltage and Relay Switching Matrix for Fluidic Control on the 'COPI' device	88
Table 3.2	Different buffer conditions used in CPT off-chip	88
Table 3.3	(a) Voltage and Relay Switching Matrix for Fluidic Control of Microchip (b) Mixed Vacuum,Voltage and Relay Switching Matrix for Fluidic Control of Microchip	94
Table 3.4	The % probe cleavage and amplification factors for off-chip cycling	103
Table 3.5	The % probe cleavage and amplification factors for on-chip cycling	115
Chapter 4		
Table 4.1	Voltage and Relay Switching Matrix for Fluidic Control of Microchip	130
Table 4.2	The % probe cleavage and amplification factors	138

List of Figures

		Page
Chapter 1		
Figure 1.1	Profile across the double layer.	6
Figure 1.2	(a) The generation of EOF (b) The net migration of three ions, positive, neutral and negative under EOF	9
Figure 1.3	Schematic of the integrated PCR-CE microdevice	21
Figure 1.4	The Flow-PCR device set-up.	22
Figure 1.5	Microchannel design used for integrated rapid PCR analysis on-chip	23
Figure 1.6	Mask pattern for the 96-channel radial capillary array electrophoresis microplate	24
Figure 1.7	Instrumental set-up for on-chip cycling probe technology	25
Figure 1.8	Layout schemes of two devices used for post-column derivatization	27
Figure 1.9	Schematic of microchip used for protein separation with post-column labeling	28
Figure 1.10	Representation of a tetranucleotide	30
Figure 1.11	The DNA double helix structure	31
Figure 1.12	Scheme for Cycling Probe Technology, (CPT)	35
Figure 1.13	Schematic drawing of a proposed mechanism for the action of *E.coli* RNase H	36
Chapter 2		
Figure 2.1	Bonding of the poly(dimethylsiloxane) with capillary surface	52
Figure 2.2	Electropherogram for separation of lyzozyme and cytochrome C in PDMS coated capillary	57
Figure 2.3	Electropherogram for separation of basic proteins	58
Figure 2.4	Variations in μ_{eo} with increasing SDS concentration at different pH values	62
Figure 2.5	Schematic representation of adsorbed layers of, (a) SDS and (b) of SDS and Brij 35 on PDMS coated surface	63
Figure 2.6	Schematic representation of adsorbed layers of CTAB on bare capillary surface	64
Figure 2.7	Variations in μ_{eo} with increasing CTAB concentration at different pH values close to the point of EOF reversal	65
Figure 2.8	Variations in μ_{eo} with increasing CTAB concentration at different pH values over the full range	66
Figure 2.9	Schematic representation of the adsorption of CTAB on the hydrophobic PDMS surface	67
Chapter 3		
Figure 3.1	The reaction scheme of cycling probe technology	76
Figure 3.2	Scheme showing the different steps in making microfabricated glass chips	81
Figure 3.3	(a) Illustration of the 'COPI' device layout (b) Illustration of the GOCPTTT layout	85
Figure 3.4	Instrumental Set-up for running the 3 inch square 'COPI' device	86
Figure 3.5	The instrumental setup for performing CPT on-chip.	90
Figure 3.6	The Inverted confocal microscope	91
Figure 3.7	(a) CPT chip layout (b) Single T injection scheme	94
Figure 3.8	(a) Electropherograms for the gel free separation of the off-chip CPT reaction products (b) The calibration curve (log-log plot of peak areas versus target concentration)	96
Figure 3.9	Electropherogram of a synthetic mixture of cleaved and in intact probe	97
Figure 3.10	(a) Electropherograms for gel free separation of the off-chip CPT reaction products with spermine optimized conditions (b) Log-log calibration curve	99
Figure 3.11	Electropherograms of replicate data for the lowest amount of target detected for MRSA sample cycled off-chip	100
Figure 3.12	(a) Electropherograms of off-chip CPT reaction products in CZE mode	101

		Page
Figure 3.12	(b) Linear plot for ratio of peak areas versus target concentration	102
	(c) log-log plot of the data in Figure 3.12b	
Figure 3.13	(a) Represents a plot of peak height against voltage for 10 nM Fluorescein sample	105
	(b) Layout of the GOCPTTT device with variable injection voltage	
Figure 3.14	Electropherograms obtained for MRSA CPT products for different peltier currents	106
Figure 3.15	Diffusion plots across a 130 µm wide channel	110
Figure 3.16	(a) Electropherogram for on-chip amplification of 100 amol of MRSA DNA	113
	(b) Reproducibility between 5 repeated injections for 25 amol of MRSA DNA	114
Figure 3.17	(a) Electropherograms obtained with cycling performed on chip for different target concentrations	117
	(b) Linear plot obtained for on-chip cycling and separation of the CPT products	118
	(c) Log-log plot of the data in Figure 3.17b	
Chapter 4		
Figure 4.1	(a) CPT Chip layout	130
	(b) A single-T injection scheme	
Figure 4.2	Slab gel electropherogram for an isotopic CPT assay with *Erwinia herbicola* (EH) DNA	134
Figure 4.3	Electropherogram for an on-chip CPT reaction of 1.6 amol of EH target DNA	136
Figure 4.4	(a) Electropherograms of on-chip CPT reaction for 1.6 to 16 amol of EH target DNA	139
	(b) On-chip calibration curve for EH samples	140
	(c) On-chip calibration curve for EH sample in a log-log plot format.	
Figure 4.5	Electropherogram following 15 min incubation of 16 amol of EH target DNA	141
Chapter 5		
Figure 5.1	Electropherogram for the gel-free separation of 9 mer-DNA fragment and MRSA probe	150
Figure 5.2	New chip design	152
Figure 5.3	DARPA box	153

List of Abbreviations

Concentration nomenclature

pmol	Picomole (10^{-12})
fmol	Femtomole (10^{-15})
amol	Attomole (10^{-18})
CFU	Colony formation unit

Technical words

μ_{eo}	Electroosmotic mobility ($cm^2/V/sec$)
μ_{ep}	Electrophoretic mobility ($cm^2/V/sec$)
$\bar{\mu}$	Average electrophoretic mobilities between ions ($cm^2/V/sec$)
μ_{ob}	The observed mobility of an ion ($cm^2/V/sec$)
v_{eo}	Electroosmotic velocity (cm/s)
v_{ep}	Electrophoretic velocity (cm/s)
η	Viscosity (g/cm/s)
ρ	Surface charge density in (C/m^2)
ζ_{eo}	Zeta-potential close to plane of shear
σ	Standard deviation
R_s	Resolution between two peaks
μ-TAS	Micro-total analysis system
cmc	Critical micelle concentration
CGE	Capillary gel electrophoresis
CZE	Capillary zone electrophoresis
CPT	Cycling probe Technology
DARPA	Defense Advanced Research Project Agency
EOF	Electroosmotic Flow
pI	Isoelectric point (pH of zero charge on a protein)

Reagents

CTAB	Cetyltrimethyl ammonium bromide
EH	*Erwinia herbicola*
MRSA	methicilin resistant *Staphylococcus aureus*
RNase H	Ribonuclease H
PDMS	Poly(dimethylsiloxane) (n = 200)
SDS	Sodium dodecylsulfate
N, N, N, N' TEMED	tetramethylethylenediamine

CHAPTER 1: Introduction

1.1 Miniaturization

In chemical and biochemical analysis, separation of a mixture into its various components is often a critical requirement. The advent of high performance liquid chromatography (HPLC) was a major advancement, but the amount of waste generated by the technique was a major contributor to operating costs by chemical and biotechnology companies [1]. As demands have started to shift more towards higher speed and high throughput, other techniques need to be developed. To satisfy the demands, a focus on miniaturization has developed. Micro LC [2,3] in both open tubular and packed format was shown to have a promising future, but the technical difficulties in the design of high pressure, low-volume solvent delivery systems and operational challenges in handling the severe pressure drop in packed column chromatography deterred commercial development of capillary LC. The introduction of capillary electrophoresis (CE)[4] as a high speed separation technique which used electrokinetic forces for separation and mobilization certainly played an overwhelming role in the sequencing of the human genome [5-12]. The success of CE brought about the idea of separation on planar glass devices.

1.1.2 Micro (or Miniaturized) Total Analysis Systems

The concept of Micro (or Miniaturized) Total Analysis Systems (μ-TAS) was introduced by Manz et al [13], who proposed a state-of-the-art strategy for solving analytical problems. The concept of a total chemical analysis system, TAS, involves periodically transforming chemical information into electronic information. Techniques

such as chromatography, electrophoresis or flow injection can be integrated in a TAS. The detector or sensor in a TAS does not need high selectivity, because sample pretreatment serves to eliminate most of the interfering chemical compounds. Furthermore, calibration can be incorporated into the system. Manz and Widmer later proposed the miniaturization of a TAS for such instrumentation, creating the μ-TAS concept. With a μ-TAS, sample handling and analysis steps could be performed close to the place of sample origin. Along with the concept of μ-TAS came the concept of microfluidics and the "lab on a chip".

1.1.2.1 Microfluidics and the "Lab on a Chip"

Microfluidics is a concept that has been mainly associated with microfabricated devices for liquid phase separation. The miniaturization and mass fabrication of liquid phase separation devices also enabled a much more powerful concept to be realized. The integration of several laboratory functions on a single chip provides the equivalent of a laboratory on a chip.

Capillary electrophoresis (CE) on chip could be integrated with various other tasks such as mixing, reaction and separation as first demonstrated by Widmer and coworkers [13-14]. Such microfabricated systems are based upon planar, monolithic fabrication techniques.

The development of μ-TAS was aimed at the automation, miniaturization and integration of chemical and biochemical analysis processes. The μ-TAS concept may be applied to many types of analysis, although it is unlikely to be universal. One issue of developing importance is the automation of genetic analysis, as such procedures move from the research lab to routine clinical and forensic applications. DNA amplification and

separation are important steps that may be successfully integrated into a μ-TAS device. The exploration of such a system is a key focus of this thesis.

1.1.3 Focus of Chapter One

The first part of this chapter will present the different modes of CE as well as its theoretical basis. The second part will focus on surface modification, as both permanent coating and dynamic coating of channels are important in the separation of biomolecules and other samples. This subject was recently reviewed by Beale and St. Clair [15]. The subsequent section will focus more on the development of the μ–TAS concept. The following section will discuss different DNA amplification and analysis techniques. Finally, an overview of the scope of the present thesis work will be presented.

1.2 Mode of Capillary Electrophoresis

1.2.1 Capillary Zone Electrophoresis

Capillary zone electrophoresis (CZE), introduced by Jorgenson and Lukacs [16], is the most basic and mature method of CE. Separation occurs in a free-flow, open tubular mode, driven by electrophoretic migration and electroosmotic flow (EOF) under the influence of an electric field. Separation is based upon the differences in the electrophoretic mobilities of the individual sample compounds. These mobility differences can be optimized for a given separation by controlling voltage, electrolyte composition, pH, ionic strength and surface coatings.

1.2.2 Micellar Electrokinetic Capillary Chromatography

The charge on neutral compounds is zero, but in CZE, separation is based on differences in electrophoretic mobilities, so that neutral compounds cannot be separated by CZE. Terabe introduced micellar electrokinetic chromatography (MEKC) [17,18],

based upon differential micellar solubilization of analytes and their subsequent variation in electrokinetic migration. Separation of two neutral analytes occurs in MEKC when they differentially partition with the hydrophobic interior of the charged micelle and the aqueous phase. Although originally developed for the separation of neutral compounds, MEKC has increasingly been used to separate charged compounds which have similar electrophoretic mobilities, using both charged and neutral zwitterionic surfactants [19].

1.2.3 Capillary Gel Electrophoresis

One of the major fields in which capillary gel electrophoresis (CGE) has been widely used is in the separation of DNA sequencing fragments for the human genome project [20-24]. The gel used most frequently is polyacrylamide gel. In a gel, separation is based on molecular size and not on mobility of the species. In conventional gel electrophoresis, the matrix also stabilizes the analyte bands and prevents zone broadening produced by thermal convection and diffusion. Conventional gel electrophoresis is fairly labor intensive, but not a complicated technique. The only problem with gel electrophoresis is that the gel overheats when a large voltage is applied for separation. However, low voltages lead to extremely long separation times (several hours). In CGE, the surface of the capillary walls in contact with the volume of gel used is very large. This allows rapid dissipation of heat when a high voltage is applied. In so doing, the separation time is reduced from several hours to several minutes.

The low diffusion coefficient of DNA in a gel and higher electric fields compared to conventional gel allow for plate numbers of 10^6 in CGE of DNA [21-22]. Considerable effort to identify appropriate gels for DNA sequencing [20-29] has been made for CGE. Among the most studied gels are polyacrylamide gel and hydroxymethyl cellulose

(HPMC). Minimally entangled with low viscosity polymers such as poly(ethylene oxide) PEO and poly(vinylpyrrolidone) PVP are also successfully employed as a sieving matrix for DNA separation in coated and uncoated capillaries[26-27].

1.2.4 Capillary Isoelectric Focusing

Capillary isoelectric focusing (CIEF) [30] relies upon the achievement of a gradient in which sample molecules can be separated based upon differences in molecular properties. In isoelectric focusing, amphoteric analytes such as peptides and proteins are separated on the basis of their differing isoelectric point (pI). Sample ions are mixed with carrier ampholytes that span the desired pH range, and the mixture is loaded onto a capillary. When an electric field is applied, the ampholytes build up a pH gradient, due to migration of H^+ and OH^- from the electrolyte reservoirs, and the sample ions focus concurrently to their pH of zero charge. After focusing, sample elution can be achieved by (1) hydrodynamic flow, (2) siphoning, (3) adding salt to the buffer to create a pH imbalance gradient. In CIEF the coating of the capillary is important because the EOF must be eliminated during focusing.

1.2.5 Capillary Isotachophoresis

Capillary Isotachoporesis (CITP) [31] can be regarded as the first electrophoretic microanalysis technique. In comparison to CZE, which uses a uniform carrier buffer throughout the system, CITP is performed in a discontinuous buffer system. Isotachophoresis takes place when an electric field is applied to a system of electrolytes consisting of a sample solution introduced as a zone between a leading electrolyte and a terminating electrolyte, with each containing only one ion species having the same sign as the sample ions to be separated. The leading electrolyte must have an effective

mobility higher than that of any of the sample ions and the terminating electrolyte must have an effective mobility lower than that of any of the sample ions. When the system has reached equilibrium, all of the ions migrate with the same velocity but are separated into a discrete number of zones in immediate contact with each other, and arranged in order of decreasing mobility. Because of these identical migration velocities, a voltage gradient in the consecutive zone occurs so that by using a potential gradient detector, a stepwise pattern is recorded.

1.3 Theory of Capillary Electrophoresis

This thesis focuses mainly on CZE, hence this section will discuss the theory behind CZE.

1.3.1 Double Layer Theory

The surface of the capillaries is negatively charged at most pH values, due to deprotonation of the surface silanols groups. A charged surface in contact with an

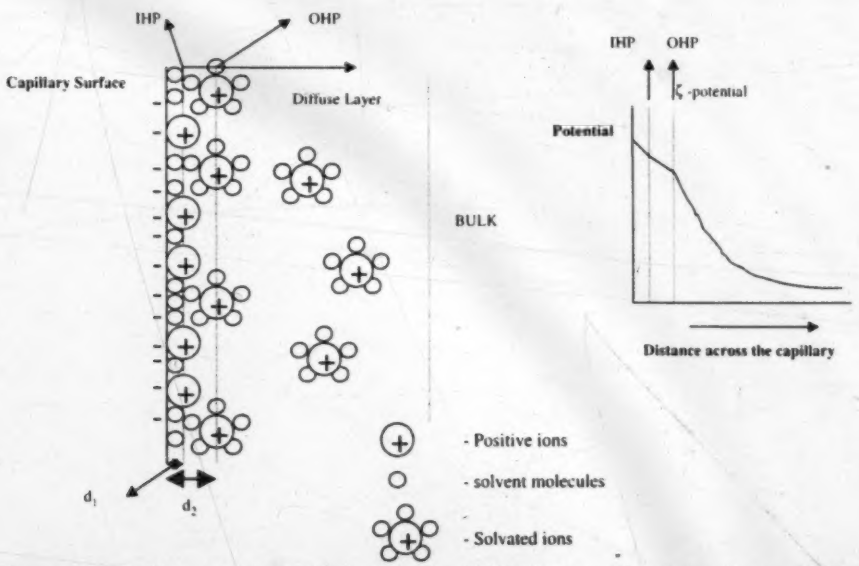

Figure 1.1 : Profile across the double layer, where IHP is the inner Helmholtz plane and OHP is the outer Helmholz plane. The diffuse layer extends from the OHP to the bulk solution. The graph represents the potential profile across the capillary.

electrolyte solution is expected to attract ions of opposite charge and to repel ions of like charge, thus establishing an ion atmosphere of opposite sign in the immediate vicinity of the surface. Two parallel layers of charge are formed: the charge on the surface itself and the layer of oppositely charged ions near the surface. This structure is called the electric double layer, and is illustrated in Figure 1.1.

The inner layer of ions is called the compact Helmholtz or Stern layer. The locus of points involving the electrical center of the specifically adsorbed ions is called the inner Helmholtz plane (IHP) with distance d_1. These are ions which are not solvated. The solvated ions can only approach the charged surface to a distance d_2; the locus of centers of these nearest solvated ions is called the outer Helmholtz plane (OHP). The interaction of the solvated ions with the charged surface involves only long-range electrostatic forces independent of the chemical properties of the ions. These ions are said to be nonspecifically adsorbed. Because of thermal agitation in the solution, non-specifically adsorbed ions are distributed in a 3-dimensional region, called the diffuse layer, which extends from the OHP into the bulk of the solution. The thickness of the diffuse layer is represented by the reciprocal of the Debye layer thickness, κ,

$$\frac{1}{\kappa} = \sqrt{\frac{\varepsilon kT}{2000e^2 N_{av} I}} \qquad (1.1)$$

where – e is the electron charge (1.6×10^{-19} C), N_{av} is Avogadro's constant, I is ionic strength [M], ε is the permitivity of the electrolyte (C/Vm), k is the Boltzman constant [1.38×10^{-23} J/K] and T is the absolute temperature [K].

1.3.2 Generation of Electroosmotic Flow

Electroosmotic flow (EOF) arises because of the motion of the diffuse layer of ions in the solution relative to the solid surface, when a potential is applied between the ends of a capillary. The diffuse layer is mobilized by the electric field and drags the bulk solution with it, thereby generating EOF, Figure 1.2a. Figure 1.2b shows the migration of charged ions in a fused silica capillary under an applied voltage. Under the influence of EOF, all the ions typically move in the same direction. The electric field causes the positive ions to move in the same direction as the EOF, giving them faster velocities than the solvent. Neutral species with no electrophoretic mobility will not move in the absence of EOF, but with EOF they move at the solvent velocity. The negative ions undergo a retardation due to electric field applying a force in the opposite direction to EOF. Typically, the electroosmotic mobility is greater than the electrophoretic mobility of the negative ions, so that their net flow is in the direction of the solvent flow.

The potential governing the magnitude of EOF is known as the Zeta potential (ζ_{eo}) and is defined as the potential at the plane of shear (slipping surface) near the outer Helmholtz plane (OHP). The ζ_{eo} potential is given by the equation

$$\zeta_{eo} = \frac{\rho}{\varepsilon k} \tag{1.2}$$

where ρ is the surface charge density [C/m^2] at the plane of shear. The linear EOF velocity, v_{eo} [m/s], can be calculated from the Von Smoluchowski equation (Eq 1.3)

$$v_{eo} = \frac{E\zeta_{eo}}{4\pi\eta} \tag{1.3}$$

where E is the electric field strength and η the viscocity of the buffer.

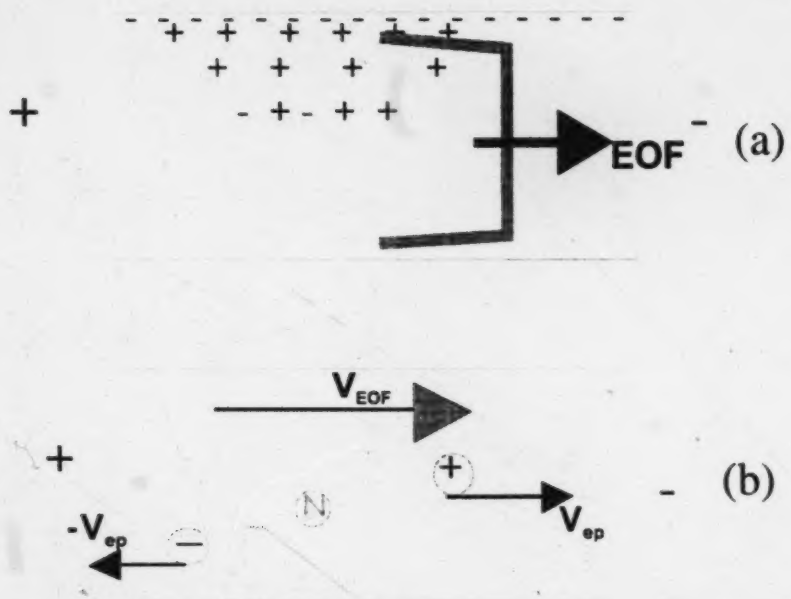

Figure 1.2: (a) The generation of EOF through the pumping action of the mobile ions in the diffuse layer, which drag their hydration sphere with them and consequently the whole bulk solution. (b) the net migration of three ions, positive, neutral and negative respectively, all going in the same direction. The separation is based on the difference in the electrophoretic mobility of the ions.

1.3.3 Fundamentals of CE

The electrophoretic migration velocity of a particular species is given by,

$$v_{ep} = \mu_{ep} E = \frac{\mu_{ep} V}{l} \qquad (1.4)$$

where v_{ep} is the velocity, μ_{ep} the electrophoretic mobility, E the electric field gradient, V the total applied voltage, and l the length of the tube. The time, t, required for a zone to migrate the entire length of the capillary is,

$$t = \frac{l}{v_{ep}} = \frac{l^2}{\mu_{ep} V} \qquad (1.5)$$

The electrophoretic separation of charged species result from the distinct electrophoretic mobilities of ions. While neutral analytes elute at a linear velocity v_{eo}, charged species experience an electrical force which can either accelerate positive ions or retard negative ions. The electrical force, F_E (N), on the ion is given by Equation 1.6,

$$F_E = qE \qquad (1.6)$$

Where q and E are the effective charge of the ion and E the applied electric field strength (V/m).

For small ions ($\kappa r << 1$), $q = \zeta_{ep} 4\pi\varepsilon r$ and can be rearranged to give Equation 1.7,

$$F_E = \zeta_{ep} 4\pi\varepsilon r E \qquad (1.7)$$

where ζ_{ep} is the zeta potential of the ion, ε is the permitivity, η the viscosity of the medium and r is the hydrodynamic radius of the ion.

The frictional drag on the ions as they move under the influence of the electric field is

$$F_F = v_{ep} 6\pi\eta r \qquad (1.8)$$

Where v_{ep} and r are the electrophoretic velocity [m/s] and the hydrodynamic radius of the ion, respectively. At steady state $F_E = F_F$, so the electrophoretic velocity can thus be written as

$$v_{ep} = \frac{qE}{6\pi\eta r} \qquad (1.9)$$

The expression shows the dependence of the mobility of a charged species upon the charge to friction ratio.

1.3.4 Efficiency of Separation

Factors contributing to Zone Broadening

The concept of separation efficiency expressed in terms of theoretical plates may be borrowed from chromatography, as suggested by Giddings [32]. The number of theoretical plates, N, is defined as

$$N = \frac{L^2}{\sigma_t^2} \tag{1.10}$$

where σ_t contains the dispersive effects, i.e. the band broadening terms and L is the length of separation. The overall variance σ_t^2 can be expressed as,

$$\sigma_t^2 = \sigma_L^2 + \sigma_{inj}^2 + \sigma_{det}^2 + \sigma_{wall}^2 + \sigma_j^2 \tag{1.11}$$

where the variance terms are σ_L^2 for longitudinal diffusion, σ_{inj}^2 for the sample injection, σ_{det}^2 for on-capillary detection, σ_{wall}^2 for analyte to wall interaction and σ_j^2 for Joule heating effects. σ_L^2 is given by the Einstein equation

$$\sigma_L^2 = 2Dt \tag{1.12}$$

where D is the molecular diffusion coefficient of the solute and t is the separation time. The term σ_{inj}^2 is given by the equation

$$\sigma_{inj}^2 = \frac{w_{inj}^2}{12} \tag{1.13}$$

and σ^2_{det} is given by

$$\sigma^2_{det} = \frac{w^2_{det}}{12} \tag{1.14}$$

where w_{inj} is the plug width and w_{det} is the length of the detector zone. The term σ_{wall}^2 can be minimized by appropriate choice of buffer and, more importantly, by surface

modification procedures. The σ_j^2 term is highly dependent on the channel cross-section, the ionic strength and the applied potential. With the dimensions of the capillary in the microfluidic devices and the concentration of buffer used, the Joule heating contributing to band broadening is usually insignificant at fields below1000 V/cm [4].

1.3.5 Characterization of Electroosmotic Flow

Electroosmotic flow will somewhat modify the equations describing the separation efficiency. Fortunately, the EOF profile approximates a "plug" shape [33] and thus the flow profile itself leads to minimal zone broadening. The velocity of electroosmotic flow may be given as

$$v_{eo} = \mu_{eo} E = \mu_{eo} \frac{V}{l} \qquad (1.15)$$

where μ_{eo} is the coefficient relating the electroosmotic velocity to the electric field gradient and l is the length of the column. The net migration velocity, v_{net} of a substance is then given by,

$$v_{net} = \mu_{ep} \frac{V}{l} + \mu_{eo} \frac{V}{l} = (\mu_{ep} + \mu_{eo}) \frac{V}{l} \qquad (1.16)$$

The signs as well as the magnitudes of μ_{ep} and μ_{eo} will be important; the signs indicate the relative direction of the flow and the electrophoretic migration. The time it takes an ion to migrate the along the capillary to the detector is

$$t = \frac{lL}{(\mu_{ep} + \mu_{eo})V} \qquad (1.17)$$

and the resulting spatial variance, if we neglect the other parameters involved in zone broadening , becomes

$$\sigma_t^2 = \frac{2DtL}{(\mu_{ep} + \mu_{eo})V} \qquad (1.18)$$

The resulting separation efficiency is

$$N = \frac{(\mu_{ep} + \mu_{eo})V}{2D} \qquad (1.19)$$

The number of theoretical plates can be computed from peak profiles by using the formula

$$N = 5.54\left[\frac{t}{w_{1/2}}\right]^2 \qquad (1.20)$$

Where $w_{1/2}$ is the full peak width at the half maximum points.

The height equivalent to a theoretical plate (H) is

$$H = \frac{L}{N} \qquad (1.21)$$

where L is the length of the separation channel up to the detection point. Replacing for N from Equation 1.10 in Equation 1.21, H can be represented as,

$$H = \frac{\sigma^2_t}{L} \qquad (1.22)$$

Combining equations 1.11, 1.12, 1.13, 1.14 and 1.22, a general expression for plate heights can written and is given by

$$H = \frac{2Dt}{L} + \frac{w^2_{inj}}{12L} + \frac{w^2_{det}}{12L} + \frac{\sigma^2_{wall}}{L} + \frac{\sigma^2_t}{L} \qquad (1.23)$$

In chromatographic theory, theoretical plates represent a phase partitioning process. In electrophoresis, there is no phase separation, but peaks have a finite width defined by their variance, so that H in Eq 1.22 remains meaningful. Separation of the components of a mixture is determined by their relative mobilities in the applied electric field. The

theoretical plate is a convenient concept used to describe the analyte peak shape, to assess the factors which affect separation, and to relate these to the column design.

1.3.6 Resolution Between Two Peaks

Equation 1.19 suggests a misleading approach to improve separation efficiency. This is to promote very large values of μ_{eo}, EOF, in the same direction as the electrophoretic mobility. Giddings [32] derived an expression for resolution in electrophoresis as

$$R_s = \frac{N^{\frac{1}{2}}}{4}\frac{\Delta v}{\bar{v}} \qquad (1.24)$$

where R_s is the resolution and $\Delta v / \bar{v}$ is the relative velocity difference of the two zones being separated. This ratio is equal to

$$\frac{\Delta v}{\bar{v}} = \frac{\mu_1 - \mu_2}{\bar{\mu}} \qquad (1.25)$$

where μ_1 and μ_2 are the electrophoretic mobilities (μ_{ep}) of the two zones and $\bar{\mu}$ is their average mobility. However, in the presence of electroosmosis this becomes

$$\frac{\Delta v}{\bar{v}} = \frac{\mu_1 - \mu_2}{\bar{\mu} + \mu_{eo}} \qquad (1.26)$$

It is readily apparent that a large value of μ_{eo} will decrease the relative velocity difference of the two zones. By substituting the expressions for the relative velocity differences (Eq 1.26) and the number of theoretical plates (Eq 1.19) into the expression for resolution (Eq 1.24) we obtain,

$$R_s = \frac{1}{4}\left[\frac{(\bar{\mu} + \mu_{eo})V}{2D}\right]^{1/2}\left[\frac{\mu_1 - \mu_2}{\bar{\mu} + \mu_{eo}}\right] \qquad (1.27)$$

and rearranging

$$R_s = 0.177(\mu_1 - \mu_2)\left[\frac{V}{D(\bar{\mu} + \mu_{eo})}\right]^{1/2} \qquad (1.28)$$

Now it is clear that a large component of electroosmotic flow in the same direction as the electrophoretic migration will decrease the actual resolution of two zones. In fact, it may be seen that the best resolution will be obtained when the electroosmotic flow just balances the electrophoretic migration

$$\mu_{eo} = -\bar{\mu} \qquad (1.29)$$

At this point substances with extremely small differences in mobility may be resolved. However, the time required can become excessive.

1.4 Surface Modification in Capillary Electrophoresis

1.4.1 Importance of Coating

For CE to become established as a routine separation technique for biomolecules, the challenges associated with the capillary surface chemistry must be addressed. Traditional theory, predicting efficiencies in the millions of theoretical plates for CE, assumes that solute-wall interaction is negligible. However, efficiencies obtained experimentally for large molecule separations using bare fused silica are well below those predicted by theory.

Proteins adsorb due to electrostatic effects; surface charge attracts the opposite charge on the protein. But there are also hydrophobic interactions that do not depend on charge and may cause adsorption even when the electrostatic interaction is not favorable. This adsorption results in poor recovery and poor reproducibility in migration times. In some cases one may be unable to detect the protein, because of complete adsorption on the walls of the channels.

Adsorption causes tailing of the sample, which leads to loss of resolution and sensitivity, due to a decrease in plate numbers. Secondly, it will change the ζ-potential of the capillary, which affects the EOF rate, changing migration times and giving poor reproducibility. Non-uniform distribution of the ζ-potential caused by local adsorption of proteins causes additional peak broadening. For example, analysis of DNA in fused silica capillaries or in microfluidic glass devices requires suppression or reduction of both EOF and channel wall interactions. Extensive studies have been done to elucidate the effect of wall interactions on efficiencies and plate height [15, 34-58]. In the following section we will briefly review different coatings that have been used.

1.4.2 Different Coating Procedures

In order to avoid adsorption problems, the inner wall of fused silica capillaries and channel walls in microfluidic devices have been coated by various methods. These methods can be categorized into two groups, i.e., covalent bonding and adsorption methods. So far, the former is more frequently used in the separation of proteins.

1.4.2.1 Covalent Bonding

Covalent modification generally results in permanent changes to the surface properties of the column. Covalent modification includes bonding via siloxane bonds,

silane bonds and silicon-carbon bonds, with the subsequent attachment of hydrophobic polymers such as polyacrylamide, poly(ethyleneglycol), poly(ethylene-propylene glycol), poly(vinylpyrrolidinone), epoxy polymers and even polysaccharides [15,34-51].

Surface modification with polyacrylamide provides a reasonably inert surface for protein and DNA separations. Polyacrylamide is hydrophobic in nature and does not interact with proteins and DNA. The coating is stable over a wide range of pH, can be used for hundreds of injections, and reduces EOF significantly. Hjërten [34] was the first to obtain near-zero EOF with bonded acrylamide capillaries, allowing the development of isoelectric focusing in capillary columns. The procedure for the polyacrylamide coating is discussed in detail in Chapter 3.

1.4.2.2 Adsorption Methods

The covalent coating process consists of multistep reactions which can be difficult to control, laborious and time consuming. Adsorption methods are less difficult so far as the coating procedures are concerned. The method may be referred to as dynamic coating, wherein the coating material is introduced in the capillaries or in microfluidic channels via the running buffer [36, 52-58]. Normally, polymers or surfactants are employed as coating materials, because these are strongly adsorbed onto the silica surface by means of Coulombic interaction, hydrogen bonding or Van Der Waals forces. When cationic surfactants are used they produce excess positive charges on the surface and reverse the EOF direction. Anionic species cannot be separated because they are attracted and adsorb onto the positive sites on the capillary wall.

An initial attempt at preventing protein-wall interaction was performed by Lauer and McManigill [55], where a combination of increasing pH, adding zwitterions, KCl and

putrescine was used. The best results for the separation of basic proteins were obtained at higher pH values, indicating protein-wall interactions were still an issue. Efficiencies were reported in the range of 50,000 to 836,000 plates/m. Green and Jorgenson [58] attempted to minimize protein-wall interactions by adding alkali metal salts to electrophoresis buffers. They showed that 0.3 M or greater concentration of K^+ in the electrophoresis buffer reduced protein adsorption, as indicated by an increase in efficiency.

1.5 The Development of Micro-Total Analysis Systems

The development of Lab-On-Chip technology is directed toward eventual automated chemical and biochemical analysis in microfabricated devices. The concept is based on miniaturizing sample processing and analysis within a single device. Compared to conventional systems, such devices could reduce solvent and sample consumption, or decrease analysis times because of their decreased dimensions. The integration of sample handling with separation and detection in miniaturized chemical analysis system on a microchip structure has recently been reviewed by Manz [59].

The pioneering work in miniaturization of instruments that perform chemical measurements was first demonstrated in 1979, when an integrated gas chromatograph was fabricated on a 5 cm diameter silicon wafer [60]. Unfortunately, this initial demonstration did not provide the performance characteristics that users desired. However, in the late 1980's, several research groups recognized that liquid phase separation techniques are more amenable to miniaturization than gas chromatography [13, 14].

Electrokinetic effects were used to advantage in miniaturized analysis systems. Electroosmotic flow provides a pumping method that is convenient for small capillaries that develop high back pressures with conventional pumps, and electrophoretic separation has been shown to be an extremely useful chemical separation technique [14]. The first CE separation on a chip was demonstrated by Harrison et al [14] using a 3-port device, 30 μm channels were etched into a glass device with dimensions of 148 mm long x 39 mm wide x 10 mm thick. Fluoresecein and calcein were separated in 7 min, generating up to 35,000 theoretical plates.

This section of Chapter one will concentrate more on the development of micro-total analysis systems for DNA or gene amplification, separation and detection. Much research has concentrated on the integration of the polymerase chain reaction (PCR) on a chip. PCR is a temperature cycling process that theoretically doubles the number of specific DNA molecules after each thermal cycle. Each cycle consists of three separate steps: melting of the double stranded DNA (dsDNA), binding of the specific primers to their target sites (annealing) and extension of the primers by the thermostable DNA polymerase enzyme. The individual steps are simply performed by alternately heating and cooling the sample to characteristic temperatures. Conventionally, PCR is performed in commercially available thermocyclers.

Demands for high-throughput, high performance and cost-effective nucleic acid analysis technologies are increasing. CE has been recognized as a powerful method for DNA fragment sizing and sequencing, because it provides rapid, high resolution, sensitive separations. To address the throughput challenges, capillary-array electrophoresis (CAE) has been developed and applied to DNA fragment sizing and

genomic sequencing [61-66]. Even more advanced approaches to high-throughput nucleic analysis are needed. One of the ways to address this problem is through the "Lab-On-Chip" technology. The fact that microfabricated CE devices have been used to perform separation of fluorescent dyes [14], fluorescently labeled amino acids [14], DNA restriction fragment PCR products, short oligonucleotides, short tandem repeats and DNA sequencing fragments [67, 68], makes them a suitable candidate for the development of integrated high throughput DNA analysis instrument.

1.5.1 μTAS for Gene Analysis

The first DNA amplification reported on a microfabricated device was by Northrup et al [69] at Transducers 93, Yokohama, Japan. The amplification of the human immunodeficiency virus (HIV)- specific target was performed in a micro-reaction channels etched on a silicon wafer (4" diameter, 500 μm thickness). The device included 2 to 3 μm thick low stress silicon nitride membranes with polysilicon (2500 Å) thin film heaters, and aluminum bond pads for contacting the heaters. Simple resistive heating and passive cooling of 50 and 25 μl-volume reaction chambers provided reaction mixture temperature rise and fall times of over 13 and 35 °C/sec, respectively. Northrup claimed amplification was performed 4 times faster than with commercial instruments at a fraction of the power and size.

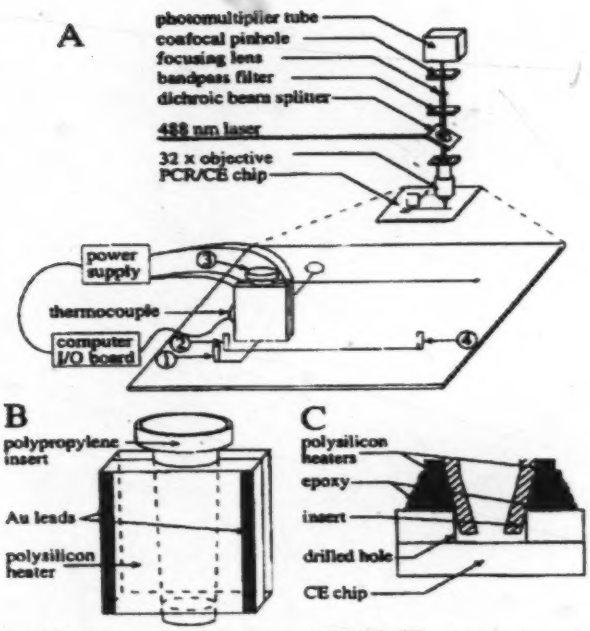

Figure 1.3: Schematic of the integrated PCR-CE microdevice. (A) Laser-excited confocal fluorescence detection apparatus and an integrated PCR-CE microdevice. (B) Expanded view of the microfabricated PCR chamber. (C) Expanded cross-sectional view of the junction between the PCR and CE devices. The size of the epoxy-filled gaps is exaggerated for viewing clarity.

Later Northrup and coworkers [70] coupled the microfabricated silicon PCR reactor and a glass CE chip, as shown in Figure 1.3, to form an integrated DNA analysis system. To demonstrate the functionality of this system, a 15 min PCR amplification of a β-globin target cloned in M13 was immediately followed by high-speed CE separation in less than 120 sec. Wilding and coworkers [71-72] also reported a PCR amplification system on microfabricated silicon glass chips. However, the separation of the PCR products was done off-line on conventional CE instruments.

Manz and co-workers [73] reported a flow-through PCR system as shown in

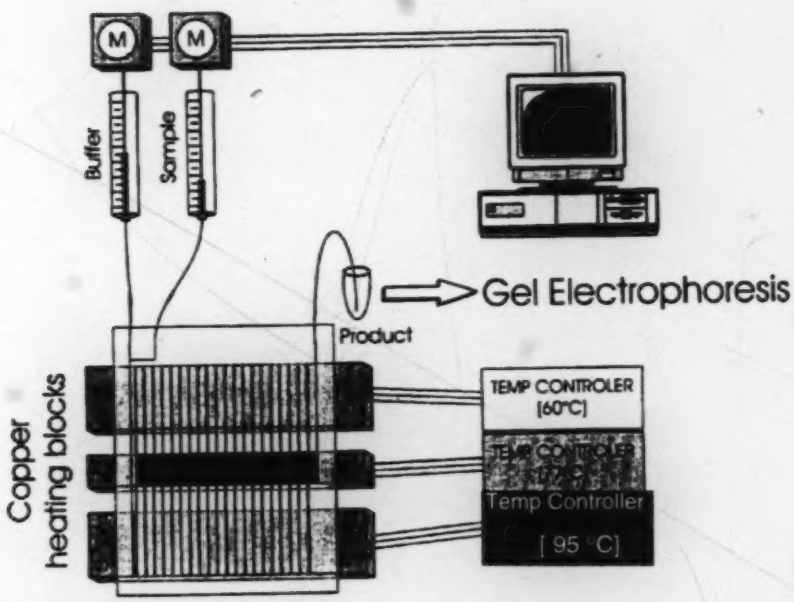

Figure 1.4: The Flow-PCR device set-up. The sample passes repetitively through the three PCR specific temperature Zones: 95°C for melting, 60 °C for hybrization of the primers and 77°C for extension of the primers to the full length product. The product is then collected as shown in the Figure for gel electrophoresis.

Figure 1.4, based on a single channel passing repetitively through three temperature well define zones. The zones were held at 95°C, 77°C and 66°C by means of thermostated copper blocks. The sample was hydrostatically pumped through a single channel etched into a glass chip. The melting, annealing and extension steps occur in different part of the channel as the reagents pass through the three temperature zones. Furthermore, the pattern defined the number of cycles n, performed per run through the chip. The chip incorporated 20 cycles giving a theoretical amplification factor of 2^{10}. A flow rate that provided a total cycling time of 10 min gave 70% of the yield of a fast concentration PCR

thermocycler in which the equivalent number of cycles takes, 50 min. After PCR the products were separated using gel electrophoresis.

Ramsey and co-workers [74] reported an integrated system for rapid PCR- based DNA analysis in microfluidic devices. The system couples a compact thermal cycling assembly based on dual Peltier thermoelectric elements with a microchip gel electrophoresis platform, as shown in Figure 1.5. The system does not actually perform PCR on the device, but rather in the reservoirs of the device, as shown in Figure 1.5. Nevertheless, the system with an on-chip DNA concentration injection scheme involving a porous membrane can detect PCR products after only 10 thermal cycles in less than 20 min. The starting number of template copies was less than 15 per injection volume.

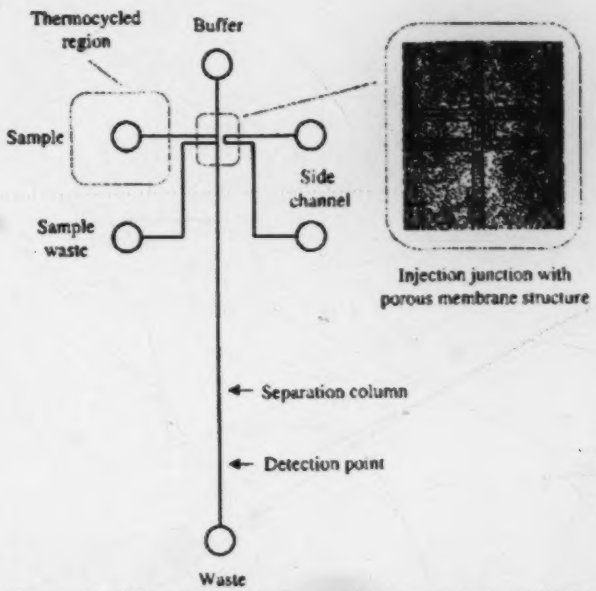

Figure 1.5: Microchannel design used for integrated rapid PCR analysis on-chip. A porous membrane structure is incorporated in the injection valve (CCD image in theinset) to utilize the on-chip DNA concentration feature.

Mathies and co-workers [75] recently reported a radial capillary array electrophoresis microplate and scanner for high-performance nucleic acid analysis, Figure 1.6. The microplate consisted of a central common anode reservoir, as depicted in Figure 1.6, coupled to 96 microfabricated separation channels connected to sample injectors on the perimeter of the 10-cm diameter wafer. Detection was accomplished by a laser excited, rotary, confocal scanner with four color detection channels. Loading of 96 samples in parallel was achieved using a pressurized capillary array system. Separation of 96 PBR322 restriction digest samples was achieved in < 120 s. At the μTAS 2000 conference in University of Twente, Netherlands, the idea of integrating heating elements with the 96 channel microplate was presented by the same research group [76], for the purpose of performing PCR. However, results were not presented.

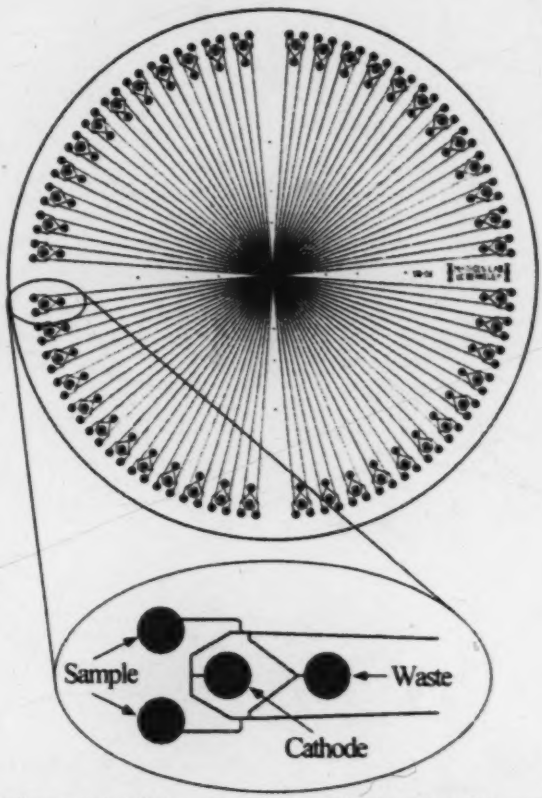

Figure 1.6: Mask pattern for the 96-channel radial capillary array electrophoresis microplate. Separation channels with 200-μm twin-T injectors were masked to 10 μm width and then etched to form 110-μm-wide by ~50-μm-deep channels. The diameter of the reservoir holes is 1.2 mm. The distance from the injector to the detection point is 33 mm. The substrate is 10 cm in diameter.

From the commercial point of view, Nanogen [77] has presented an integrated microelectronic system for rapid multiplex hybridization analysis for genomic research and diagnostic applications. At μTAS 2000, Cepheid [79] reported a PCR DNA diagnostic system based upon a hybrid microfluidic platform. The sample was prepared in a reusable plastic section of the microfluidic platform, which releases the sample, processes it through a series of complex fluidic operations and delivers it to the PCR thermal cycling and amplification section, which is a disposable plastic module. A variety of new commercial instruments are starting to emerge in the market, e.g., Caliper gene separation chip and Micralyne (former Alberta Microelectronic Corporation) Microfluidic Tool Kit.

For the present thesis work an integrated μTAS for gene amplification and detection is presented [79]. Figure 1.7 shows the experimental set-up used. More details on its function are presented in Chapter 3. The DNA amplification method used is cycling probe technology (CPT), which is

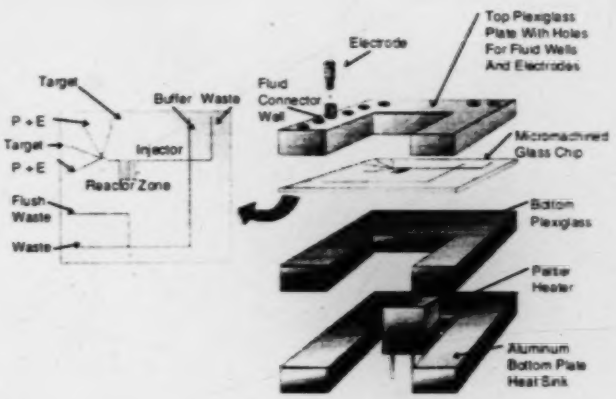

Figure 1.7: The set-up used to perform cycling probe technology on chip. The device is sandwiched between two pexiglass plates which sits on a bottom aluminum block (used as heat sink). The device contains a reaction coil which sits on a heating element. P and E are probe and enzyme respectively. Fluidic and electrical interface are in the top plexiglass as shown in the figure.

an isothermal signal amplification technique developed by ID Biomedical, Vancouver, BC. More details on CPT will be presented in the next section where most of the DNA amplification technologies will be briefly discussed.

In general, genetic analysis involves chemical amplification steps, typically the PCR reaction. To implement these technologies complex thermal modeling and design methods were applied to create these devices. It was necessary used to avoid surface chemistry problems associated with surface denaturing of the enzymes and/or adsorption of DNA due to high-temperature cycles required in PCR. The surface also nucleates gas bubble formation when temperature is varied (60 to 95 °C). Hence, most of the works involving PCR as an amplification technique were done on two devices mated together and not on a single monolithic fluidic device. The isothermal nature of the CPT reaction made it possible to integrate all the processes of mixing, reaction, separation and detection on a single device. It is true that CPT is not as sensitive as PCR, but it is a convenient method to be integrated on chip, whereby there is reduced, gas bubble formation and surface chemistry problems, which are detrimental when performing PCR.

1.5.2 Mixing

When developing a μ-TAS, several issues have to be considered. If an on-chip reaction is performed the mixing of reagents is certainly an issue that should be addressed. Microfabrication offers substantial advantages for pre- and post-column derivatization methods in particular, since mixing intersections with essential zero dead volume can be integrated onto the CE chip.

Post-column reactions in liquid chromatography are performed after the separation is complete. However, in CE, the separation will continue between the reagent

mixing and detection points due to the electric field gradient. The post-column reaction must be rapid, and mixing of the sample and reagent streams must be efficient in order to reduce band-broadening arising from differences in the reactant and product mobilities. It seems likely, then that the geometry of a channel intersection at which mixing occurs is an essential element.

At the μ-TAS 94 Conference, Harrison et al [80(i)] demonstrated a pre-separation mixing of fluorescent compound on a chip, and post-separation fluorescent labeling on a chip. The device used for pre-separation mixing incorporated a mixing chamber. Reagents were driven through the chamber using electrokinetic pumping and the main driving force for mixing of the solutions within the chamber was diffusion. The post-column labeling was later described in

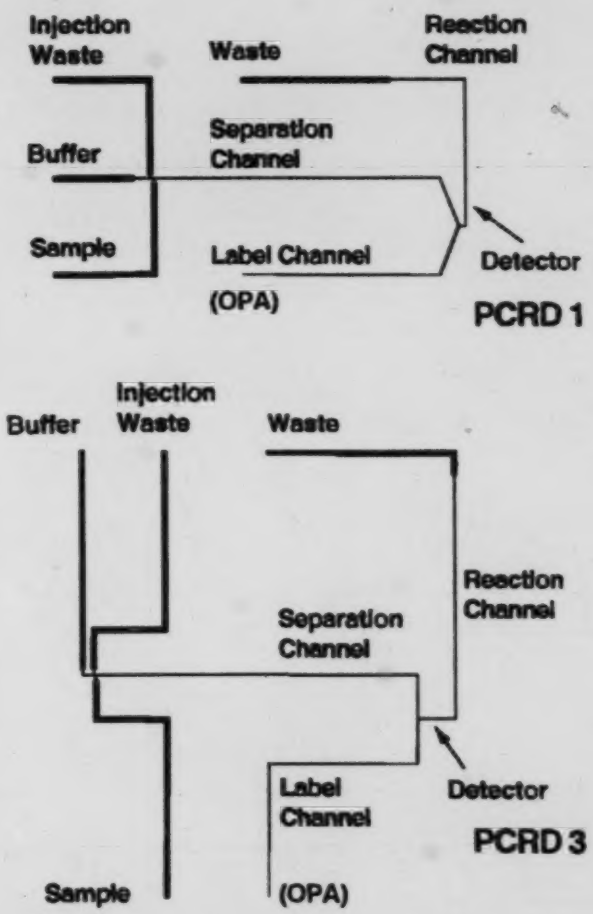

Figure 1.8: Layout schemes of two devices used for postcolumn derivatization reactions with o-phthaldialdehyde (OPA).

more detail [80(ii)]. Quartz and glass devices in which post-column reactors were integrated are shown in Figure 1.8. On-chip post-column reaction of o-phthaldialdehyde (OPA) and amino acids gave theoretical plate numbers of up to 83,000 and ~90 ms peak widths, corresponding to 0.5 μm theoretical plate heights (HETP). Later the PCRD3 device was used for post-column labeling of CE separated human serum protein [81].

Ramsey and co-workers [82] reported an electrophoretic separation of proteins on a chip with non-covalent, post-column labeling, Figure 1.9. A fluorogenic dye, NanoOrange was used for post-column labeling of β-lactoglobulin. The device used is shown in Figure 1.9. The number of theoretical plates obtained was on the order of 11000. In this case diffusive mixing occurs rapidly in the post-column labeling format and band distortion, caused by the difference in mobilities of labeled and unlabeled compound is minimized. Also earlier work from Ramsey and co-workers [83] reported the effects of injection schemes and column geometry on the performance of microchip electrophoresis. In one of his designs, Ramsey used a serpentine column geometry (similar to the reaction coil in the GOCPTTT device, Figure 1.7, to study the contribution of plate

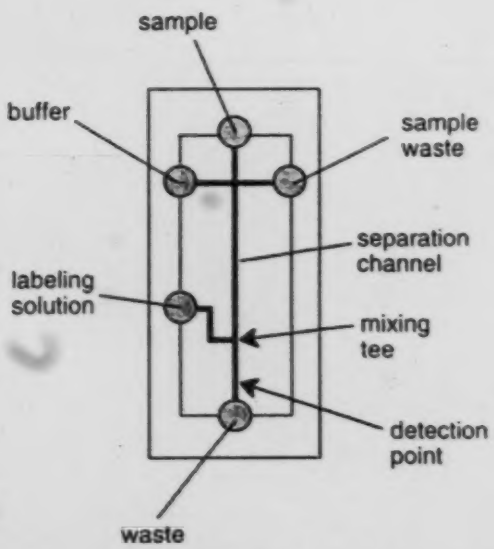

Figure 1.9: Schematic of microchip used for protein separation with post-column labeling.

height of this geometry to band-broadening. The contribution to the plate height equation due to the turns in the serpentine pattern of separation column is written as

$$H_{geo} = \frac{n(\omega\theta)^2}{12L} \qquad (1.30)$$

where n is the number of identical turns, ω is the width at the top of the channel, and θ is the angle of a single turn. Most importantly the expression shows that the plate height decreases as the square of channel width. Reduction of the channel widths should allow reduction of this effect to an acceptable level.

In the present work, the device used, i.e. GOCPTTT (named after G. Ocvirk and T. Tang), performs pre-column reactions in a reaction zone integrated on the device. The reaction zone contains 160 nl volume, Figure 1.7. After the CPT reagents are driven to the reaction coil by electrokinetic pumping, the voltages are turned off and the reagents allowed to mix and react at an elevated temperature of 60 °C. In light of the results obtained from previous work [80-83], we expected sufficient mixing would occur due to diffusion. Most of the optimum conditions necessary for reaction and separation of the CPT products will be discussed in Chapter 3. We did not worry about contributions to band broadening due the serpentine geometry because separation was not performed in this part of the design.

1.6 Basic DNA Concepts

1.6.1 Deoxyribonucleic Acid (DNA) Structure

Genetics is the study of genes, which are carrier of information in all cellular life as well as in many viruses [84-85]. A gene is the basic functional unit of heredity. It is composed of a section of a long, threadlike biological molecule called deoxyribonucleic acid, best known as DNA. DNA is composed of only four basic molecules called nucleotides, which are identical except that each contains a different nitrogen base. Each nucleotide contains phosphate, sugar (of the deoxyribose type) and one of the four bases. The four bases are adenine (A), guanine (G), cytosine (C) and thymine (T). Two of the bases, adenine and guanine, are similar in structure and are called purines. The two other bases, cytosine and thymine, being similar, are called pyrimidines. The first to succeed in finding a reasonable DNA structure were James Watson and Francis Crick in 1953. On

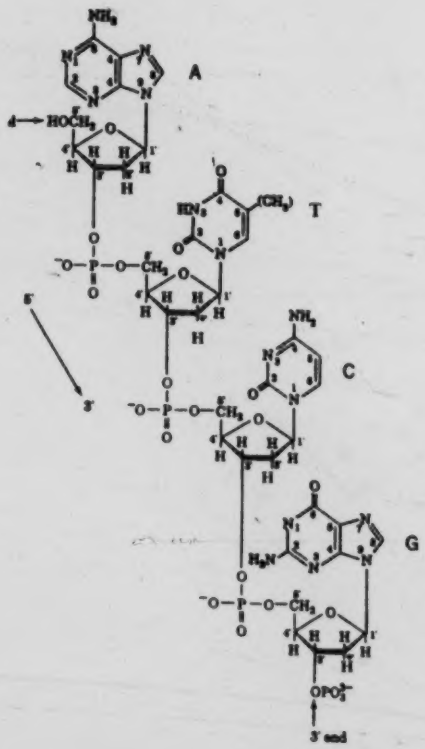

Figure 1.10 : Representation of a tetranucleotide. The sugar atom numbers are primed to distinguish them from the atomic positions of the bases. By convention, a polynucleotide sequence is written with its 5' end at the left and its 3' end to the right. Thus, reading left to right, the phosphodiester bond links neighboring ribose residues in the 5'-3' direction. The above sequence may abbreviated ATCG.

the basis of the X-ray structure of DNA and Chargaff's rule where the amount of T is always equal to the amount of A and the amount of C is always equal to G, Watson and Crick derived the double helix structure of DNA. Each helix, Figure 1.10, is a chain of nucleotides held together by phosphodiester bonds, in which a phosphate group forms a bridge between –OH groups on two adjacent sugar residues. The two helices are held together by hydrogen bonds as shown in Figure 1.11. In the figure the two backbones run in opposite directions; they are said to be antiparallel, and (for reasons apparent in Figure1.11), are called 5'→3' and the other 3'→ 5'.

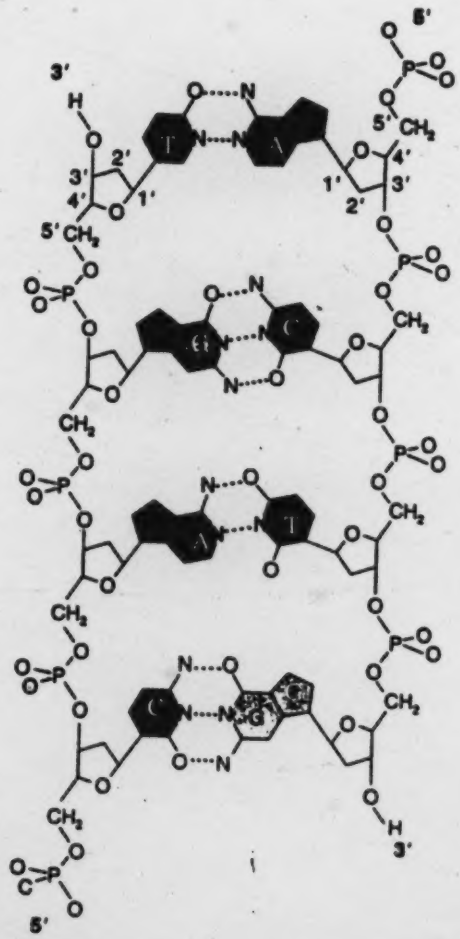

Figure 1.11: The DNA double helix, unrolled to show the sugar-phosphate backbones and base-pair rungs.

In three dimensions, the bases actually form rather flat structures (more like steps) in a ladder and these flat bases stack on top of one another in the twisted structure of the double helix. This stacking of bases adds tremendously to the stability of the complex by excluding water molecules

molecules from between the base pairs. Other names for double helix DNA are double stranded DNA (dsDNA) and duplex DNA.

1.6.2 Properties of RNA

Although RNA is a long-chain macromolecule of nucleic acid (as in DNA), it has very different properties. First, RNA is usually single-stranded, not a double helix. Second, RNA has ribose sugar, rather than deoxyribose, in its nucleotides (hence, its name). Third, RNA has the pyrimidine base uracil (U) instead of thymine (T), where the CH_3 group on the base is replaced by H.

1.6.3 Denaturation and Renaturation of DNA

When a solution of double stranded DNA is heated above a characteristic temperature, its native structure collapses and its two complementary strands separate and assume a random coil conformation. The denaturing of DNA is accompanied by a change in physical properties compared to native DNA. For example, single stranded DNA is less viscous than native DNA, which possesses a certain rigidity in the molecule that is lost when denatured. The denaturing of DNA may be described as the melting of a one-dimensional solid and the temperature at which this occurs is called the melting temperature, T_M.

1.6.3.1 Renaturation

If a solution of denatured DNA is rapidly cooled below its T_M, the resulting DNA will be only partially base paired because the complementary strands will not have had sufficient time to find each other before the partially base paired structures become effectively "frozen in". If, however, the temperature is maintained ~ 25 °C below T_M, enough thermal energy is available for short base paired regions to rearrange by melting

and reforming. Long complementary stretches will not melt again. Under such annealing conditions, denatured DNA eventually completely renatures. Likewise, complementary strands of RNA and DNA, in a process known as hybridization, form RNA-DNA hybrid double helices or duplexes that are only slightly less stable than the corresponding DNA double helices.

1.6.4 Identification of Microorganisms or Bacteria by Conventional Methods

Identification of a bacterium requires a pure growth culture (8h incubation) for reliable result, [86]. Observations of colony morphology, Gram reaction, cell morphology and arrangement are necessary to determine the genus type. The designation of the genus name and species relies heavily on detailed examination of the metabolic and nutritional abilities of these tiny cells.

Biochemical tests are performed in an ordered manner, to subdivide the bacteria into smaller groups called sections. Once the section that bacterium belongs to is known, further biochemical tests can be done, following the methods in Bergey's Manual of Determinative Bacteriology [87] for identification.

1.6.5 Polymerase Chain Reaction

Polymerase Chain Reaction (PCR) [88,89] is a DNA amplification technique which mass amplifies a target DNA. A temperature-resistant polymerase from the bacterium *Thermus aquaticus*, Taq polymerase. is used to catalyze growth from DNA primers. Primers on opposite strands are extended in different directions, towards each other. After completion of the replication of the segment between the two primers (one cycle), the two new duplexes are heat-denatured to generate single-stranded templates, and a second cycle of replication is carried out by lowering the temperature in the

presence of all the components necessary for polymerization. Repeated cycles of synthesis and denaturation result in an exponential increase in the number of segments replicated. Amplifications of up to a millionfold can be readily achieved. With PCR, on the order of 10 copies of human gene be can detected after amplification, provided primers can be synthesized corresponding to the known sequences of the gene [90].

PCR is an example of a mass amplification technique [88,89,91]. Other examples involving target amplification are Transcription Mediated Amplification (TMA), Nucleic Acid Sequence-Based Amplification (NASBA), Self-Sustained Sequence Replication (3SR) and Strand Displacement Amplication (SDA) [91].

In contrast to mass amplification methods, the DNA technology used in this thesis work is a signal amplification technique. The target DNA is not amplified, but participates in cleavage of a probe molecule with the help of endonuclease restriction enzyme RNase H. The amplification arises from the target participating repeatedly in probe cleavage reactions. The amount of cleaved probe is an indication of amount of target initially present. Other signal amplifications of DNA in the literature are techniques such the Branch DNA assay [91] and the smart probe technique [92].

1.6.6 Cycling Probe Technology

CPT is a probe amplifier technology suitable for use in large-scale automated clinical diagnostics [93,94]. It is relatively fast, sensitive and is performed at constant temperature. The system functions by allowing a single target DNA molecule to act as a catalyst for converting a large number of probe molecules to a unique detectable form, with the use of a restriction enzyme. Restriction enzymes are produced by bacteria as a defense mechanism against phages. The enzymes act like scissors, cutting up the DNA of

the phage and thereby inactivating it. However, restriction enzymes do not cut randomly, but at specific target sequences called palindromes, which makes them suitable for DNA and RNA manipulation. An endonuclease restriction enzyme is an enzyme that cleaves the phosphodiester bond within a nucleotide chain [84-85].

The basis of the CPT system is a probe based amplification technology. In essence CPT can be compared to an enzyme-linked immunosorbent assay (ELISA). ELISA offers a similar type of amplification, where the signal for a particular antigen is monitored through the turnover of a substrate by an enzyme bound within an antibody-protein-antibody-enzyme complex. CPT utilizes a chimeric DNA-RNA-DNA probe to hybridize with a target DNA molecule at a specific constant temperature, which is dependent upon the sequence and length of the probe. Ribonuclease H (RNase H), an enzyme which specifically digests RNA in an RNA-DNA duplex, cleaves the probe and the resulting fragments dissociate from the target, as shown in Figure 1.12. The target molecule is then available to pair with another probe molecule and the cycle is repeated. The probe fragments accumulate during incubation for certain amounts of time at about 60 °C. Measurement of the ratio of cleaved to intact probe forms the basis

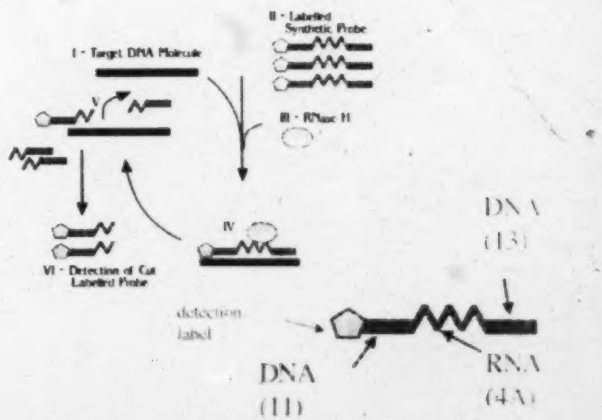

Figure 1.12 : Scheme for Cycling Probe Technolgy. (CPT). (iv) Probe-target hybridization, enzyme action and probe cleavage. (v) dissociation. Courtesy of W.E. Lee from Defence Research Establishment Suffield, AB, Canada.

for detection of the target. The term cycling comes from cycling of the target to cleave intact probes and is not to be confused with thermal cycling in PCR. In essence incubation would have been a more informative name for the process.

The development of CPT was rendered possible due to the specificity of the endonuclease enzyme RNase H, which specifically degrades the RNA portion of the DNA/RNA hybrid and does not cleave single-stranded DNA or RNA.

1.6.6.1 DNA-RNA Hybrid Recognition by RNase H

Two papers, in the literature, describe in detail the mode of action of the enzyme RNase H and the role of Mg^{2+}, which serves as a cofactor to the enzyme to enhance enzymatic activity [95,96]. Investigation of the interaction between the RNA strand of the DNA-RNA hybrid duplex and the Mg^{2+} ion in the ternary complex is required for the elucidation of the mechanism for the RNase H cleavage reaction. One proposed mechanism by Nakurama et al [95] states that the Mg^{2+} ion is not coordinated to the non-bridging oxygens of the phosphodiester bond. In his proposed mechanism, shown in Figure 1.13, the Mg^{2+} neutralises the charge on the phosphate, making the phosphorus center susceptible to nucleophilic attack by a water

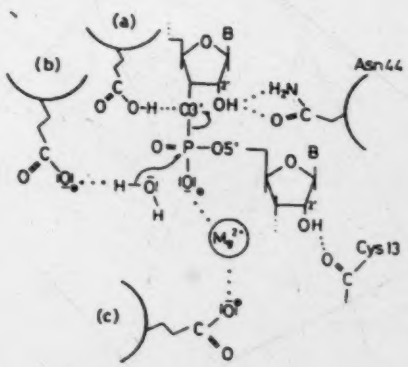

Figure 1.13: Schematic drawing of a proposed mechanism for the action of E.coli RNase H. Three carboxylates, (a, b and c) are involved in catalytic activity, but they are not definitely identified among Asp-10, Glu-48 and Asp-70. Carboxylate accepts a proton from a water molecule, which cleaves the P-O-3' bond. The nucleophilic attack of the water molecule is facilitated by electrostatic interactions among a,c, Mg^{2+} ion, and the phosphate. The side chain amide of Asn-44 and the backbone oxygen of Cys-13 make hydrogen bonds with the 2'-hydroxyls of the ribonucleotide chain of the substrate hybrid.

molecule, which subsequently cleaves the phosphodiester bond. The various species involved in the mechanism for the enzyme include three carboxylates from the amino acids, Asp-10, Glu-48 and Asp-70. One of the carboxylates accepts a proton from a water molecule, which then cleaves the phosphodiester bond. The nucleophilic attack of the water molecule is facilitated by electrostatic interactions among the two remaining carboxylates, the Mg^{2+}, and the phosphate. The side chain amide bonds of Asn-44 and backbone oxygen of Cys-13 make hydrogen bonds with 2'-hydroxyls of the ribonucleotide chain of the substrate hybrid.

In the previous paragraph we discussed the importance of Mg^{2+} in the cycling medium. Most of the preliminary work was done by incubating the CPT reagents in a conventional thermalcycler and running the separation on the 'COPI' device, as described in the experimental section of Chapter 3. Since the chip-based CE separation was run off-line, the CPT reaction required quenching. The quenching buffer used contained urea and EDTA. The high concentration of urea (~ 3.5 M) used was to prevent hybridization of the probe and target DNA. The EDTA was added to the reaction mixture for complexation with the Mg^{2+} ions, to prevent further enzymatic action. However, according to the work done at ID Biomedical, the CPT reactions occurs only at elevated temperature of about 60 °C, hence if the temperature is lowered, the reaction kinetics should slow down, enough to prevent any further probe cleavage.

1.6.6.2 Application of CPT Published to Date

Since the cycling probe technology is quite new, there are few papers on the subject. While most deal with optimizing CPT [94, 97-98], one application of the technology has been reported from work done by ID Biomedical in collaboration with the

University of Arkansas [97]: the development of a diagnostic assay based on the detection of a 36 –bp direct repeat (DR) region in *Mycobacterium tuberculosis*. A CPT probe complementary to the DR was engineered and tested with synthetic and genomic target. The lower limit of detection reported was approximately 250 cell equivalents. The conclusion from the work was that CPT was a viable option among the collection of amplification technologies. Its attractive features include rapidity, simplicity and lack of sensitivity to amplicon contamination.

1.6.7 Physical Artifacts in DNA and RNA

1.6.7.1 Hairpin Loop Formation

Self-annealing of primers (or probe molecules) causes the formation of hairpin structures in solution which may reduce the effective concentration of the reagent, because of the competition between self-annealing and target annealing [91]. Self-complementarity at 3' end of a primer should be especially avoided, because it will reduce the effective concentration of the primer or probe. In the case of CPT it can influence the amount of probe present which can affect calibration. To correct for eventual hairpin loops in designing probes and primers, several computer programs are now available for predicting self- complementarity [99-102].

1.6.7.2 Primer-Dimer

The term 'primer-dimer' refers to an accumulated short PCR product that is roughly the size of the DNA duplex that would be created by two adjoining primers. In the context of CPT, the term primer-dimer would refer to a probe-dimer artifact. Such an artifact can influence quantitation. Again computer programs are available for predicting such interactions [99-102]. However in CPT, apart from probe-dimer artifact, probe-

target artifacts are still a possibility, and their influence on quantitation still need to be studied. In the context of this thesis, urea was used to prevent hybridization after incubation. In the on-chip experiments, with the GOCPTTT device such artifacts should still be considered.

1.7 Scope of the Thesis

The present thesis work is primarily about developing an integrated system that performs online mixing of reagents, DNA hybridization and enzymatic reactions to produce detectable CPT products, followed by separation and detection of the products. The initial system design was done by two former graduate students, T. Tang and G. Ocvirk. The key contribution of this thesis was to develop methods to successfully perform the on-chip CPT process in a quantitative fashion. The system was designed to perform DNA assays that can be ultimately used in the field of clinical diagnostics and biodetection. To reach this goal, numerous conditions had to be optimized and this effort is the main focus of Chapter 3, being the heart of the thesis.

The efforts described in the second chapter, address the frequent need to coat the walls of microfluidic devices to prevent adsorption. The chapter reports the study of electroosmotic flow in poly(dimethylsiloxane) (PDMS) coated capillaries and the use of surfactants to modify the EOF rates. Preliminary work by N. Chiem and M. Wong in this group had suggested PDMS might be a suitable generic coating material. However, the need for adding surfactant to prevent protein adsorption meant it was not suitable for the later CPT project.

Chapter 3, which is the heart of the project, focuses more on (1) the development of a free flow capillary electrophoresis system on chip for separation of CPT DNA

products, avoiding the use of gels, and (2) the coupling of the reaction component to the free flow CE system on the GOCPTTT device. The DNA sample was from methicilin resistant *Staphylococcus aureus* (MRSA), representative of typical clinical assays.

The Fourth chapter tests the GOCPTTT system developed in Chapter 3 for biodetection by running samples derived from *Erwinia herbicola* (EH), a model (simulant) of pathogens in the environment. The work established that the methods developed in Chapter 3 could be easily and quickly applied to a second CPT assay.

Chapter 5 focuses on future work, and on overall conclusions from the thesis effort.

1.8 References

1. Oda, R. P., Landers J. P., "Handbook of CE" 2nd Edition, Landers J. P., CRC Press, Inc., Chapter 1, 1997.
2. Ishii, D., Hirose, A., Hibi K., Iwasaki, Y., *J. Chromatogr.*, 157, 43-50, 1978.
3. Kucera, P., and Guiochon, G., *J. Chromatogr.*, 283, 1-20, 1984.
4. Jorgenson, J. W., Lukacs, K., *Anal. Chem.*, 53, 1298-1302, 1981.
5. Liu, S., Shi, Y., Ja, W. W., Mathies, R. A., *Anal. Chem.*, 71, 566 -573, 1999.
6. Cohen, A. S., Najarian, D. R., Paulus, A., Guttman, A., Smith, J. A., Karger, B. L. *Proc. Natl. Acad. Sci.* U.S.A., 85, 9660-9663 1988.
7. Kasper, T. J., Melera, M., Gozel, P., Brownlee, R. G., *J. Chromatogr.*, 458, 303-312 1988.
8. Drossman, H.; Luckey, J. A., Kostichka, A. J., D'Cunha, J., Smith, L. M. *Anal. Chem.*, 62, 900-903, 1990.
9. Cohen, A. S., Najarian, D. R., Karger, B. L., *J. Chromatogr.*, 516, 49-60, 1990.

10. Swerdlow, H.; Wu, S.; Harke, H.; Dovichi, N. J., *J. Chromatogr.*, 516, 61-67, 1990.

11. Zhang, J. Z., Fang, Y., Hou, J. Y., Ren, H. J., Jiang, R., Roos, P., Dovichi, N. J., *Anal. Chem.*, 67, 4589-4593, 1995.

12. Carrilho, E., Ruiz-Martinez, M. C., Berka, J., Smirnov, I., Goetzinger, W., Miller, A. W.; Brady, D., Karger, B. L., *Anal. Chem.*, 68, 3305-3313, 1996.

13. Manz, A., Graber, M., Widmer, H. M., *Sens. Actuators*, B, 1, 244-248, 1990.

14. (i) Manz, A., Harrison, D. J, Verpoorte, E., Fettinger, J. C., Paulus, A., Ludi, H., Widmer, H. M., *J. Chromaotgr.*, 593, 253-258, 1992.

(ii) Harrison, D. J., Manz, A., Fan, Z., Lüdi, H., Widmer, H. M., *Anal. Chem.*, 64, 1926-1932, 1992.

(iii) Harrison, D. J., Fluri, K., Seiler, K., Fan, Z., Effenhauser, C. S., Manz, A., *Science*, 261, 895-897, 1993.

15. (i) Beale, S. C., *Anal. Chem.*, 70, 279R-300R, 1998.

(ii) St. Clair, R. L., *Anal. Chem.*, 68, 569R-586R, 1996.

16. Jorgenson, J. W., Lukacs, K., *Science*, 222, 266-272, 1983.

17. Terabe, S., Otsuka, K., Ichikawa, K., Tsuchiya, A., Ando, T., *Anal. Chem.*, 56, 111-113, 1984.

18. Terabe, S., Otsuka, K., and Ando, T., *Anal. Chem.*, 57, 834-841, 1985.

19. Chan. K. C., Muschik, G. M., Issaq, H. J., Snader, K. M., J. High Resolution Chromatogr., 17, 51, 1994.

20. Swerdlow, H., Gestland, R., *Nucleic Acids Res.*, 18, 1415-1419, 1990.

21. Guttman A., Cohen , A.S., Heiger, D. M., Karger, B. L., *Anal. Chem.*, 62, 137-141, 1990.

22. Luckey J.A., Drossman, H., Kostichka, A. J., Mead, D. A., D'Cunha, J. Norris, J. B., Smith, L. M., *Nucleic Acids Res.*, 18, 4417-4421, 1990.

23. Huang, X. C., Quesada, M. A., Mathies, R. A., *Anal Chem.*, 64, 2149-2154, 1992.

24. (i) Chen, D. Y., Harke, H. R., Dovichi, N. J., *Nucleic Acids Res.*, 20, 4873-4880, 1992.

(ii) Lu, H., Arriaga, E., Chen, D. Y., and Dovichi, N. J., *J. Chromatogr.*, 680, 497-501, 1994.

(iii) Swerdlow, H., Dew-Jager, K. E., Brady, K., Gestland, R., Grey, R., Dovichi, N. J., *Electrophoresis*, 13, 475, 1992.

(iv) Swerdlow, H., Zhang, J. Z., Chen, D., Harke, H. R., Grey, R., Wu, S., Fuller, C., Dovichi, N. J., *Anal. Chem.*, 63, 2835-2841, 1991.

(v) Figeys, D., Dovichi, N. J., *J. Chromatogr.*, 645, 311-317, 1993.

25. Gao, Q., Yeung, E. S., *Anal. Chem.*, 70, 1382-1388, 1998.

26. Preisler, J., Yeung, E. S., *Anal. Chem.*, 68, 2885-2889, 1996.

27. Gao, Q., Yeung E. S., *Anal. Chem.*, 72, 2499-2506, 2000.

28. Han, F., Huynh, B. H., Ma Y. Lin, B., *Anal. Chem.*, 71, 2385-2389, 1999.

29. Schure, M.R, Murphy, R. E., Klotz, Willie Lau, W., *Anal. Chem.*, 70, 4985-4995, 1998.

30. Hjerten, S., Liao, J., Yao K., *J. Chromatogr.*, 403, 47-61, 1987.

31. Kenndler, E., *Chromatographta.*, 30, 713-718, 1990.

32. Giddings, J.C., *Sep. Sci.*, 4, 209-21, 1969.

33. (i) Pretorius, V., Hopkins, B. J., Schieke, J. D., *J. Chromatogr.*, 99, 23-30, 1974.

(ii) Rice, C. L., Whitehead, R. J., *J. Phys. Chem.*, 69, 4017-4024, 1965.

34. Hjerten S., *J.Chromatogr.*, 347, 191-198, 1985.

35. Hjerten, S., Kubo, K., *Electrophoresis*, 14, 390-395, 1993.

36. Mazzeo, J. R., Krull, I. S., *Biotechniques*, 10, 638, 1991.

37. Schomburg, G., Belder, D., Giles, M., Motsh, S., *J. Capillary Electrophoresis*, 3, 219-223, 1994.

38. Bruin, G. J. M., Chang, J. P., Kulman, R. H., Zegers, K., Kraak, J. C., and Poppe, H., *J.Chromatogr*, 471, 429-436, 1989.

39. Swedberg S., *Anal. Biochem.*, 149, 642, 1990.

40. Srinivasan, K, Pohl, C., Avdalovic, N., *Anal. Chem.*, 69, 2798-2805, 1997.

41. Cobb, K. A., Dolnik, V., Novotny, M., *Anal. Chem.*, 62, 2478-2483, 1990.

42. Giles, M., Kleemiss, G., Shomburg, G., *Anal. Chem.*, 66, 2038-2046, 1994.

43. Strege, M. A., Lagu, A. L., *J.Chromatogr.*, 630, 337-344, 1993.

44. Gelfi, C., Curcio, M., Righetti, P. G., Sebastiano, R., Citterio, A., Ahmadzadeh, H., Dovichi, N. J., *Electrophoresis*, 19, 1677-1682, 1998.

45. Tsuji, K., Little, R. J., *J. Chromatogr.*, 594, 317-324, 1992.

46. Chiari, M., Dell'Orto, N., Gelain, A., *Anal. Chem.*, 68, 2731-2736, 1996.

47. Huang, M., Bigelow, M., Byers, M., *Am. Lab.*, 28 (Oct), 32, 1996.

48. Liu, Y., Kuhr, W. G., *Anal. Chem.*, 71, 1668-1673, 1999.

49. McCormick, R., *Anal. Chem.*, 60, 2322-2328, 1988.

50. Towns, J. K., Regnier, F. E., *Anal. Chem.*, 63, 1126-1132, 1991.

51. Zhao, Z., Malik, A., Lee, M. L., *Anal. Chem.*, 65, 2747-2752, 1993.

52. Melanson J. E., Baryla, N. E., Lucy, C. A., *Anal. Chem.*, 72, 4110-4114, 2000.

53. Baryla, N. E, Lucy, C. A., *Anal. Chem.*, 72, 2280-2284, 2000.

54. Heinig, K., Vogt, C., Werner, G., *Anal. Chem.*, 70(9); 1885-1892, 1998.

55. Lauer, H. H., McManigill, D., *Anal. Chem.*, 58, 166-170, 1986.

56. Yeung, K. C., Lucy, C. A., *Anal. Chem.*, 69, 3435-3441, 1997.

57. Rundlett, K. L., Armstrong, D. W., *Anal. Chem.*, 68, 3493-3497, 1996.

58. Green, J. S., Jorgenson, J. W., *J. Chromatogr.*, 478, 63-70, 1989.

59. Manz, A., *Biochem. Soc. Trans.*, 25, 278-281, 1997.

60. Terry, S. C., Herman, J. H., Angell, J. B. "A GC Air Analyser Fabricated on a Silicon Wafer" , *IEEE Trans. Elec. Dev.*, 26, 1880,1979.

61. Mathies, R. A., Huang, X. C., *Nature* (London), 359, 167-169, 1992.

62. Ueno, K.; Yeung, E. S., *Anal. Chem.*, 66, 1424-1431, 1994.

63. Dovichi, N. J., *Electrophoresis*, 18, 2393-2399, 1997.

64. Kheterpal, I., Mathies, R. A., *Anal. Chem.*, 71, 31A-37A, 1999.

65. Mansfield, E. S., Vainer, M., Harris, D. W., Gasparini, P., Estivill, X., Surrey, S., Fortina, P. *J. Chromatogr. A.*, 781, 295-305, 1997.

66. Mullikin, J. C., McMurray, A. A., *Science*, 283, 1867-1868, 1999.

67. Woolley, A. T.; Mathies, R. A., *Proc. Natl. Acad. Sci.* U.S.A., 91, 11348-11352, 1994.

68. Effenhauser, C. S.; Paulus, A.; Manz, A.; Widmer, H. M., *Anal. Chem.*, , 66, 2949-2953, 1994.

69. Northrup, M. A.; Ching, M. T.; White, R. M.; Watson, R. T. In Digest of Technical Papers: *Transducers 1993; IEEE:* Yokohama,Japan, pp 924-926, 1993.

70. Woolley, A. T., Hadley, D., Landre, P., deMello, A. J, Mathies, R. A., and Northrup, A. M., *Anal Chem.*, 68 4081-4086,1996.

71. Wilding, P., Shoffner, M. A., Kricka, L. *J. Clin. Chem.*, 40, 1815-1818, 1994.

72. Cheng, J., Shoffner, M. A., Hvichia, G. E., Kricka, J. L, Wilding P., *Nucleic Acid Res*, 24, 381-385, 1996.

73. Kopp, M. U., deMello, A. J., Manz, A., *Science*, 280, 1046-1048, 1998.

74. Khandurina, J., McKnight, T. E., Jacobson, S. C,. Waters, L. C,. Foote, R. S, Ramsey, J. M., *Anal Chem.*, 72; 2995-3000, 2000.

75. Shi, Y., Simpson, P. C., Scherer, J. R., Wexler, D., Skibola, C., Smith, M. T., Mathies, R. A., *Anal. Chem.*, 7; 5354-5361, 1999.

76. Lagally, E. T., Paegel, B. M., Mathies, R. A., *μTAS Proc'd 2000*, pp 217-220, 2000.

77. Heller et al, Nanogen, *μTAS Proc'd 98*, pp 221-224, 1998.

78. Pourahmadi et al, Cepheid , *μTAS proc'd 2000*, pp 243-248, 2000.

79. Badal, M. Y., Tang, T., Lee, W. E., Dickingson-Laing, T., Bader, D. E., Harrison, D. J., *μTAS proc'd 2000*, pp 423-426, 2000.

80. (i) Harrison, D. J., Fluri, K. Fan, Z., Seiler, K., *μTAS proc'd 94*, pp 105-115, 1994. (ii) Fluri, K., Fitzpatrick, G., Chiem, N., Harrison, D. J., *Anal. Chem.*, 68; 4285-4290, 1996.

81. Colyer, C. L., Mangru, S. D., Harrison, D. J., *J. Chromatogr.* A., 781, 271-276, 1997.

82. Liu, Y., Foote, R. S., Jacobson, S. C., Ramsey, R. S., Ramsey, J. M., *Anal.Chem.*, 72; 4608-4613, 2000.

83. Jacobson., S. C., Hergenroder, R., Koutny, L. B., Warmack, R. J., Ramsey, J. M., *Anal. Chem.*, 66, 1107-1113, 1994.

84. Voet, D., Voet. J.G., "Biochemistry" second edition, Chapter 28-30, 1995.

85. Griffiths, A. J. F., Miller, J.H., Suzuki, D.T., Lewoutin, R.C., Gelbart, W. M., "Genetic Analysis" sixth edition, 1996.

86. Madigan, M. T., Martiko, J. M., Parker, J., "Brok Biology of Microorganism" 9th Edt, Prentice Hall, Inc., 2000.

87. Bergey D. H., Holt, J. G., "Bergey's Manual of Determinative Bacteriology" 9th Edt., Baltimore, Williams and Wilkins, 1994.

88. Saiki, R., Scharf, S., Faloona, F., Mullis, K., Horn, G., Erlich, H., Arnheim, N., *Science*, 230, 1350-1354, 1985.

89. Mullis, K., Faloona, F., Scharf, S., Saiki, R., Erlich, H., Cold Spring Harbor *Symp. Quantum Biol.*, 51, 263-273, 1986.

90. Corey, E., Arfan, E. W., Oswin, M. M., Melchior, S. W., Tindlass, D. J., Young, C. Y., Ellis, W. J., Yessalka, R. L., *Urology*, 50, 184-8, 1997.

91. Persing, D. H., Smith, T. F., Tenover, F. C., White, T. J., " Diagnostics Molecular Microbiology, *Principles and Applications*", 1993.

92. Knemeyer, J. P., Marmé, N., Sauer, M., *Anal. Chem.*, 72, 3717-3724, 2000.

93. Duck, P., Alvarado-Urbina, G., Burdick, B. & Collier, B., *Biotechniques*, 9, 142-7, 1990.

94. Bekhaoui, F., Poisson, I., Crosby, W., Cloney, L., Duck, P., *Biotechniques*, 20, 240-8, 1996.

95. Nakaruma, H.,Oda, Y., Iwai, S., Inoue, H., Ohtsuka, E., Kanaya, S., Kimura, S., Katsuda, C., Katayanagi., K., Morikawa, K., Miyashiro, H., Ikehara, M. , *Proc., Natl. Acad. Sci. USA*, 88, 11535-11539, 1991.

96. Uchiyama, Y., Shigenori, I., Uena Y., Ikehara, M., Ohtsuka Eika., *J. Biochem.*, 116, 1322-1329, 1994.

97. Beggs, M. L., Cave, M. D., Cloney, L., Marlowe, C., Duck, P., Eisenach, K. D. *J. Clin. Microbiol.*, 34, 2985-9, 1996.

98. Modrusan, Z., Bekhaoui, F., and Duck, P., *Molecular and cellular Probes.*,12, 107-116, 1998.

99. Lucas, K., Busch, M., Mossinger, S., Thompson, J. A., *Comput. Appl. Biosci.*, 7, 525-529, 1991.

100. Mcgraw, R. A., Steffe, E. K., Baxter, S. M., *Biotechniques*, 8, 674-678, 1990.

101. Osborne, B. I., *Comput. Appl. Biosci.*, 8, 83-93, 1992.

102. Rychlik, W., Rhoades, R. E., *Nucleic Acids Res.*, 17, 8543-8551, 1989.

CHAPTER 2: Electroosmotic Flow Study on Poly(dimethylsiloxane) Coated Capillaries

2.1 Introduction

Capillary Zone Electrophoresis (CZE) [1] is a versatile technique for separation of analytes. Unfortunately, CZE performance may be limited because of the charged capillary walls, which invite analytes such as proteins to adsorb. Such interaction or adsorption causes zone broadening and tailing, resulting in low separation efficiencies. As a result, surface modification of capillary walls is required for protein separation in the CZE mode. Modification of the capillary walls within fused silica capillaries or microchips [2] can be achieved through coatings. Separation of large proteins is highly useful in the pharmaceutical industry for evaluation of recombinant protein products to be used as therapeutic agents. Separation can also be used to study various aspects of post-translational modification, such as glycosylation, phosphorylation, protein folding, etc. Analysis of the whole protein can help in the detection and characterization of isoenzymes [3-5], making coating procedures that facilitate protein analysis important.

Various permanent and dynamic coatings have been reported in the literature [6-32] and all of them exhibit some level of experimental difficulty. The alternate procedure of capillary gel electrophoresis (CGE)[33-50] is a well established technique for protein and DNA separation. However, CGE also requires coating of the capillary walls, to reduce electroosmotic flow (EOF).

Controlling the flow in a particular separation experiment can help to determine the optimum condition for high separation efficiency and resolution. The parameters

which describe a high quality separation are summarized in Equations 2.1 to 2.4 for the migration time, t, the total number of theoretical plates, N, and the resolution, R.

$$t = \frac{l^2}{\mu_{ob} V} \qquad (2.1)$$

$$N = \frac{\mu_{ob} V}{2D} \qquad (2.2)$$

$$R_s = 0.177 \Delta\mu_{ob} \left\{ \frac{V}{D(\bar{\mu} + \mu_{eo})} \right\}^{1/2} \qquad (2.3)$$

$$\mu_{ob} = \mu_{ep} + \mu_{eo} \qquad (2.4)$$

Here l is the capillary length, μ_{ob} is the observed electrophoretic mobility of the solute, μ_{ep} is the electrophoretic mobility, $\Delta\mu_{ob}$ is the difference between the observed electrophoretic mobilities of two analytes. $\bar{\mu}$ is the average of the electrophoretic mobilities of the two analytes, μ_{eo} is the electroosmotic mobility, V is the separation voltage between injection and detection locations and D is the diffusion coefficient. In order to improve migration time, plate numbers and resolution between analytes such as a protein, we may adjust the EOF and influence all four equations. The best resolution would be when $\bar{\mu} = -\mu_{eo}$, but it would then take an enormous amount of time for components to reach a detector. Also, we know from Equations 2.1 and 2.4 that in CZE, the EOF affects the amount of time a solute resides in the capillary, and in this sense, both separation efficiency and resolution are related to the direction of flow and the rate of electroosmosis.

Several research groups have reported various ways to control EOF. Lee et al [51] reported the use of an external electric field for direct control of EOF by coupling an

externally applied potential with the potential inside the capillary. The ζ-potential can be controlled so as to be made positive, zero, or negative. The ability to control EOF in this fashion was very interesting. But to separate large biomolecules, surface modification was still needed to prevent adsorption. Further work on the control of EOF using an external field by Ewing and co-workers [52] was done using Nafion coated capillaries. The authors reported a dramatic decrease in analysis time of a peptide mixture at pH 1.4. The authors also reported that the technique offered better EOF control at low pH.

Another method to control charge on capillary walls is to adjust the pH of the running buffer [20,30,53]. Acidic pH may be used to repress the ionization of silanols or basic pH to produce a negative charge on the protein, which is then repelled by negatively charged walls. However, many proteins are denatured by extreme pH, making such methods not universal. Regnier and co-workers [21] reported a more universal technique of both controlling the flow and reducing protein adsorption on the capillary surface. Regnier's work followed the study by Borgerding and Hinze [54] which examined the effect of Brij 35 (polyoxyethylene(23)-dodecanol) on chromatography performed on an octadecylsilane column. Borgerding and Hinze reported the substantial adsorption of Brij 35 on the reverse-phase surface. The most definitive work on the effects of neutral surfactants in exclusion media for large molecules was contributed by Desilets et al [55]. The author reports that the polyoxyethylene-based surfactants apparently create a semipermeable membrane, a hydrophilic layer of adsorbed surfactant on an alkylsilane derivatized surface that prevents the adsorption of proteins. Regnier [21] used the technique in a capillary format for CE, where the capillary surface was

permanently coated with an alkylsilane and proteins were separated using neutral surfactants such as Brij 35 or the Tweens as dynamic adsorbants.

Lucy and co-workers [25-28] reported various studies on EOF control using ionic and neutral surfactants in bare capillaries. These methods provide a dynamic coating that may be more general than the external electric field procedure. Recently, Lucy and co-workers [27] reported the simultaneous separation of cationic and anionic proteins using zwitterionic surfactants in CE. The zwitteronic surfactant (AM CAS U) formed a dynamic coating that prevented protein adsorption, and efficiencies as high as 1.5 million plates/m were reported. The same group reported a double-chained surfactant, didodecyldimethylammonium bromide (DDAB) [26] for semipermanent wall coatings. The authors claimed efficiencies on the order of 10^5-10^6 plates/m for separations of basic protein mixtures. Similar, earlier work has been done by Cifuentes et al [23] in 1996 and Fritz and co-workers [24] in 1997, who reported plate numbers on the order of 10^5/m where C_{16}TAB was used in the analysis of basic proteins, all in bare capillaries. Roeraade and co-workers [33] also reported the separation of basic and acidic proteins in the presence of cationic and anionic fluorosurfactants in bare capillaries.

Four qualities that a coating should possess have been identified by Mazzeo and Krull [56] and these are: (1) high separation efficiency, (2) high protein recovery (~100%), (3) stability, evidenced by negligible changes in migration from run to run or day to day, and (4) ease of electroosmotic flow control, so that cationic and anionic proteins can be separated in one run. In this work we show that a capillary with a permanent coating of poly(dimethylsiloxane) (PDMS) can be used to separate large proteins. Furthermore, PDMS coated capillaries not only offer the four qualities

mentioned above, they are also inexpensive and relatively easy to make. The bonding in the permanent modification of the capillary wall surface is most likely an Si--- O---Si which is shown in Figure 2.1 [57].

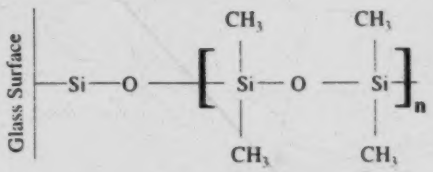

Figure 2.1 : Bonding of the poly(dimethylsiloxane) with the silanol group on the capillary surface (n = 200).

The PDMS coating interacts with surfactants. Consequently it can provide an adsorptive surface for the deposition of charged surfactants that may be used to modify EOF. We have used PDMS in this fashion, with a combination of neutral and charged surfactants in a modification of the procedure used by Lucy, Cifuentes and Fritz [23-28]. In this work commercially available neutral surfactant could be used instead of zwitterionic surfactant which Lucy selected, due to the affinity of PDMS for surfactants. Sodium dodecylsulfate (SDS) and cetyltrimethyl ammonium bromide (CTAB) were used as charged species to modify EOF, with Brij 35 as a neutral surfactant. The effect of pH on EOF in the presence of these surfactants was also evaluated.

2.2 Experimental

2.2.1 Instrumentation

All experiments were performed on a Beckman P/ACE 5010 CE instrument. P/ACE system software was used for data acquisition. Polymicro capillaries (Phoenix , AZ) with an inner diameter of 50 µm, an outer diameter of 345 µm and a total length of 27 cm (20 cm to the detector) were used. Detection was by UV absorbance at 254 nm.

2.2.2 Reagents

The phosphate buffers of ionic strength 50 mM were prepared from potassium phosphate monobasic (KH_2PO_4 - Fischer) and di-potassium hydrogen orthophosphate (K_2HPO_4 -BDH)[1] using the phosphate buffer nomogram [58]. The nomogram was used to prepare the desired pH for buffers without having to adjust with acid or alkali. Different proportions of the two phosphates were used to make the different pH value buffers and the value measured from the pH meter was used.

Poly(dimethylsiloxane) [PDMS] 200 (Aldrich) was used as received for coating purposes. A 1% PDMS solution in dichloromethane (dried and distilled before use) was prepared and used to coat the capillaries, after filtering with a 0.2 µm nylon filter. All water used in the experiments was from a Milli-Q UV plus water purifier. Protein samples used included: lysozyme (chicken egg white), myoglobin (horse skeletal muscle), cytochrome C (horse neart), α-chymotrysinogen A (bovine pancreas) and ribonuclease A (bovine pancreas), which were all from Sigma and used as received. The neutral marker used to measure electroosmotic flow (EOF) was 1% (v/v) benzyl alcohol prepared by dissolving in 5 ml methanol and adjusted to 100 ml volume with phosphate buffer (ionic strength ajusted to 50 mM). The surfactants were sodium dodecylsulfate ($C_{12}H_{25}SO_4$- Na) (SDS) (SERVA)), cetyltrimethyl ammonium bromide 95% ($CH_3(CH_2)_{15}N(CH_3)_3Br$ (CTAB), (Aldrich)) and Brij 35 (Aldrich), used as received. All solutions were filtered through 0.2 µm nylon filters prior to use.

2.2.3 Coating of Capillaries

For each individual coating a 100 cm capillary was used and the Beckman instrument was used for the conditioning and coating of the capillaries. The capillaries were conditioned by flushing with 0.1 M NaOH for 30 min and water for another 45 min.

Finally, nitrogen gas was flushed through to drive out the remaining water for about 15 min. The capillary was coated by rinsing with dichloromethane for 5 min followed by 1% PDMS solution for another 2 min, after which the PDMS was allowed to sit inside the capillary for a further 10 min. The last stage was to flush nitrogen through for 10 min. The final step involved placing the capillary in a programmable oven (Model 6-525, J.M. Ney Co., Yucaipa, CA, USA) for thermal curing of the coating. The program used for curing was (**1.** 10 °C/min rise to , 400°C, then 0.5h at 400°C, followed by **2.** Natural cooling to room temperature).

2.2.4: Protein Separation

The 27 cm lengths for each study were tested by separating a sample mixture of lysozyme and cytochrome C on the Beckman. The sample concentration was 0.2 mg/ml of each enzyme in 50 mM phosphate buffer. The running buffer was 50 mM phosphate buffer containing 0.01% Brij 35 (83.3 μM) at pH 7.3. The sample injection time was 2 sec (pressure injection) and the separation voltage was 20 kV. A mixture of 5 different proteins was separated, containing 1 mg/ml each of lysozyme, cytochrome C and ribonuclease and 0.5 mg/ml of α-chymotrypsinogen A and myoglobin, using the same buffer conditions.

2.2.5: EOF Measurement

Coated capillaries of 27 cm length were used for each trial. The capillary was rinsed with water for 15 min, followed by the respective buffer for another 30 min. The neutral marker, benzyl alcohol (1% in 50mM phosphate buffer), was then pressure injected for 2 sec and separated at 20 kV separation voltage. The migration time was

obtained from the neutral marker peak, from which electroosmotic mobility was calculated from the following expression

$$\mu_{eo} = \frac{v_{eo}}{E} = \frac{L_{det} l}{tV} \qquad (2.5)$$

where v is the velocity of the EOF, E is the electrical potential defined as the applied voltage, V, divided by the total length of the capillary (l = 27 cm), L_{det} is the length of the capillary to the detector (20 cm) and t is the observed migration time for the neutral EOF marker, benzyl alcohol.

2.3 Results and Discussion

2.3.1 Coating Evaluation

Table 2.1 shows the migration for the neutral marker in PDMS coated and uncoated capillaries for differing pH values. Compared to an uncoated capillary, the PDMS coating suppresses EOF to 50% of the original value. With 0.01% Brij 35 (83.3 μM) added to the buffer, a 75% suppression of EOF was observed from the bare capillary. These results show that the PDMS coating reduces the effect of charged sites on the surface and that the Brij 35 adds another hydrophobic layer to further reduce the effect of surface charge and so reduce EOF. This coating should, therefore, reduce protein interaction with the walls, unless hydrophobic interaction are significant. Note Brij 35 critical micelle concentration (cmc) is 92 μM in water. The 0.01% Brij 35(83.3 μM) in solution was close to its cmc [59].

Table 2.1: The electroosmotic mobility (μ_{eo}) at different pH values

	μ_{eo} $cm^2/Vsec$		
pH of buffers*	**6.3**	**7.36**	**8.2**
Uncoated	6.32×10^{-4}	7.24×10^{-4}	7.88×10^{-4}
PDMS coated	3.51×10^{-4}	3.65×10^{-4}	4.43×10^{-4}
PDMS/Brij 35 coated	1.58×10^{-4}	1.65×10^{-4}	1.66×10^{-4}

* Phosphate buffer with the ionic strength adjusted to 50 mM was used.

The separation of lysozyme and cytochrome C in a PDMS/Brij 35 coated capillary (50 mM phosphate buffer pH 7.3) is shown in Figure 2.2a and b. The high resolution of 1.969 achieved in the separation of these two proteins, (Figure 2.2a), which could not be separated in bare capillaries [21], showed the improvement due to the coating. The variations in migration time from run to run was within 1% RSD. On the other hand Figure 2.2b shows the separation efficiency after 50 runs, indicating very little deterioration was observed. Separation was achieved with fairly good resolution of 1.62 and 8% RSD variation in migration time. The highest plate numbers achieved with the separation of those proteins was 7.5×10^4 plates/m. Figure 2.3 shows the separation of five different proteins with the same buffer conditions as mentioned above. The data in Figure 2.3 shows the ability to separate large proteins with significantly different pI values (Table 2.2) and hydrophobic characters [21].

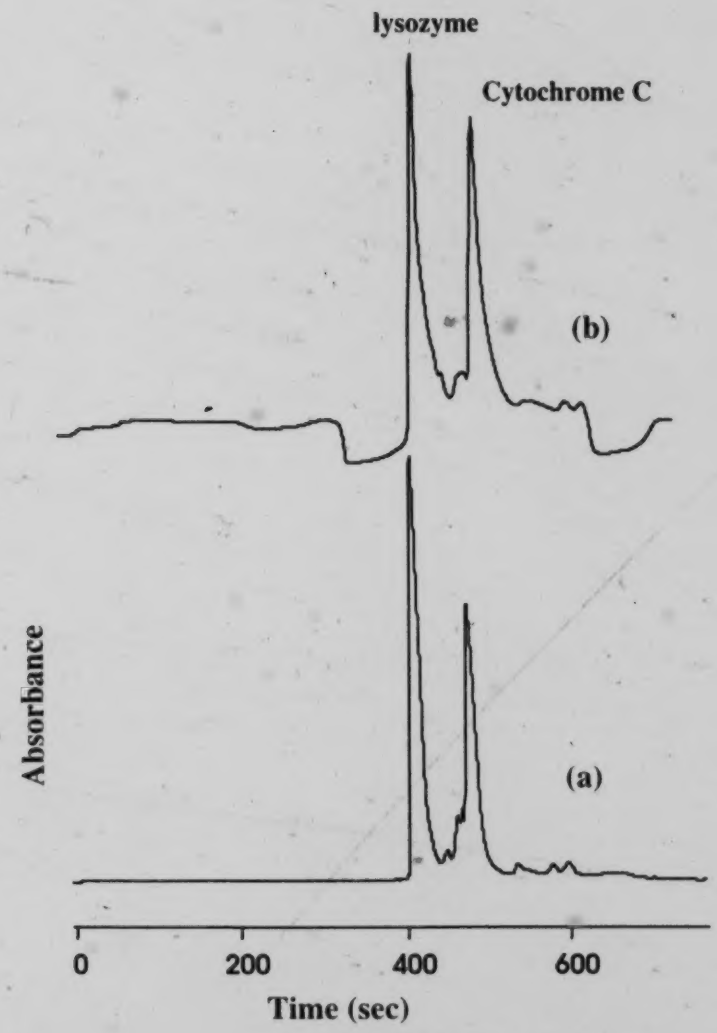

Figure 2.2: Electropherograms show: (a) Separation of two proteins, lyzozyme and cytochrome C in PDMS coated capillaries, giving 7.5 x 10^{-4} plates/m and an R value between the two peaks is 1.97. Separation was achieved in 50 mM phosphate buffer (pH 7.3), 0.01% Brij 35. A 2 s pressure injection was performed and 20 kV separation voltage was used across 27 cm length capillary. Variation between the first 5 injections was within 1 % RSD. (b) Separation after 50 runs with an R value of 1.62, % RSD of ~8 in migration time.

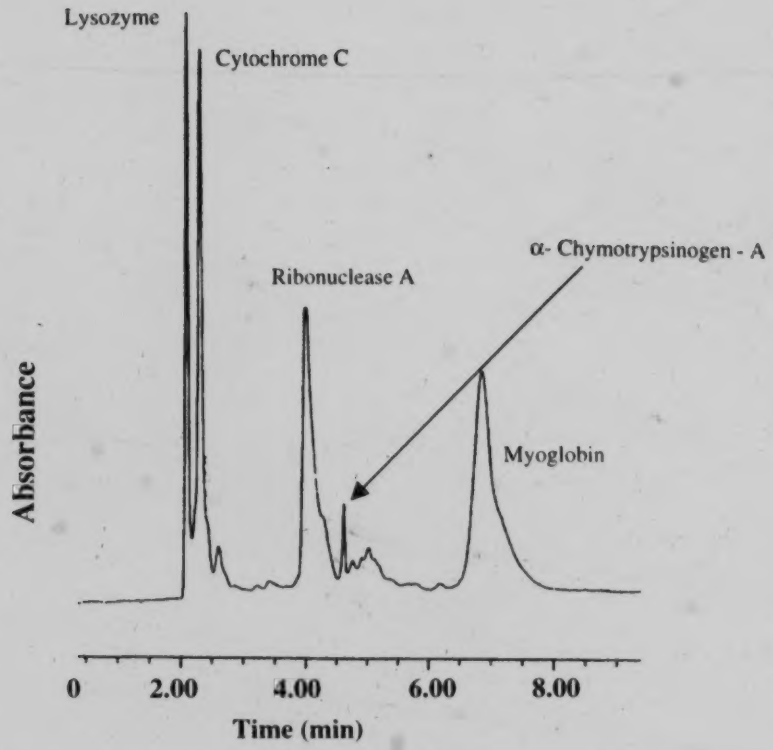

Figure 2.3: Electropherogram for separation of 5 proteins in a PDMS coated capillary. Separation was achieved in 50 mM phosphate buffer (pH 7.3), 0.01% Brij 35. Pressure injection of 2 s with a 20 kV separation voltage in a 27 cm long capillary. Sample mixture was 1 mg/ml of Lysozyme, Cytochrome C , Ribonuclease A and 0.5 mg/ml of α- Chymotrypsinogen - A , Myoglobin.

Table 2.2: pI values of different proteins [21]

Protein	pI value
Lysozyme	11.0
Cytochrome C	10.2
Ribonuclease	9.3
α-chymotrypsinogen A	9.2
Myoglobin	7.3

2.3.2 Effect of pH on the EOF in Coated Capillaries

Table 2.1 shows how the mobility changed on moving from lower pH to higher pH in bare and PDMS coated capillaries. There were measurable changes in mobility on moving to higher pH values in bare capillaries and PDMS coated capillaries. However, with Brij 35 in the buffer, the changes in mobility in coated capillaries with pH changes were rather insignificant. With Brij 35 in the running buffer, the surface charge was less susceptible to pH variation.

A 75% reduction in EOF is certainly not as good as values reported by Hjerten [6] and Dovichi [15] in their respective work on polyacrylamide coating and surface modification based on Si-C sublayers. In the case of Hjerten, the value reported was near zero EOF and in the case of Dovichi and co-workers a one order of magnitude reduction in EOF was observed, which worked very well with DNA separations. But as Regnier and coworkers [21] reported, a decrease in EOF does not correspond to an increase in separation efficiency of proteins. One important thing to note is that it is necessary to reduce the negative silanol charges on the capillary wall that cause protein adsorption yet

still allow for sufficient electroosmotic pumping to drive analyte molecules of different pI values to the detector. Hence the PDMS coating is a possible candidate which can be used for the separation proteins.

2.3.3 Effect of SDS on the EOF

Charged surfactants that adsorb on the PDMS can be used to modify and control the EOF [21]. For surfactant adsorption on a silica/PDMS surface, several parameters will be important. These include the pH, which modifies the charge of the silica, and the concentration of surfactant. The presence of a neutral surfactant such as Brij 35 may also have a modifying effect on the ability to fine tune the value of EOF. Such effects have been shown by Lucy and co-workers [25-28], using surfactants such as CTAB, coco(amidopropyl)hydroxyldimethylsulfobetaine (Rewoteric AM CAS U), and more recently a double-chained surfactant didodecyldimehylammonium bromide (DDAB). Most of those studies were in bare capillaries where the zwitterionic surfactants acted as a dynamic coating into which the charged surfactants were presumed to dissolve.

In the present study the experiments were done at three different pH values in the presence and absence of 0.01% Brij 35 in the running buffer. Different concentrations of SDS were used to modify EOF within the PDMS coated capillaries. A comparative study was done in a bare capillary at pH 6.3 where no significant change in μ_{eo} was observed, as shown in Table 2.3. The results show that SDS, being negatively charged, is repelled by the negatively charged capillary walls, consequently no change in EOF is observed with increasing SDS concentration.

Table 2.3: μ_{eo} of bare capillaries at different SDS concentrations at pH 6.3

% SDS in buffer	0	0.0005	0.005	0.05
μ_{eo} x 10^{-4} cm^2/Vsec	6.11	6.12	6.12	6.14

For PDMS coated capillaries, significant changes were observed in μ_{eo} with increasing concentration of SDS, as shown in Figure 2.4a, b and c. In the absence of Brij 35 it was found that the mobility increases and reaches a plateau for each pH. A constant EOF is observed in the range of 0.02 to 0.08% of SDS (0.7mM to 2.8mM). The cmc level for SDS is 8.1 mM in water and 2.2 mM in buffer with an ionic strength of 50 mM [60]. We note that at 0.02% SDS in the running buffer, we are still below the cmc level of SDS by one order of magnitude. At this concentration (below cmc) many proteins would not denature [61].

In the presence of 0.01% Brij 35, the neutral surfactant, there is a continuous increase in μ_{eo} with increasing SDS. No plateau was observed even at 0.08% SDS. Therefore in the presence of Brij 35 it is possible to control the μ_{eo} across a range of 1.5 to 6.0 cm^2/Vsec, by adjusting the SDS concentration. A plausible explanation of the observed change in μ_{eof} with increasing SDS concentration in the presence and absence of Brij 35 can be illustrated in Figure 2.5. In the absence of Brij 35, SDS molecules adsorbed on the PDMS surface to form hydrophobic interactions. Increasing SDS concentration saturated the PDMS coated surface. The point of constant EOF was reached. Both Brij 35 and SDS can adsorb on the PDMS surface through hydrophobic interactions. In the presence of Brij 35 a competition between SDS and Brij 35 for

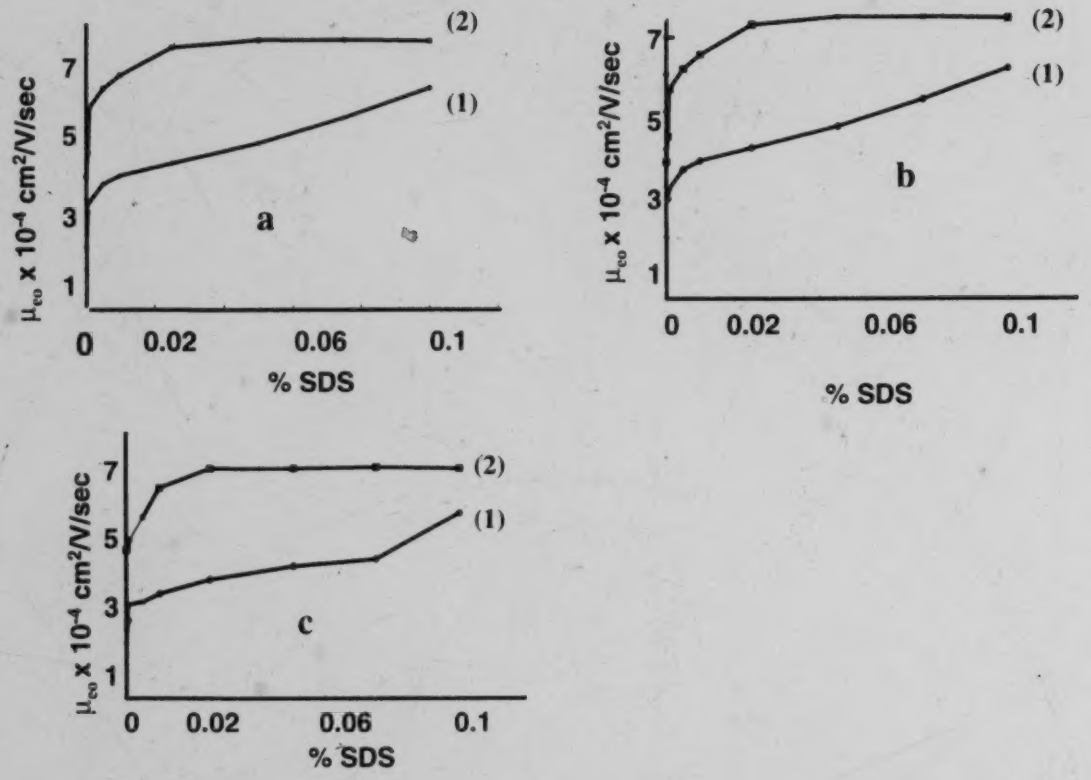

Figure 2.4 : Variations in μ_{eo} with increasing SDS concentration in the running buffer at different pH values. Separation voltage was 20 kV in 27 cm capillaries. [a] pH =6.3, [b] pH =7.36, [c] pH = 8.2. In all of the three cases the study was done (1) with 0.01% Brij 35 in the running buffer, (2) without Brij 35 in the buffer.

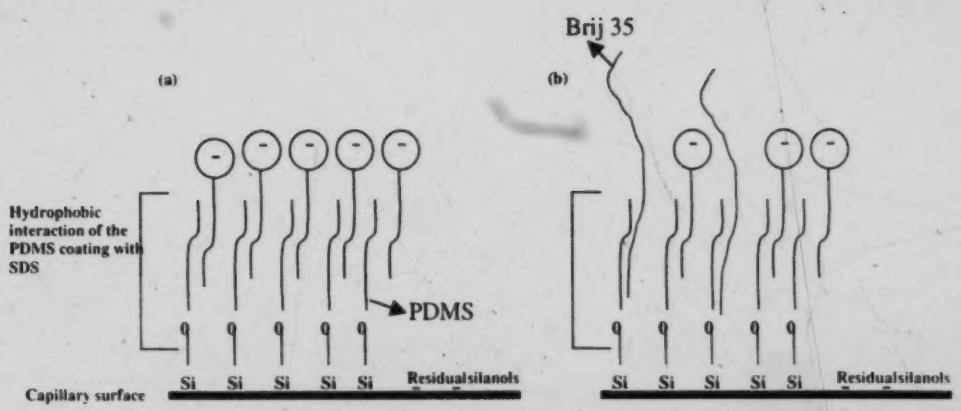

Figure 2.5: (a) Illustrates the adsorption of SDS hydrophobic tails on the PDMS coated capillary surface. (b) Illustrates the competitive binding of SDS and Brij 35 on the PDMS surface.

adsorption occurs, so that more SDS is needed to cause saturation. In the present study, we cannot comment on the kinetics and thermodynamics of interaction of the surfactants on the surface. However, the results demonstrate a reasonable control on EOF in the presence Brij 35.

2.3.4 Effect of CTAB on the EOF

CTAB is a cationic surfactant that can adsorb strongly on the negatively charged walls of the capillary and will not be repelled by the surface charge, in contrast to SDS. As a result, it was expected that more SDS would be needed to achieve a change in surface charge state in comparison to CTAB. The use of long-chain alkylammonium salts to reverse EOF was first reported by Reijenga et al [62]. Typically, when flow reversal is desired for a separation, it is achieved by addition of 0.5 mM CTAB to the electrophoretic buffer [63-64]. At this concentration, the EOF is reversed and stable.

To explain the changes in surface charge, Lucy et al [25] propose the formation of "hemimicelles" as described by Fuerstenau and Gaudin [65]. The "hemimicelle" formation is due first to the adsorption of the cationic head of the surfactants with the surface of the negatively charged capillary walls through electrostatic interaction. With

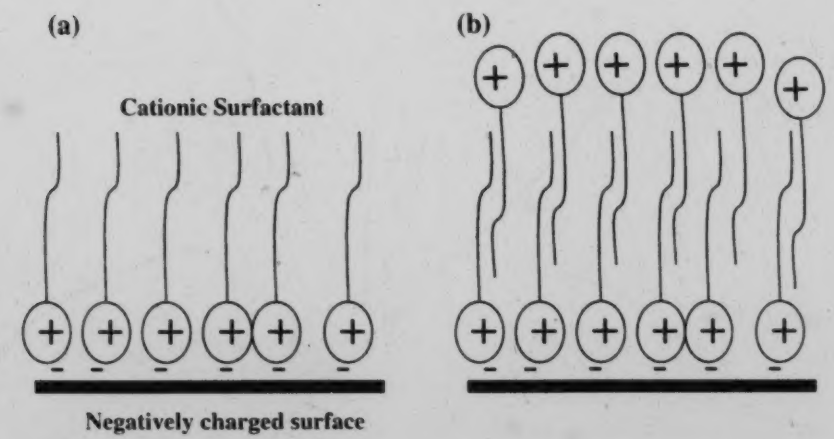

Figure 2.6: Schematic representation of, (a) formation of first adsorbed layer on negatively charged capillary walls and, (b) Adsorption of second layer of cationic surfactant through hydrophobic interaction forming the bilayer i.e "hemimicelles".

increasing surfactant concentration, the surface of the walls becomes saturated, with all the silanol groups being neutralized. This is the point of zero EOF, as shown in Figure 2.6a. Further increase in the surfactant concentration causes the CTAB molecules to orient in such a way that their hydrophobic tails come into contact with the hydrophobic tails of the CTAB molecules on the first layer, forming hydrophobic bonds, as shown in Figure 2.6b. At this point hemimicelles are formed and EOF reversal occurs. The concentration at which this secondary adsorption occurs is always a fraction of the cmc.

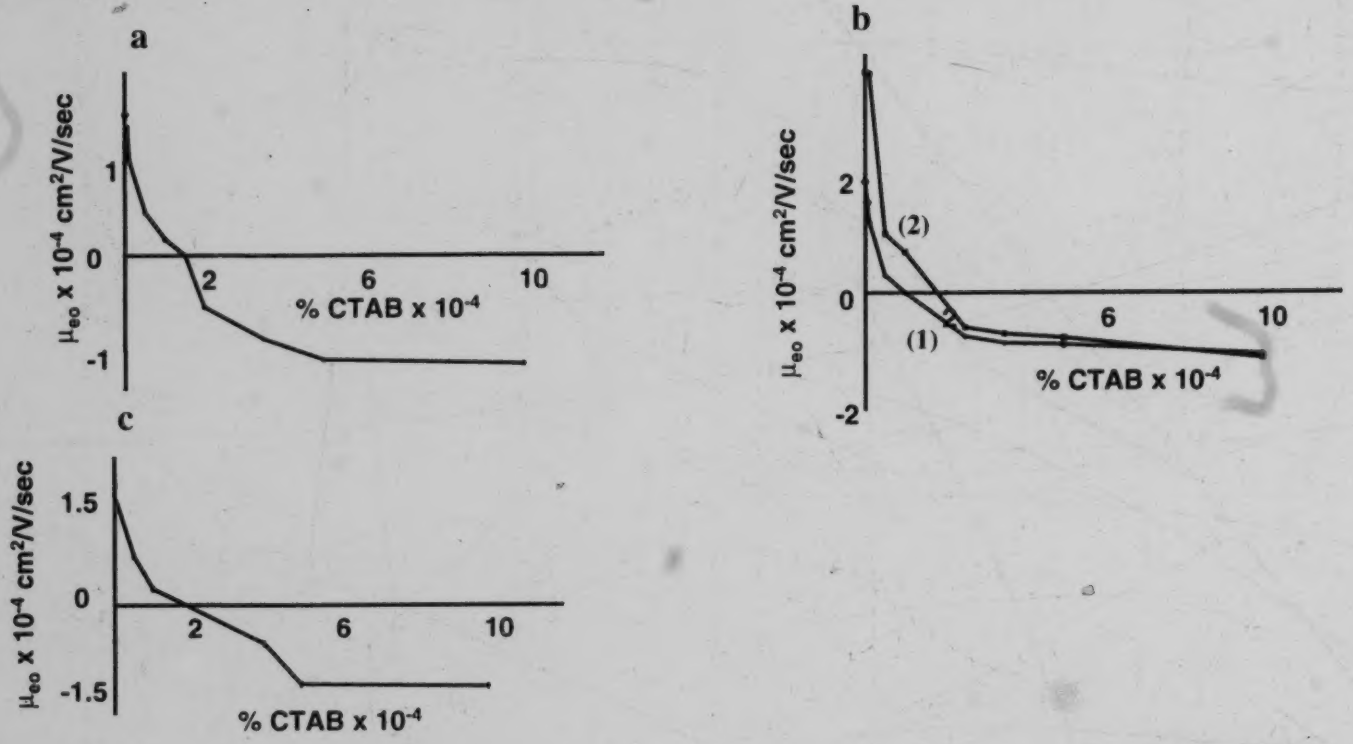

Figure 2.7: Variations in μ_{eo} with increasing CTAB concentration in the running buffer at different pH values. Separation voltage was 20 kV across 27 cm length capillary. [a] pH = 6.3 with 0.01 % Brij 35, [b] pH = 7.36, (1) with 0.01% Brij 35 and (2) without Brij 35 and [c] pH = 8.2, with 0.01% Brij 35.

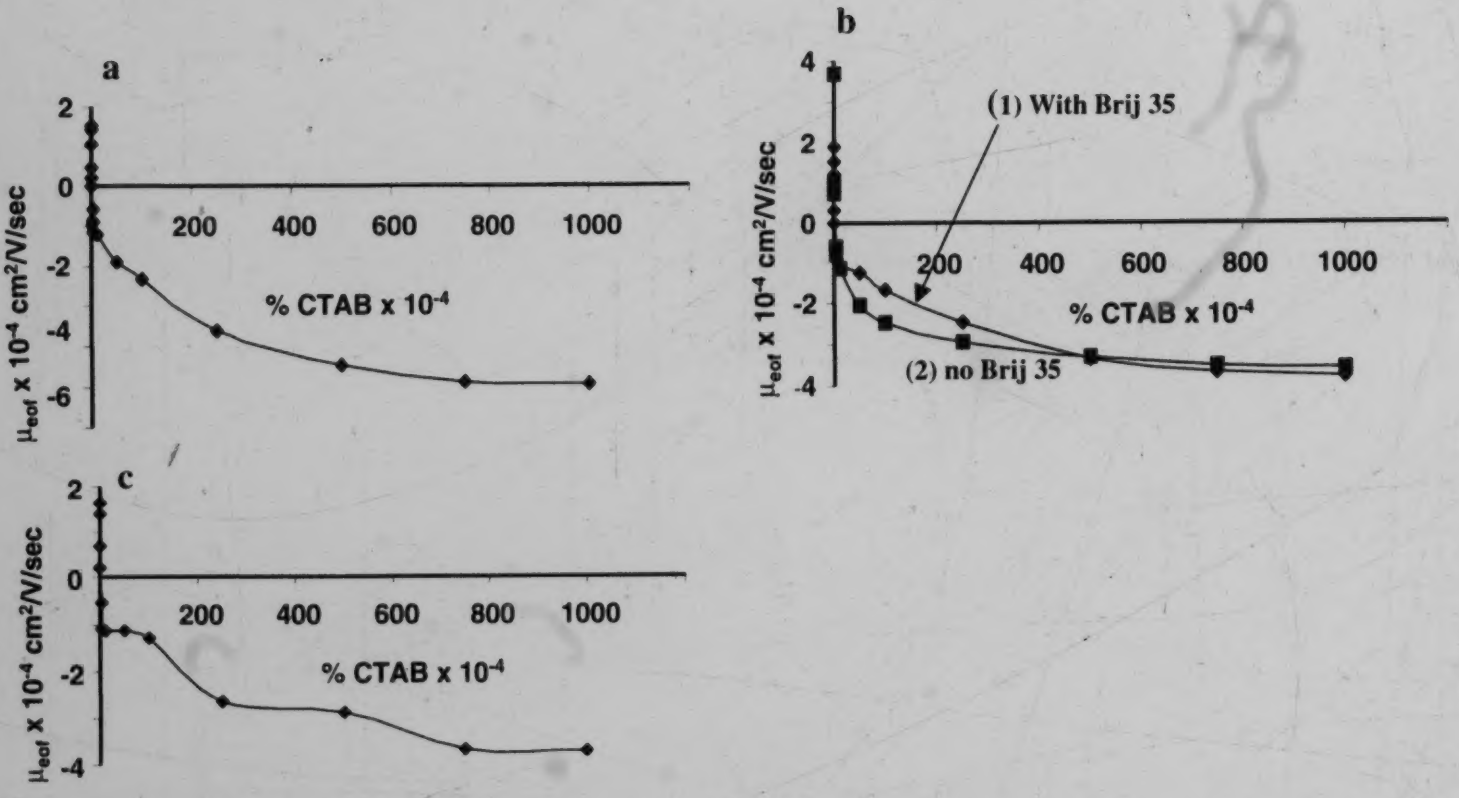

Figure 2.8: Illustrates the full range study of the data in Figure 2.6 for the variations in μ_{eo} with increasing CTAB concentration. Curves a, b and c represent the study done at pH 6.3, 7.36 and 8.2 respectively.

Figures 2.7a,b and c show the behaviour of μ_{eo} with increasing CTAB concentration in the presence of 0.01% Brij 35 in the running buffer at three different pH values. The results show how predictable the flow can be in the pH range 6.3 to 8.2. Figures 2.7a, b and c show a narrow range of CTAB concentration near the point of flow reversal. The mobility decreased with increasing CTAB concentration until the flow was reversed. The flow then increased in the reverse direction until it reached a plateau, as shown in Figures 2.8a, b and c. The plateau was observed because of equilibrium achieved due to saturation of CTAB on the walls of the capillaries. One thing to note is that the point of zero EOF was not exactly known for any of these experiments. The CTAB concentration range in which these points lay was 1×10^{-4} % (2.7 μM) to 2.3 x 10^{-4} %(6.3 μM) of CTAB in the running buffers. No peaks for the neutral marker could be observed over 2 h intervals in normal and reversed flow in this CTAB concentration range. The cmc level for CTAB measured at pH 9 in 50 mM ionic strength phosphate buffer is ~0.1 mM [25], so the reversal occurs well below the cmc. Janini et al

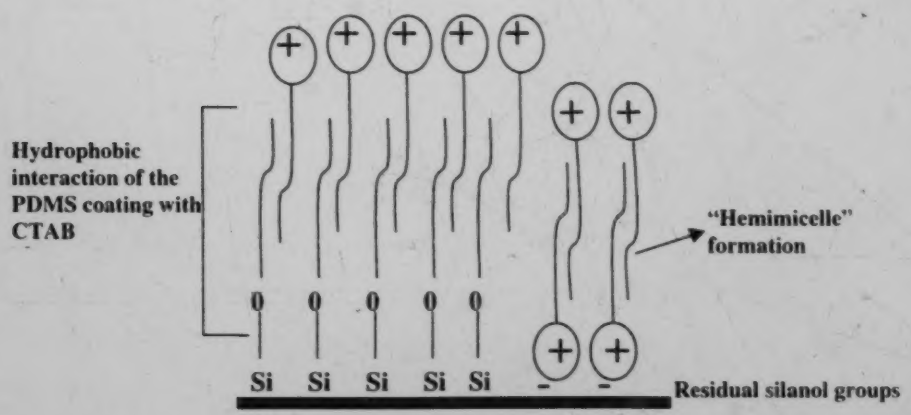
Hydrophobic interaction of the PDMS coating with CTAB
"Hemimicelle" formation
O O O O O
Si Si Si Si Si
Residual silanol groups

Figure 2.9: Schematic representation of the adsorption of CTAB on the hydrophobic PDMS surface and "hemimicelles formation on the residual silanol groups.

[18] reported reversal of flow with CTAB in the μM range in C_8-coated surface, at low pH. Janini's work involved the study of the effect of pH on EOF at constant CTAB concentration. Also, Pfeffer and Yeung [16] reported flow reversal in the μM concentration of CTAB with a fused silica column coated with hydrophobic cross-linked polymer PS-264.

In the present study and similar to Janini's and Yeung's work, the capillary walls were already coated with a PDMS hydrophobic layer. In this case CTAB may adsorb directly onto the PDMS coating, as well as through ion pairing with residual exposed surface silanol groups. The hemimicelle model need not be invoked in order to explain flow reversal, due to direct adsorption on the PDMS. However, hemimicelles may still be formed, as illustrated in Figure 2.9.

Figure 2.7b and Figure 2.8b show the results of experiments done at pH 7.36 in the presence and absence of Brij 35. There is only a slight difference, with the reversal of flow occurring at lower CTAB concentration in the presence of Brij 35. This was presumably because less CTAB was needed to completely neutralize the residual silanol groups in the presence of Brij 35, since adsorption of the Brij 35 may have already masked these groups. The plateau at ($\mu_{eo} = -3.7 \times 10^{-4}$ cm^2/V/sec) was reached at almost the same concentration of CTAB (2.2 mM) for both experiments. At pH 6.3 and 8.3, μ_{eo} reached their respective constant values at -5.0×10^{-4} and -3.7×10^{-4} cm^2/V/sec.

Similar studies done by Lucy et al [25] on bare capillaries showed reversal of EOF with a CTAB concentration equal to or greater than 0.2 mM, while the μ_{eo} plateaued at ~ -0.5 cm^2/V/sec in 10 mM phosphate buffer (adjusted to ionic strength of 50 mM with KCl). The pH range studied was from 3.5 to 9.0.

The results obtained in the present study showed that less CTAB was needed to cause EOF reversal on PDMS coatings than on bare silica surface [25]. The amount of CTAB needed to cause flow reversal is well below the cmc level (~0.1 mM). The reverse μ_{eo} seen in the present study was ~ -3.7×10^{-4} $cm^2/V/sec$, compared to -0.5×10^{-4} $cm^2/V/sec$ on a bare surface at pH 7 [25]. Ding and Fritz [24] also observed reversal of EOF in Tris buffer at pH 3.45 with a CTAB concentration of 0.6 mM, in bare capillaries. Ding and Fritz reported very little control of the change in EOF due to CTAB unless the pH was varied. In contrast, on the PDMS surface the data in Figure 2.8 show that the μ_{eo} can be easily controlled in a range –1 to –5 $cm^2/V/sec$. Control close to the flow reversal point remained difficult to achieve.

2.3.5 Effect of pH on the Study in the Presence of Charged Surfactants

The effect of pH on the EOF study with SDS and CTAB was not very significant. In the case of SDS, the maximum μ_{eo} ~7 to 7.7×10^{-4} $cm^2/V/sec$ (Figure 2.4) for the three different pH values studied in the absence of Brij 35. In the presence of Brij 35 no significant difference was observed for all three pH values.

With the CTAB study little difference was observed near the point of flow reversal at the three pH values, as seen in Figure 2.7. The point of zero EOF lay in almost the same range in the presence of Brij 35. The results obtained in the present study show small differences were observed at high CTAB concentration (> 0.14 mM), as seen in Figure 2.8. Better control of EOF was achieved at pH 6.3 and 7.36. While these changes are small, they contrast with Lucy's results [25] for bare capillaries, in which EOF was largely independent of pH. Janini and co-workers [18] reported the pH at which EOF is maximum varies slightly depending on the concentration of CTAB in C_8-coated

capillaries which is comparable to the data shown in Figure 2.8. In Figure 2.8, the maximum reversed EOF at pH 6.3 was $\mu_{eo} = -5.0 \times 10^{-4}$ cm^2/V/sec, and the plateau for pH 7.36 and 8.2 was $\mu_{eo} = -3.7 \times 10^{-4}$ cm^2/V/sec.

The data shown in Figure 2.4, Figures 2.7 and Figure 2.8 demonstrate that it is possible to control the EOF across distinct ranges of surfactant concentration. In the case of SDS, the EOF can still be varied across a wide range of SDS concentration with Brij 35 in the running buffer. On the other hand, in the case of CTAB, varying EOF near the point of flow reversal (Figure 2.6) requires careful control of the CTAB concentration. With increasing CTAB concentration (>cmc), the EOF can be varied over a wide range before μ_{eo} plateaus. The results show that the PDMS coated capillaries provide a surface on which charged surfactants of either sign readily adsorb. Mixtures of SDS and Brij 35 appear to adsorb together as indicated by the slowly varying values of EOF with SDS concentrations when Brij 35 is present. However, CTAB showed very little Brij 35 dependence. The results suggests the adsorption of CTAB was strong enough to be unaffected by Brij 35. The ease with which the flow can be controlled should aid in the separation of analytes in the cationic forms, neutral and anionic form, when adjustment of EOF is required to optimize a separation.

2.4 Conclusion

The EOF study shows that the addition of surfactants in the running buffer provides an element to fine tune the EOF in PDMS coated capillaries without having to adjust the pH. If the electrophorectic mobility of a certain analyte is known, the amount of surfactant needed can always be determined and added to the running buffer so that μ_{ep} and μ_{eof} could be made nearly equal and opposite, to improve the separation efficiency.

The combination of PDMS and a dynamic coating not only prevents analyte-wall interactions, it can also be used as a pump to induce flow in whichever direction is required.

2.5 Reference

1. Jorgenson, J. W., Lukacs, K. D., *Science*, 222, 266-272, 1983.
2. Harrison, D. J.; Fluri, K.; Seiler, K.; Fan, Z.; Effenhauser, C. S.; Manz, A., *Science*, 261, 895-897, 1993.
3. Robey, F. A., 7th International Symposium on HPLC of proteins, Peptides, and Polynucleotides, Nov 2-4, Washington, DC, paper 701, 1987.
4. Mortensen, H. B., Cristophersen, C., *Biochim. Biophys. Acta.*, 707, 154-163, 1982.
5. SiragElden, E., Gercken, G., Voight, K. D., *J. Clin. Chem. Clin. Biochem.*, 24, 283-292,1986.
6. Hjerten S., *J.Chromatogr.*, 347, 191-198, 1985.
7. Hjerten, S., Kubo, K., *Electrophoresis.*, 14, 390-395, 1993.
8. Schomburg, G., Belder, D., Giles, M., Motsh, S., *J. Capillary Electrophoresis*, 3, 219, 1994.
9. Bruin, G. J. M., Chang, J. P., Kulman, R. H., Zegers, K., Kraak, J. C., Poppe, H., *J. Chromatogr.*, 471, 429-436, 1989.
10. Swedberg S., *Anal. Biochem.*, 149, 642-650, 1990.
11. Srinivasan, K, Pohl, C., Avdalovic, N., *Anal. Chem.*, 69, 2798-2805, 1997.
12. Cobb, K. A., Dolnik, V. , Novotny, M., *Anal. Chem.*, 62, 2478-2483, 1990.
13. Giles, M., Kleemiss, G., Shomburg, G., *Anal. Chem.*, 65, 2038-2046, 1994.
14. Strege, M. A., Lagu, A. L., *J. Chromatogr.*, 630, 337-344, 1993.

15. Gelfi, C., Curcio, M., Righetti, P. G., Sebastiano, R., Citterio, A., Ahmadzadeh, H., Dovichi, N. J., *Electrophoresis*, 19, 1677-1682, 1998.

16. Pfeffer, W. D., Yeung, E. S., *Anal. Chem.* 62, 2178-2183, 1990.

17. Chiari, M., Dell'Orto, N., Gelain, A., *Anal. Chem.*, 68, 2731-2736, 1996.

18. Janini, G. M., Chan, K. C., Barnes, J. A., Muschik, G. M., Issaq, H. J., *J. Chromatogr.*, A, 653, 321-327, 1993.

19. Liu, Y., Kuhr, W. G., *Anal. Chem.*, 71, 1668-1673, 1999.

20. McCormick, R., *Anal. Chem.*, 60, 2322-2328, 1988.

21. Towns, J. K., Regnier, F. E., *Anal. Chem.*, 63, 1126-1132, 1991.

22. Zhao, Z., Malik, A., Lee, M. L., *Anal. Chem.*, 65, 2747-2752, 1993.

23. Cifuentes, A., Rodriguez, M. A., Garcia-Montelengo, F. J., *J. Chromatogr.*, A, 742, 257-266, 1996.

24. Ding, W., Fritz, J., *J. High Resolut. Chromatogr.*, 20, 575-580, 1997.

25. Lucy, C. A., Underhill, R. S., *Anal. Chem.*, 68, 300-305, 1996.

26. Melanson J. E., Baryla, N. E., Lucy, C. A., *Anal. Chem.*, 72, 4110-4114, 2000.

27. Baryla, N. E, Lucy, C. A., *Anal. Chem.*, 72, 2280-2284, 2000.

28. Yeung, K. C., Lucy, C. A., *Anal. Chem.*, 69, 3435-3441, 1997.

29. Heinig, K., Vogt, C., Werner, G., *Anal. Chem.*, 70, 1885-1892, 1998.

30. Lauer, H. H., McManigill, D., *Anal. Chem.*, 58, 166-170, 1986.

31. Rundlett, K. L., Armstrong, D. W., *Anal. Chem.*, 68, 3493-3497, 1996.

32. Green, J. S., Jorgenson, J. W., *J. Chromatogr.*, 478, 63-70, 1989.

33. Hult, H. L., Roeraade, E. J., *J. Chromatogr A.*, 757, 255-262, 1997.

34. Guttman A., Cohen , A.S., Heiger, D. M., Karger, B. L., *Anal. Chem.*, 62, 137-141, 1990.

35. Luckey J.A., Drossman, H., Kostichka, A. J., Mead, D. A., D'Cunha, J. Norris, J. B., Smith, L. M., *Nucleic Acids Res.*, 18, 4417-4421, 1990.

36. Huang, X. C., Quesada, M.A., Mathies, R.A., *Anal Chem.*, 64, 2149-2154, 1992.

37. Chen, D. Y., Harke, H. R., Dovichi, N. J., *Nucleic Acids Res.*, 20, 4873-4880, 1992.

38. Lu, H., Arriaga, E., Chen, D. Y., and Dovichi, N. J., *J. Chromatogr.*, 680, 497-501, 1994.

39. Swerdlow, H., Dew-Jager, K. E., Brady, K., Gestland, R., Grey, R., Dovichi, N. J., *Electrophoresis*, 13, 475-483, 1992.

40. Swerdlow, H., Zhang, J. Z., Chen, D., Harke, H. R., Grey, R., Wu, S., Fuller, C., Dovichi, N. J., *Anal. Chem.*, 63, 2835-2841, 1991.

41. J. Yan, N. Best, J Zhong Zhang, H. Ren. R. Jiang, J. Hou, N.J. Dovichi. *Electrophoresis*, 17, 1037-1045, 1996.

42. Figeys, D., Dovichi, N. J., *J. Chromatogr.*, 645, 311-317, 1993.

43. Yeung, E. S., Fung, E. N., *Anal. Chem.*, 67, 1913-1919, 1995.

44. Gao, Q., Yeung, E. S., *Anal. Chem.*, 70, 1382-1388, 1998.

45. Preisler, J., Yeung, E. S., *Anal. Chem.*, 68, 2885-2889, 1996.

46. Gao, Q., Yeung E. S., *Anal. Chem.*, 72, 2499-2506, 2000.

47. Han, F., Huynh, B. H., Ma Y. Lin, B., *Anal. Chem.*, 71, 2385-2389, 1999.

48. Schure, M.R, Murphy, R. E., Klotz, Willie Lau, W., *Anal. Chem.*, 70, 4985-4995, 1998.

49. Hjerten, S., Liao, J., Yao K., *J. Chromatogr.*, 403, 47-61, 1987.

50. Kenndler, E., *Chromatographta.*, 30, 713-718, 1990.

51. Lee, C. S., Blanchard, C. W., Wu, C., *Anal Chem.*, 62, 1550-1552, 1990.

52. Hayes, M. A., Kheterpal, I., Ewing, A. G., *Anal. Chem.*, 65, 27-31, 1993.

53. Walbroehl, Y., Jorgenson, J. W., *J. Microcolumn Sep*, 1, 41-45, 1989.

54. Borgerning, M. F., Hinze, W. L., *Anal. Chem.*, 57, 2183-2190, 1985.

55. Desilets, C. R, Rounds, M. A., Regnier, F. E. *J. Chromatgr.*, 544, 25-39,1991.

56. Mazzeo J. R, Krull I.S, " Handbook of Capillary Electrophoresis", Landers, J. P., Ed.; CRC Press: Boca Raton, FL, Chapter 18, 1994.

57. Harris, D. C., "Quantitative Chemical Analysis" 5th Edt, pp 678, *Freeman Press*, 1998.

58. Boyd, W. C., *J. Biol. Chem.*; 210, 4097-4105, 1965.

59. (i) Lever, M., *Anal. Biochem.*, 83, 274-282, 1997.

(ii) Ashani, Y., Catravas, G. N., *Anal. Biochem.*, 109, 55-62, 1980.

60. Hiemertz, P. C., Principles of Colloid and Surface Chemistry 2nd Edition; Marcel Decker, New York, chapter 8, 1986.

61. Tanford, C., "The Hydrophilic Effect: Formation of Micelles and Biological membranes", Wiley, New York, 1980.

62. Reijenga, J. C., Verheggen, T. P. E. M., Everaerts, F. M., *J. Chromatogr.* 260, 241-251, 1983.

63. Jones, W. R., Jandik, P., *J. Chromatogr.* 546, 445-458, 1991.

64. Jones, W. R., Jandik, P., *J. Chromatogr.* 608, 385-393, 1992.

65. Gaudin, A., Fuerstenau, D. W., *Trans. Am. Inst. Min., Metall. Pet. Eng.* 202, 958, 1955.

CHAPTER 3: Methicilin Resistant *Staphylococcus aureus* DNA Assay using Cycling Probe Technology with Capillary Zone Electrophoresis on a Chip

3.1 Introduction

Electrokinetic effects provide a convenient method to control the delivery of sample and reagents through electroosmosis [1], while also providing separation via electrophoresis. Consequently, electrokinetically actuated microfluidic devices [2] are potentially well suited to DNA assays. For this study we used the mixing, reaction and separation steps, shown by Chiem et al [3] for immunoassays in microfabricated glass chips, for DNA assays. However, the present study introduced several more steps as compared to the immunoassay case. Firstly, the channels in the chips were coated to reduce adsorption and secondly, the DNA amplification reaction which, is known as cycling probe technology (CPT), must be done at an elevated temperature of about 60 ^{o}C.

CPT represents a unique method for the detection of specific target sequences [4,5]. The two main reagents of the CPT reaction are a chimeric DNA-RNA-DNA probe which in this study was 29 bases long, and the endonuclease enzyme RNase-H. The probe provides an RNase-H sensitive cleavage region when it binds to a complementary target DNA sequence, as suggested in Figure 3.1 [2]. CPT reactions are performed at constant temperature (60 ^{o}C), which allows hybridization of the chimeric probe to the complementary single stranded target DNA. The resulting probe-DNA duplex is recognized by the RNase-H, which cleaves the RNA at one of the phosphodiester bonds. Enzymatic binding to the RNA portion is enhanced by the co-factor Mg^{2+} [6-8]. At the

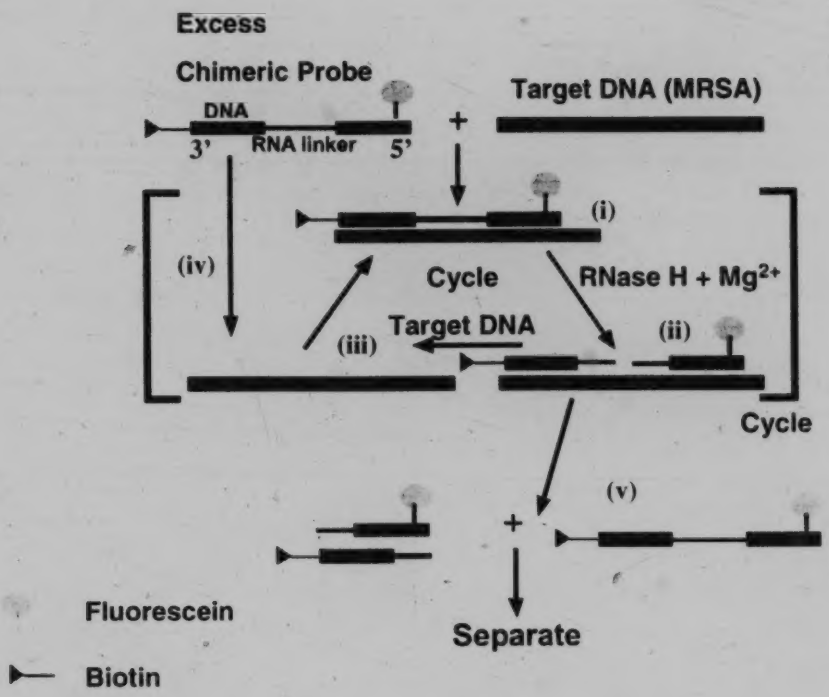

Figure 3.1: Illustrating the reaction scheme of cycling probe technology. (i) Hybridization of probe to target DNA, (ii) enzyme action, (iii) dissociation of fragmented probes, (iv) target mediate the cleavage of another probe, (v) 30 min incubation time and separation using CE.

temperature used, the fragmented probe/target complex dissociates, allowing the target to mediate the cleavage of another probe following hybridization. After incubating this reaction cycle for a period of time, the accumulated fragmented probes are then separated from the excess intact probe and detected. When capillary electrophoresis (CE) is used for separation, detection is usually done with laser induced fluorescence (LIF). The accumulation of probe fragments allows the amount of target DNA to be amplified and quantified. The measured variation of the cleaved probe to intact probe gives the amount of target present.

CPT has several advantages. Apart from being isothermal and rapid, it is a signal amplification technique compared to PCR which is a mass amplification. The signal amplification in CPT is linear when the amount of target is small compared to the amount of probe. Quantitation can be easier with linear amplification, compared to the exponential amplification observed with PCR. Also, work on PCR on a chip encountered surface chemistry problems associated with surface denaturing of the enzymes and/or adsorption of the DNA, particularly at the highest temperatures used in PCR. The surfaces also nucleate air bubble formation, which is a significant problem when temperatures are varied between 60 and 95 °C. CPT, is an isothermal process. This means there are reduced surface chemistry and gas bubble formation problems, because the maximum temperature used is ~60 °C, and the temperature is not frequently changed. To overcome such problems, most work involving PCR on-chip [9-14] was done in two microfabricated devices of which one was a microreactor for PCR and the second was for CE separation and detection. These elements were then mated together, rather than being integrated monolithically.

All the advantages associated with CPT make it suitable for automation and integration on a single chip. The principle underlying the CPT reaction has been demonstrated in a system containing synthetic DNA and a chimeric probe [4-5, 15-17]. CPT has also been used with genomic DNA to discriminate between strains of mycobacteria [15]. Diagnostic tests for tuberculosis are based on either detection of *Mycobacterium tuberculosis* in a clinical sample or recognition of the host response *to M. tuberculosis*. Acid-fast microscopy of sputum, followed by culture confirmation, remains the cornerstone of the diagnosis of tuberculosis. These traditional bacteriological methods are slow and expensive [18]. PCR assays have been developed for the laboratory diagnosis of disease such as tuberculosis [19], but how easily the technology can be integrated onto microfabricated devices for rapid analysis at low cost remains to be determined.

In this study we demonstrate a gel-free DNA separation system on a device we named GOCPTTT, incorporating a series of mixing, DNA amplification reaction, separation and LIF detection steps. The device consists of four inlet ports for CPT reagents introduction and a reaction chamber in the form of a serpentine, where the reagents are mobilized and reacted at an elevated temperature of 60°C. The final process involved mobilization to a double T injector followed by gel-free separation of the CPT reaction products and LIF detection. This GOCPTTT device was designed by G. Ocvirk and T. Tang in this research group.

DNA molecules known to have constant charge to friction ratio cannot be separated in free solution or capillary zone electrophoresis (CZE) mode [1]. In earlier work done by T. Tang, CPT products were separated in a gel matrix on chip. The poor

reproducibility of migration times in the gel rendered identification and quantitation a difficult task. Also, introducing gel inside the channels of a microfluidic device was very time consuming and hard to do. The first part of the study involved optimizing the CPT assay for gel-free separation. Gel-free separations were optimized by performing off-chip CPT reactions and on-chip separation using a device called 'COPI'. We show that introducing a biotin label on the 3' end of the probe (Figure 3.1), helps in the separation by providing a moiety of the DNA mer with a perturbed charge to friction ratio [20]. In CZE [1], separation is based on the difference in charge to friction ratio. Because the fluorescein labeled end of the cleaved probe had no biotin label while the intact probe had a 3' end labeled with biotin, separation was achieved in a gel-free medium. The cleaved probe emerges first followed by the intact probe during CZE. With increased reproducibility in migration time and peak area ratios for the cleaved and intact probe, calibration was possible when reacting probe and target off-chip and separating the products on chip in the CZE mode.

The second part of the study dealt with the integration of all steps in the CPT analysis of DNA samples: mixing, CPT reaction, separation and detection. We show the gel-free system developed in the first part of the study was readily transferable to the GOCPTTT-chip, giving a completely integrated system. This integrated system was thus a micro-Total Analysis System, (μ-TAS). The μ-TAS not only performs all the steps mentioned, but with different target concentrations a calibration curve can be constructed to provide quantitation. Such a system allows for 5 min reagent mobilization, 30 min reaction and ~2 min separation. A total analysis time of less than 40 min was possible for

an individual sample. Conventional methods [18], based on growth culture and biochemical tests to identify organisms, would require several hours.

3.2 Experimental

3.2.1 CPT Components and Conditions

All CPT components and DNA fragments used were obtained from ID Biomedical Corp., Vancouver, BC (Canada). Target DNA used in this study was from methicilin resistant *Staphylococcus aureus* (MRSA) sequence. The 29 base-long chimeric probe was engineered and synthesized to complement MRSA. The stock concentration was 5 μM. The two probes used were tagged with either three or, later, one biotin label at the 3' end, and a fluorescein label on the 5' end. The enzyme RNase H was from *thermus thermophilus*, stock concentration of 1 μg/μl.

All materials used (PCR tubes, pipette tips) when performing CPT were from Rose Scientific (Edmonton, AB, CANADA) and were certified RNase and DNase free. Other chemical reagents used were all Molecular Biology grade from Sigma Chemicals, including phosphate buffer (K_2HPO_4 and KH_2PO_4), $MgCl_2$, urea, Triton-X-100, spermine hydrochloride, dodecyl(trimethyl ammonium bromide)(DTAB), acrylamide, potassium persulfate, γ-[(methacryloyoxy)propyl]trimethoxysilane and N,N,N,N'-tetramethylethylenediamine (TEMED).

3.2.2 Device Design and Fabrication

Photomasks for the devices were designed on L-Edit software (Tanner Research, Pasadena, CA, USA) by T. Tang and G. Ocvirk and the 5" x 5" photomasks were fabricated by Adtek (Photomask, Montreal, Quebec, Canada).

Devices were fabricated in 3"x 3", 2.32 mm thick Schott Borofloat glass and 4" x 4" 540 µm thick 0211 glass (Corning, NY) at the Alberta Microelectronic Corporation (Edmonton, Canada) and at the University of Alberta. The microfluidic devices were made by thermally bonding the etched substrate to the cover plates, in which 1.9 mm access holes were previously drilled.

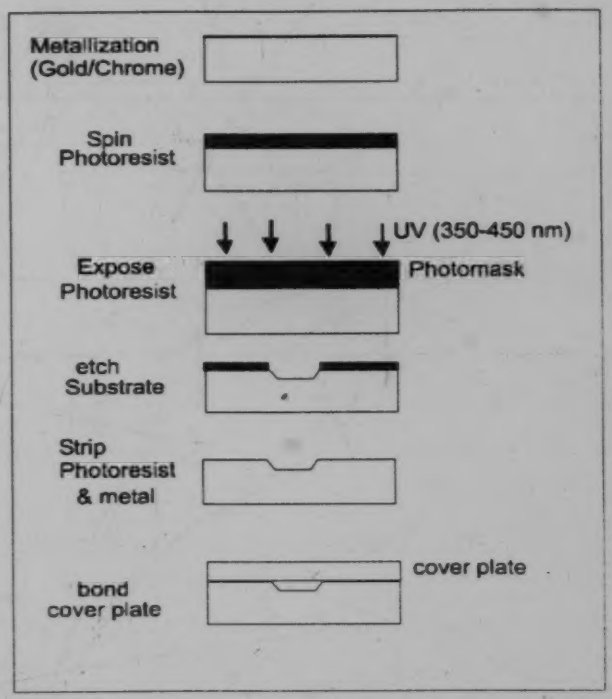

Figure 3.2: Scheme showing the different steps in making microfabricated glass chips. (a) Metallization. (b) Photoresist deposition. (c) Photolithography and development. (d) Metal etch and substrate etch. (e) Strip photoresist. (f) Bond cover plate to make the microfluidic device.

3.2.3 Method of Fabricating the Drilled Cover Plates

To drill the holes in the cover plates, a glass slide was heated on a hot plate up to 150 °C and a thin layer of Crystalbond (CrystalBondTM 509, Aremco, Ossining, NY, USA) was spread onto the top of the slide. The cover plate was then bonded by laterally sliding the latter on the glass slide. The Crystalbond was then spread on the cover plate and yet another cover plate slide was placed on top of it. About four cover plates could be stacked on each other before finally sealing the whole thing with another glass slide on top. The cover plates were sandwiched between two glass slides acting as sacrificial plates. A metal template on which the holes were drilled was then scotch taped on top. Holes were then drilled in the sandwiched plates using a

Lunzer drill with a diamond core drill bit (0.076" OD x ¼" DL, Lunzer, Saddle Brook, NJ, USA). After drilling, the cover plates were taken apart by heating on the hot plate and then were cleaned with acetone. All the cover plates were then further cleaned with acetone in an ultrasonic bath for 30 min.

3.2.4 Method of Fabricating the Etched Plates

The lithographic patterning of the etched plates has been described before [21-23]. The first step involved the cleaning of glass substrates by dipping them in a cold piranha bath (H_2SO_4/H_2O_2=3/1) for 10 min. Au/Cr was sputtered onto the glass substrates as shown in Figure 3.2. A solution of photoresist (Waycoat HPR 504, Olin Hunt) was then spin coated onto the substrates (**1.** 5 sec at 500 rpm, **2.** 5 sec at 50 rpm and, **3.** 60 sec at 3000 rpm) using a photoresist coater (Solitec Wafer Processing, San Jose, CA, USA), followed by soft baking at 110 °C for 30 min. The substrates were transferred one by one to a contact mask aligner (ABM, San Jose, CA, USA) which was used to align the substrate with the photomask for UV exposure. The exposed photoresist was removed with Microdeposit 354 developer (Shipley, Newton, MA, USA). Developed substrates were hard baked for 30 min at 110°C. The gold and chrome layers were etched respectively with an aqueous potassium iodide/iodine solution and a commercial Cr etch (KTI chemicals, Sunnyside, CA). Glass substrates were then etched using a mixture of concentrated HF:HNO_3:H_2O (20:14:66). The etching rate was 2 µm/min. The final depths were measured with an alpha-step profilometer (Alphastep 200, Tencor Instrument, KLA-Tenor Corp., San Jose, CA). The photoresist was removed with acetone and further cleaned with acetone in an ultrasonic bath for 30 min.

3.2.5 Cold Bonding the Substrate with the Cover Plate to Make the Microfluidic Device

The drilled cover plates and etched substrates were placed in warm piranha (1:3, H_2O_2:H_2SO_4) solution for 30 min for removal of any organic residues. After thorough aqueous washing, the plates were then cleaned extensively by mounting them in a 4" x 4" wafer frame with a Medium tack blue plastic film (1807465, Semiconductor Equipment Corporation, Moor Park, CA, USA), scrubbed with a sponge soaked in dilute detergent and pressure washed using a pressure cleaning station (Model 2066, MicroAutomation, Fremont, CA, USA). The cleaning process was repeated at least three times, scrubbing for at least 3 min each time. The last pressure washing was followed by a drying step in the pressure washer.

After cleaning the cover and etch plate, the two were bonded together freehand while holding the frames in the light, to make sure the holes were properly aligned with the channels. After the two plates made contact, they were pressed together to bond them.

3.2.6 Thermal Bonding of the Substrates

The final step involved thermal bonding in a programmable oven (Model 6-525, J.M. Ney Co., Yucaipa, CA, USA). The program used for the 3" x 3" borofloat devices was: (**1.** 10 °C/min, 550 °C, 0.5 h; **2.** 10 °C/min, 610 °C, 0.5h; **3.** 10 °C/min, 635 °C, 0.5 h; **4.** 5°C/min, 643 °C, 6 h; **5.** Natural cooling to room temperature. The program for the 0211 devices was: (**1.** 10 °C/min, 440 °C, 0.5 h; **2.** 2°C/min, 473°C, 0.5 h; **3.** 2 °C, 595 °C, 6 h; **4.** 4.0 °C/min, 473 °C, 0.5 h; **5.** Natural cooling to room temperature.

3.2.7 Device Layouts

Two types of devices were used in the CPT study. The first one was the 'COPI' device shown in Figure 3.3a, consisting of a double T injector and a separation channel, etched 15 µm deep. The second was the 'GOCPTTT' device, which included four inlet ports to drive reagents to a reaction coil which could contain 160 nl volume, with a double T injector and separation channel etched 15 µm deep, as shown in Figure 3.3b.

3-2-8 Channel Derivatization

Channel walls were coated with polyacrylamide with minor modification to the Hjerten procedure [24]. First the channel walls were conditioned with 0.1 M NaOH for 30 min. After washing with water for 1 h the channel walls were dried by flushing nitrogen through for 30 min. Then the walls were silanized with a 0.4% (v/v) solution of γ-(methacryloxy)propyl]trimethoxysilane (Sigma) in acetic acid buffer at pH 3.5 for 5 h. The channels were rinsed afterwards with water (30 min) and dried by flushing with nitrogen for 30 min. The channels were filled with a degassed 4% (w/v) acrylamide solution containing 0.01% (w/v) potassium persulfate and 0.01% (v/v) N,N,N,N'-tetramethylethylenediamine (TEMED). The solution was allowed to polymerize for 30 min and washed out by flushing with water (30 min), then allowed to dry by flushing with nitrogen for 1 h.

3.2.9 Instrumentation Set-up and Optimization to Perform CE on a Chip

The device shown in Figure 3.4 was run by in-house built computer controlled power supply. The supply consisted of five different power supplies of which 2 are 10 kV and the rest ± 3 kV, with associated high voltage relays. The chip was clamped on the station on a chip holder as shown in Figure 3.4. The chip holder was mounted on X-Y

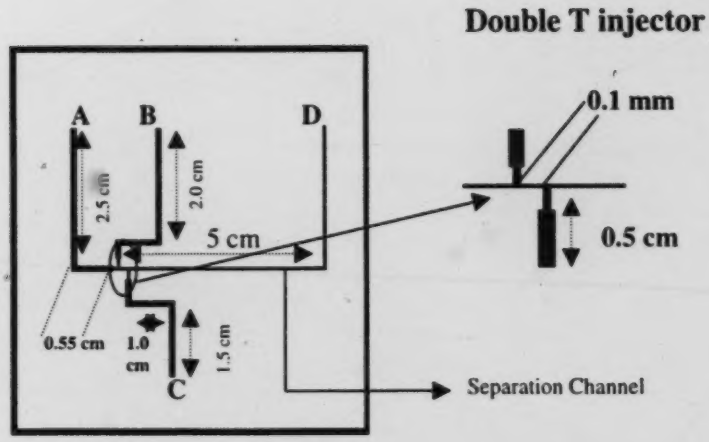

Figure 3.3 :(a) Illustration of the 'COPI' device layout also called AMC 27, patterned on borofloat glass. The channels were etched to a depth of 15 µm. The separation and the wide introduction channel are 40 and 220 µm at the top surface of the etch, respectively. Letters indicate reservoir labels. The length of the double T injector was 0.1 mm.

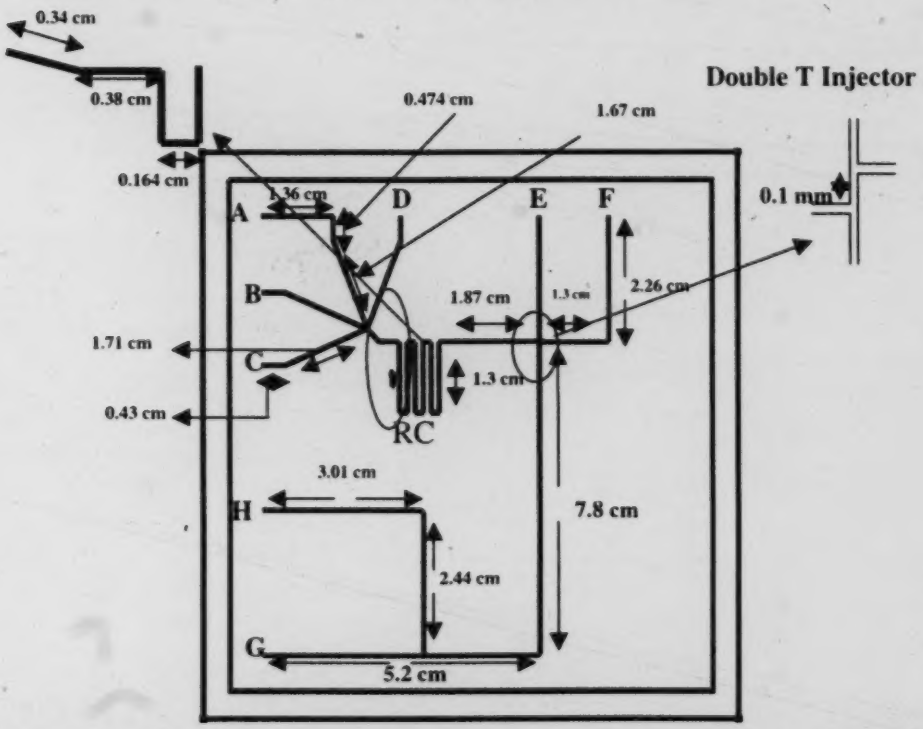

Figure 3.3: (b) Illustration of the GOCPTTT layout patterned, on 0211 glass and etched 15 µm deep. The device consists of 4 inlet reservoirs labeled A to D, which deliver reagents in the reaction coil(RC) through 40 µm wide channels. The reaction coil consists of 130 µm wide channels and can contain 160 nl volume.The arm linking the reaction coil to the double T injector is 80 µm wide. The double T injector and the separation channel are 40 µm wide.The Sample Waste channel after the double T injector to reservoir F is an 80 µm wide channel. The letters mark the reservoirs.

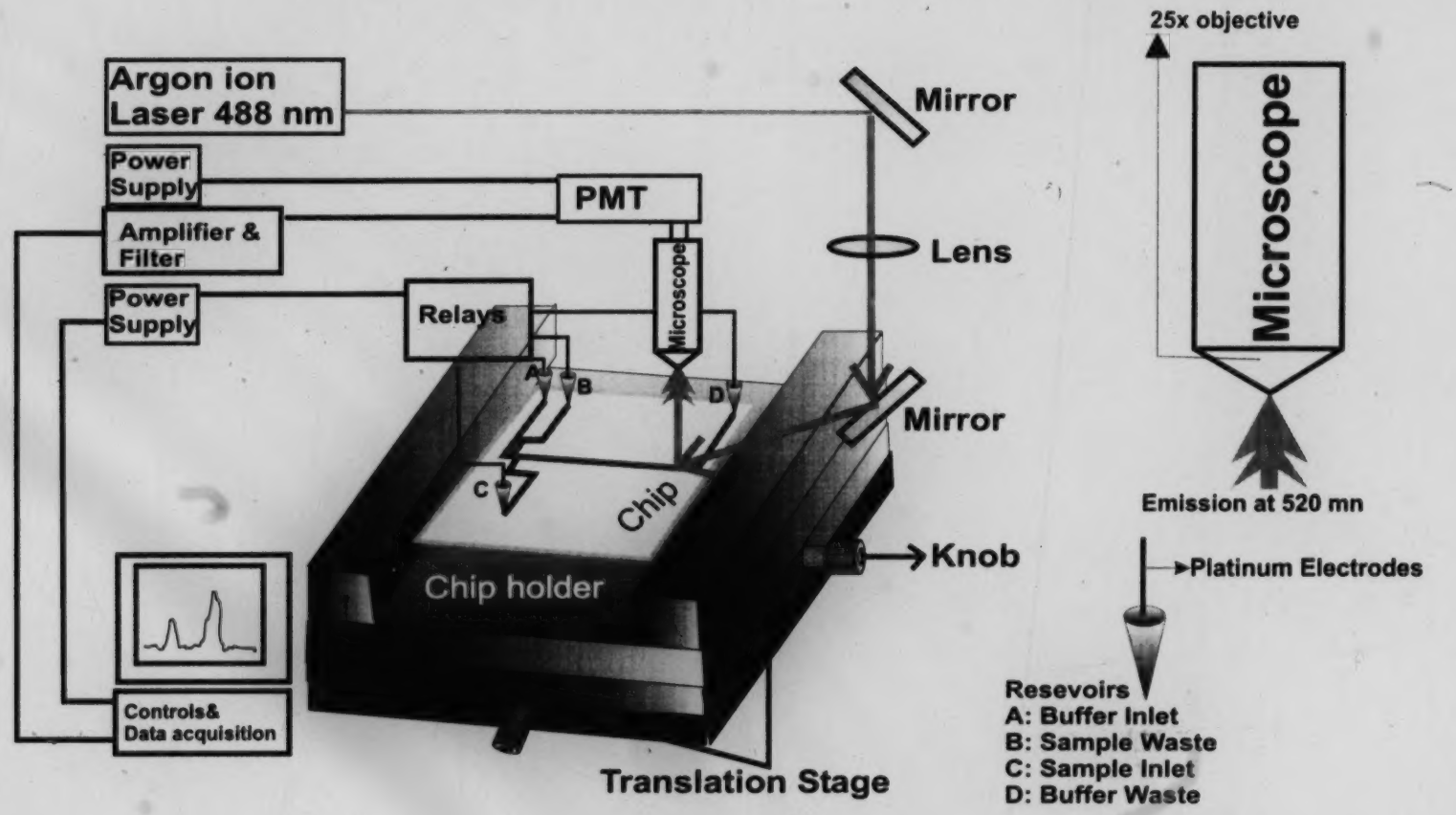

Figure 3.4: Instrumental Set-up for running the 3 inch square 'COPI' device . The 488 nm laser beam is directed to the detection point in the device. The 520 nm emission beam is then collected by the 25x objective, through a 600 μm pinhole to a bandpass filter and Notch filter to the PMT. The signal is filtered and amplified, before being sent to a computer. The data acquisition, voltage and relay switching are done using the Labview sofware. Reservoirs A, B, C and D are Buffer Inlet, Sample Waste, Sample Inlet and

translation stages. The microscope was mounted on a Z translation stage to focus at the point of detection on the chip with a 25x objective (New Focus Inc. Santa Clara, CA). The laser beam was then directed at the point of detection in the separation channel. All this alignment was done with an eyepiece on top of the microscope, with a long pass yellow filter used to avoid direct contact of the reflected light with the eyes.

3.2.10 Signal Optimization

For detection, a 600 µm pinhole with a photomultiplier tube (PMT, Hamamatsu R1477, Tokyo, Japan, (Bias, 700-850 V)) was mounted onto the microscope as shown in Figure 3.4. The emission beam went through two interference filters, a 514.5 nm bandpass filter (9 nm bandpass, Melles Griot) and a Notch filter (Beckman Instruments, Fullerton, CA) for rejection of 488 nm light. The whole 'COPI' device was first filled with buffer and allowed to equilibrate. To ensure proper operation of the device a voltage of 3.5 kV was applied on the Buffer Inlet reservoir (A) and the Buffer Waste reservoir (D). The current was monitored, and when a constant current was maintained the chip was ready for experiments. A solution of 10 nM fluorescein was injected in the device via the Sample Inlet (C) and directed towards the Buffer Waste (D) reservoir, as shown in Figure 3.4. The Sample Inlet (C) was at -2.5 kV and D was at ground. After obtaining the saturation curve with fluorescein, the signal was further optimized to obtain maximum output.

Once the detector and chip were optimized, the chip was cleaned with buffer and readied for sample. The sample obtained after performing the CPT reaction in a thermal cycler was loaded in the sample reservoir. Loading the reservoirs can put the device out of optical alignment. The chip alignment was thus re-optimized as described above. After

optimization, voltage was switched on reservoir A and D to flush buffer through the channel, thereby lowering the baseline to its original level. The chip was then ready for sample injection through the double T injector, followed by separation (Table 3.1). All the voltage and relay control was via a PC computer (Pentium 200) and the data acquisition was controlled with Labview software. The data analysis was done using Igor Pro (Wavemetrics, OR, USA). The PMT signal was amplified and filtered with a 25 Hz cut-off filter (Krohn-Hite 3442), before being captured by the computer's A/D converter. Electropherograms were recorded at a sampling rate of 50 Hz.

Table 3.1: Voltage and Relay Switching Matrix for Fluidic Control on the 'COPI' Device.

Reservoirs	A	B	C	D	Time (sec)
Injection	-	GND	-2.5 kV	-	5
Separation	-3.5 kV	-	-	GND	180

The cycling and separation buffers were optimized for doing gel-free separation of DNA fragments on chip. The first conditions used are shown in Table 3.2 below.

Table 3.2: Different buffer conditions used in the cycling, quenching and separation process in CPT.

Cycling Buffer	**Quenching Buffer**	**Separation Buffer**
10 mM phosphate buffer (pH 6.8)	10 mM phosphate buffer	10 mM phosphate buffer
0.05% Triton-X 100	0.05% Triton-X 100	0.05% Triton-X 100
4 mM $MgCl_2$	4 mM $MgCl_2$	4 mM $MgCl_2$
	7 M urea	3.5 M urea
	50 mM EDTA	25 mM EDTA

Urea and EDTA were both added as quenching reagents. Urea was added to prevent hybridization of probe and target, and EDTA was added as a chelating agent to complex the Mg^{2+}, hence preventing further enzyme activity. After a set of experiments designed to improve the peak shape, 0.2 mM spermine tetrahydrochloride (Sigma) was added to all, cycling, quenching and separation buffers. For cycling off-chip, different vials (PCR tubes) were used with different target concentrations. The amount of probe and enzyme in all vials remained constant at 20 nM and 0.04 µg/µl, respectively. To provide a control, one vial contained no target (called the C2 control). The buffer in which the CPT reagents were mixed is shown in Table 3.2 as the cycling buffer.

All the vials were placed in a thermal cycler (Techne, Mandel Scientific) where the CPT reactions were performed at a constant temperature of 60 °C for 30 min. The reaction was quenched using a quenching buffer as shown in Table 3.2, where the quenching buffer volume and reaction volume was in a 1:1 ratio. The final probe and enzyme concentrations were 10 nM and 0.02 µg/µl. The separation and quantitation on chip was done in the 'COPI' device, shown in Figure 3.3a and Figure 3.4. 5 sec injections were performed at -2.5 kV. Separation was done at 3.5 kV (350 V/cm) whereby the sample is detected about 5 cm from the injector. The C2 control was the first sample run, followed by the lowest target concentration sample and so on to minimize carryover effects.

3.2.11 Instrumentation Setup and Optimization for On-chip Cycling and Separation

The device shown in Figure 3.3b and Figure 3.5 was run by a previously described, [21-23] in-house built, computer controlled power supply system (-15 kV, MJ

series, Glass high voltage, Whitehouse Station, NJ) with high voltage relays (30 kV, Kilovac, Santa Barbara, CA). The optical set-up used in Figure 3.5 was the epifluorescence confocal design which has been described by Ocvirk et al [25]. The chip was mounted onto an X-Y-Z translation stage (Newport 423, Irvine, CA).

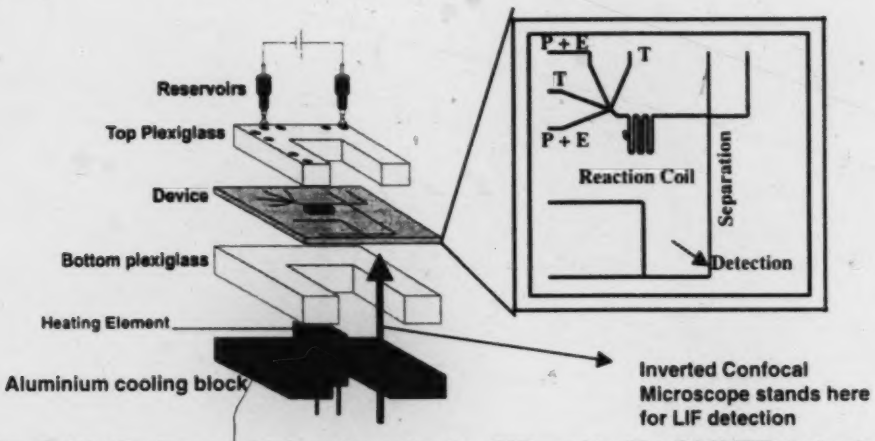

Figure 3.5: The instrumental setup for performing CPT on-chip. The GOCPTTT device is sandwiched between two plexiglass plates. The reaction coil sits on a Peltier operated in reverse mode for heating. The reservoirs are short 1/16'' male nut tightened down with a flangeless ferrule to provide a seal. The Peltier heater was manually controlled and the voltages were computer control. The confocal microscope for LIF detection sits under the device. P, T and E are probe, target and enzyme reservoirs respectively. Wafer was a 4 inch square. The whole setup sits on an aluminum cooling block.

3.2.12: LIF Detection Using an Inverted Confocal Microscope

Excitation light from an air cooled argon ion laser (488 nm, Cyonics, Uniphase, CA, USA) was passed through a dichroic mirror (505DRLP02, Omega) and focused onto a glass device. The objective used to focus the beam on the device was a 40x from New Focus Inc. (Santa Clara, CA). The fluorescence emission was collected by the same objective lens, passed through the dichroic mirror and reflected by a mirror to a 200 µm pinhole. A photomultiplier tube (PMT), (Hamamatsu R1477, Tokyo, Japan, Bias, 700-850 V) was mounted onto the microscope as shown in Figure 3.6. The emission beam

went through two interference filters, a 514.5 nm bandpass filter (9 nm bandpass, Melles Griot) and a Notch filter (Beckman Instruments, Fullerton, CA) for rejection of 488 nm light. The beam was then collected in the PMT to give an analog signal, which was amplified and filtered with a 25 Hz cut-off filter (Krohn-Hite 3442). Electropherograms were recorded on a PowerPC Macintosh 7100/80 with an NB-MI016 A/D board and a program written in Labview (National Instruments, Austin, TX, USA) at a sampling rate of 50 Hz. All data were smoothed using an eleven points box smooth algorithm, which is included in the data analysis program (Igor Pro Wavemetrics, Lake Oswego, OR, USA).

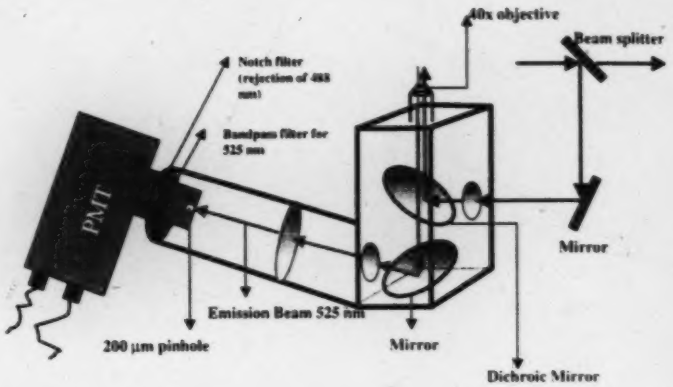

Figure 3.6: The inverted confocal microscope design used for Laser Induced Fluorescence Detection for the set-up shown Figure 3.5.

3.2.13 Instrumentation Alignment for Optimum Fluorescent Signal

With no chip mounted on the station and the objective lens removed, a mirror was mounted at the chip holding site to reflect the incident laser beam coming from the dichroic mirror. The mirror and beam splitter were then adjusted so that the reflected light followed exactly the same path as the incident beam. To ensure the reflected beam followed the same path, the reflected laser spot must be as close as possible to where the original laser beam entered. This procedure ensured that the beam reflected off the dichroic mirror at 90°. Once the device was mounted on the station, the only way to

ensure optical alignment was to place a mirror on top of the device, move the laser spot out of the channel and then focus to the laser spot on the top plate of the device. If the spot was still round it meant the optical alignment was fine. Otherwise a small adjustment of the mirror and beam splitter was needed to get a round spot. The spot was viewed through the eyepiece with a long pass yellow filter.

For further optimization, 10 nM fluorescein was run through the chip and fluorescent signal optimized, as in the case of the 'COPI' device. Once the chip was optimized, it was cleaned with buffer using electrokinetic pumping.

3.2.14 On-chip Cycling and Separation

The buffer used through the process of mixing, cycling (incubation) and separation was 10 mM phosphate (pH 6.8), 0.05% Triton X-100, 4 mM $MgCl_2$ and 0.2 mM spermine. The amount of probe and enzyme used in the reservoir was 100 nM and 0.02 µg/µl respectively. The device used was named GOCPTTT and is shown in Figure 3.7a. The device consisted of 4 inlet ports to drive reagents by electrokinetic pumping (step 1, Table 3.3a) or hydrodynamic pumping (step 1, Table 3.3b) to the reaction coil, which sat on a heating element (Peltier operated in reverse mode). When reaching the reaction coil all reagents were diluted by a factor of two because of the 1:1 mixing at intersection of the four inlet channels. All voltage and relay switchings are shown in either in Table 3.3a or Table 3.3b. The separation channel was then flushed (step 2, Table 3.3a&b). 5 repeated single T injections (Figure 3.7b) and separations, (step 3, 20 sec and step 4, 300 sec), used as control experiments (On-chip control), were then performed prior to CPT reaction. Cycling (incubating) at 60 °C for 30 min (step 5) was then performed. After cycling the CPT products were driven to the double T junction of the

device (step 6, 60 sec). The separation channel was cleaned by flushing with buffer (step 7, 180 sec). Then, 5 repeated single T injections and separations were performed (step 8, 20 sec and step 9, 300 sec), after which fresh reagents were loaded to reaction coil (step 1) for another series of experiments. Note all relays and voltages were controlled by the Labview software (National Instruments, TX).

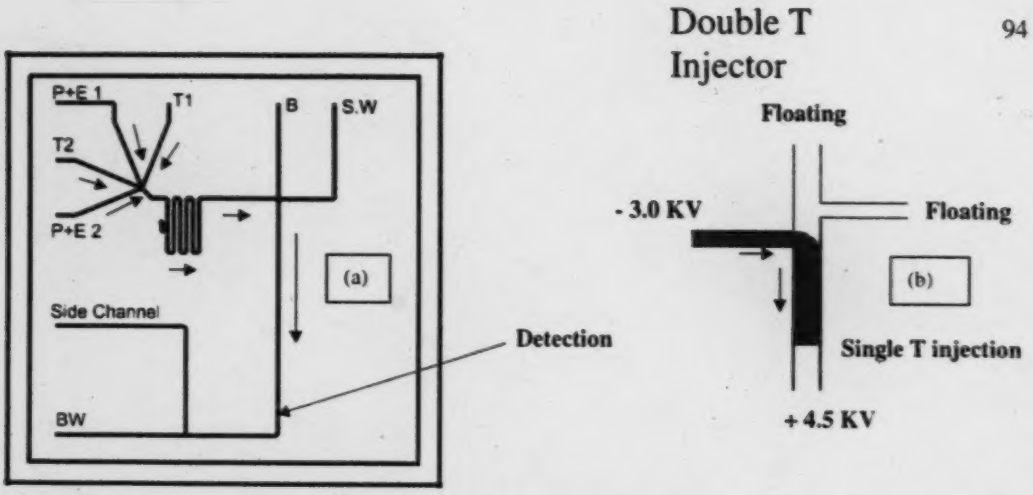

Figure 3.7: (a) CPT Chip layout, where P+E1and P+E2 represent probe and enzyme reservoirs and T1and T2 represent target reservoir respectively. B, BW and SW are Buffer Inlet, Buffer Waste and Sample Waste reservoirs. (b) Illustrates a single T injection scheme.

Table 3.3:(a) Voltage and Relay Switching Matrix for Fluidic Control of Microchip

		Reservoir voltage (kV)								
Step	**Reservoirs**	P+E[1]	P+E[2]	T1	T2	B	BW	SW	Side	Time (sec)
1	Fill Reactor	-3.5	-3.0	-3.0	-3.0		+ 4.5	-	-	600
2	Flushing					GND	+5.0			180
3	Injection	-3.5	-3.0	-3.0	-3.0		+4.5			20
4	Separation	-	-	-	-	GND	+5.0			300
5	Reaction	-	-	-	-	-	-	-	-	1800
6	Mobilization	-3.5	-3.0	-3.0	-3.0	-	-	+ 4.5	-	60
7	Flushing					GND	+5.0			180
8	Injection	-3.5	-3.0	-3.0	-3.0	-	+ 4.5	-	-	20
9	Separation	-	-	-	-	GND	+ 5.0		-	300

Table 3.3:(b) Mixed Vacuum, Voltage and Relay Switching Matrix for Fluidic Control of Microchip

		Reservoir voltage (kV)								
Step	**Reservoirs**	P+E[1]	P+E[2]	T1	T2	B	BW	SW	Side	Time (sec)
1	Fill Reactor	-	-	-	-			Vacuum	-	60
2	Flushing					GND	+5.0			180
3	Injection	-3.5	-3.0	-3.0	-3.0		+4.5			20
4	Separation	-	-	-	-	GND	+5.0			300
5	Reaction	-	-	-	-	-	-	-	-	1800
6	Mobilization	-3.5	-3.0	-3.0	-3.0	-	-	+ 4.5	-	60
7	Flushing					GND	+5.0			180
8	Injection	-3.5	-3.0	-3.0	-3.0	-	+ 4.5	-	-	20
9	Separation	-	-	-	-	GND	+ 5.0		-	300

3.3 Results and Discussion

3.3.1 Cycling Probe Technology and Capillary Electrophoresis

In initial work done by T. Tang in our Laboratory, the CPT products were separated on chip using capillary gel electrophoresis (CGE). The poor reproducibility of migration time when performing CGE on chip made it difficult to routinely identify peaks and rendered quantitation difficult. Also, the requirement for the gel added extra effort to the chip preparation. Earlier work with DNA has shown that with increase in the viscosity of the solvent, the rate of hybridization is significantly decreased [26-29], indicating that diffusion plays an important role in the hybridization process. Hence, the presence of gel in the microchip channel network could interfere with the CPT reaction by impeding probe-target hybridization or the reaction with the RNase H enzyme.

In order to eliminate the need for gel-filled capillaries, asymmetric probes were used that contained 3 biotins for early experiments and 1 biotin residue for later experiments. The biotin was located on the 3' end of the polynucleotide, while the 5' end was labeled with fluorescein. The biotin residues acted as an anchor, altering the charge to friction ratio so that separation could be carried out in the non-gel, open tubular capillary format, which is known as capillary zone electrophoresis (CZE). In this mode, separation was based solely on electrophoretic mobility.

Performance of a complete integrated CPT assay required the on-chip optimization of both the reaction and the separation. To achieve this, we initially carried out the CPT reactions off-chip, then analyzed the products on-chip by LIF-CZE. In the initial experiments with off-chip CPT and on-chip CZE, the electropherograms of the CPT reaction products provided good separation between the cleaved and intact probes

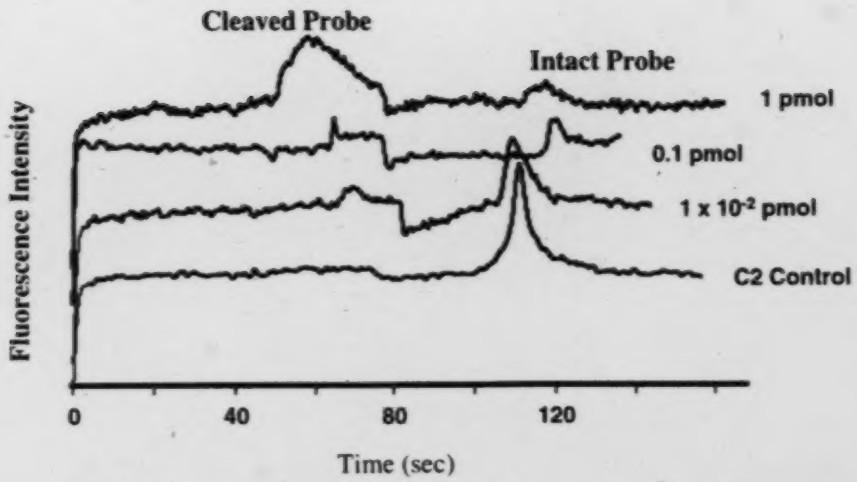

Figure 3.8: (a) Electropherograms for the gel free separation of the off-chip cycling CPT reaction products, after 30 min cycling in 25 µl reaction volume and quenching with 25 µl of the quenching buffer . The separation was achieved in 10 mM phosphate buffer, 0.05% Triton X-100, 4 mM $MgCl_2$, 25 mM EDTA and 3.5 M urea. Injection was at 2 kV for 5 s and the separation voltage was 3.5 kV (700 V/cm). The traces from the bottom represent the control with no target, 1 x 10^{-2} to 1 pimol of target . C2 control were performed in the absence of target DNA.

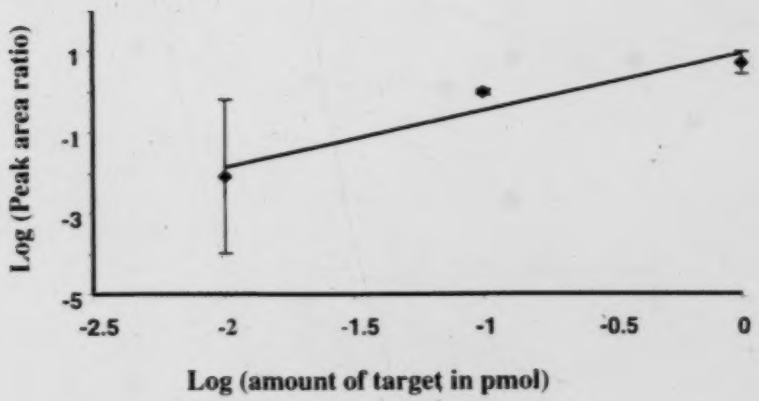

Figure 3.8: (b) The calibration curve (Log-Log plot) obtained for the data in Figure 3.8a where peak area ratio is the peak area of the cleaved probe to peak area of intact probe. The amount of target was in 50 µl volume.

(Figure 3.8a). However, the peak shapes were markedly non-Gaussian, and reproducibility between injections was very poor (Figure 3.8b). The poor shapes arose from the presence of RNase H, which interacted with the reaction products during electrophoresis. Separation of a synthetic mixture of fragmented and intact probe in the absence of RNase H, as shown in Figure 3.9, confirmed that the presence of RNase H caused the poor separations. The electropherograms in Figure 3.8 were obtained with 3 biotin labels at the 3' end, while all subsequent work was done with a single biotin label.

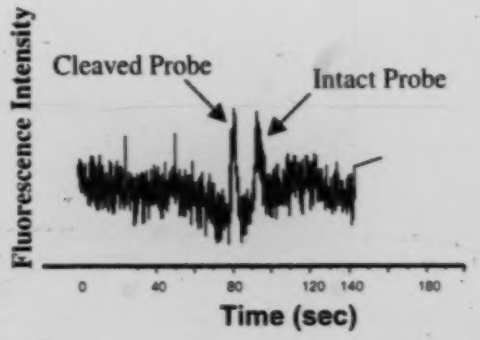

Figure 3.9: Electropherogram of a synthetic mixture of cleaved and in intact probe (0.5 picomole/50 µl volume) in the absence of enzyme. Separation was performed in 10 mM phosphate, 0.01% Triton X-100, 4 mM $MgCl_2$, 3.5 M urea, 25 mM EDTA. Injection at 2kV for 5 s and separation at 3.5 kV (700 V/cm) was used, in the COPI device.

We found that the addition of spermine to the reaction improved the peak shapes in CZE separation of CPT reaction products. Spermine is a linear polyamine (positively charged at physiological pH) that has been shown to bind to duplex nucleic acids in a minor groove of the double helix structure [30-33]. Also, Modrusan et al [17] reported that spermine can displace RNase H from single stranded DNA. The presence of spermine in the reaction mixture alleviated the peak distortion. It is likely that the spermine displaced the enzyme from the DNA, improving its migration performance. With added spermine, Guassian-shaped peaks, separated by approximately 8 s, were observed in gel free columns (Figure 3.10a), for sample containing RNase H. Also, the shapes and migration

times of these peaks were similar in appearance to the gel free separation of a synthetic mixture of intact probe and fluorescent fragment alone, shown in Figure 3.9.

Electropherograms of off-chip CPT and on-chip separation using spermine-optimized conditions are shown for target concentrations of 0.1 and 0.01 picomoles of target in 50 µl volume (Figure 3.10a). As the target concentration was increased, the relative size of the fluorescent fragment peak in the reaction mixture increased and the size of the intact probe peak decreased. To conduct the experiments for the data shown in Figure 3.10a, which is a subset of the data plotted in Figure 3.10b, samples had to be changed and the reservoirs rinsed before introducing new sample (see section 3.2.10 and 3.2.11). Performing the tasks of rinsing and loading each new sample disturbed the optical alignment from run to run. Consequently, total intensity (total area under the peaks) varied slightly. Nevertheless, the electropherograms clearly showed that the amount of probe cleavage in the CPT reaction increased with added target. The calibration curve was linear in log-log format, as shown in Figure 3.10b, however, the slope was ~½, indicating the peak ratio did not vary linearly with concentration. According to IDB, the CPT reaction follows linear kinetics only at very low target concentration, relative to probe concentration, which is consistent with the bimolecular nature of the reaction.

With the plate numbers obtained in Figure 3.10a (500 plates, 5 cm migration distance), detection of low target concentration by CPT seemed very difficult. Sample wall interactions was suspected to be the cause of the low plate numbers. As a result, we attempted to improve the polyacrylamide coating on the walls of the channel. It was

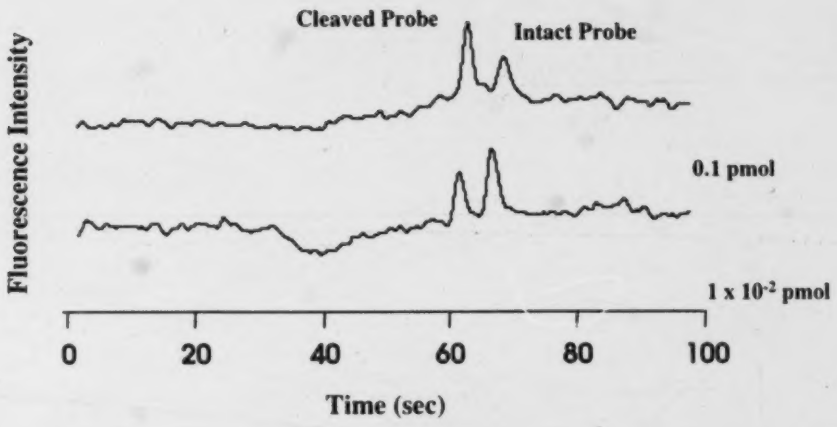

Figure 3.10:(a) Electropherograms of gel free separation of the off-chip CPT reaction products after 30 min cycling in 25 µl reaction volumes and quenching with 25 µl of the quenching buffer . Separation was performed in 10 mM phosphate buffer, 0.05% Triton X-100, 4 mM $MgCl_2$, 25 mM EDTA, 3.5 M urea and **0.2 mM spermine.** Injection at 2kV for 5 s and separation at 3.5 kV (700 V/cm) was used for in the COPI device. The traces, from bottom to top, represent target concentration of 1 x 10^{-2} and 0.1pmol of target in 50 µl.

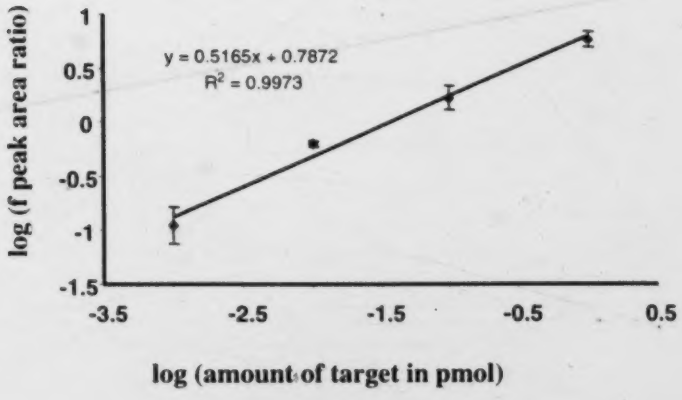

Figure 3.10: (b)The calibration curve (Log-Log plot) obtained for target from 1 x 10^{-3} to 1 picomole of MRSA target DNA where peak area ratio is the peak area of cleaved probe to peak area of intact probe. All samples were in 50 µl volume. Error bars are s.d. of 3 replicates.

found that the use of fresh reagents was very important, especially the TEMED and potassium persulfate used as the radical initiator of the acrylamide polymerization. Also, in order to decrease the residence time of the sample in the channel, DTAB was used as a cationic surfactant to improve flow in the reverse direction in the absence of EOF.

After performing all these changes, excellent quantitative data were obtained with improved plate numbers in the order of 4700 plates for 5 cm migration distance. The lowest concentration that was detected on chip was 0.1 attomoles in a 35 µl reaction volume, as shown in Figure 3.11. Figure 3.12a shows the electropherograms obtained for various concentrations of target from 0.1 attomoles to 10 femtomoles in a 35 µl reaction volume. At 0.1 attomole target, fluorescent fragments can be observed as a small peak above the control level as shown in Figure 3.11. The amplification factor was on the order of 10^5, which was calculated from the ratio of the amount of cleaved probe to the amount of target DNA used (Table 3.4). At this concentration we could readily discern

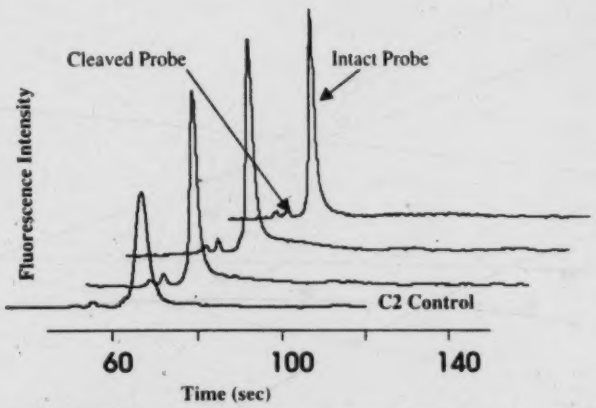

Figure 3.11: Electropherograms of replicate data for the lowest amount of target detected for MRSA sample cycled off-chip. **0.1 attomoles** in 35 µl. The % RSD for the peak area ratio was 9 and the % RSD for migration time of intact probe was 1.8. The S/N ratio of the cleaved probe was 10. 5 s injection at 2.5 kV and separation at 3.5 kV was performed in COPI. The separation buffer was 10 mM phosphate buffer, 0.05% Triton X-100, 4 mM $MgCl_2$, 0.2 mM spermine, 2.5 mM DTAB, 25 mM EDTA and 3.5 M urea. The bottom trace is the C2 control experiment where CPT was performed in the absence target.

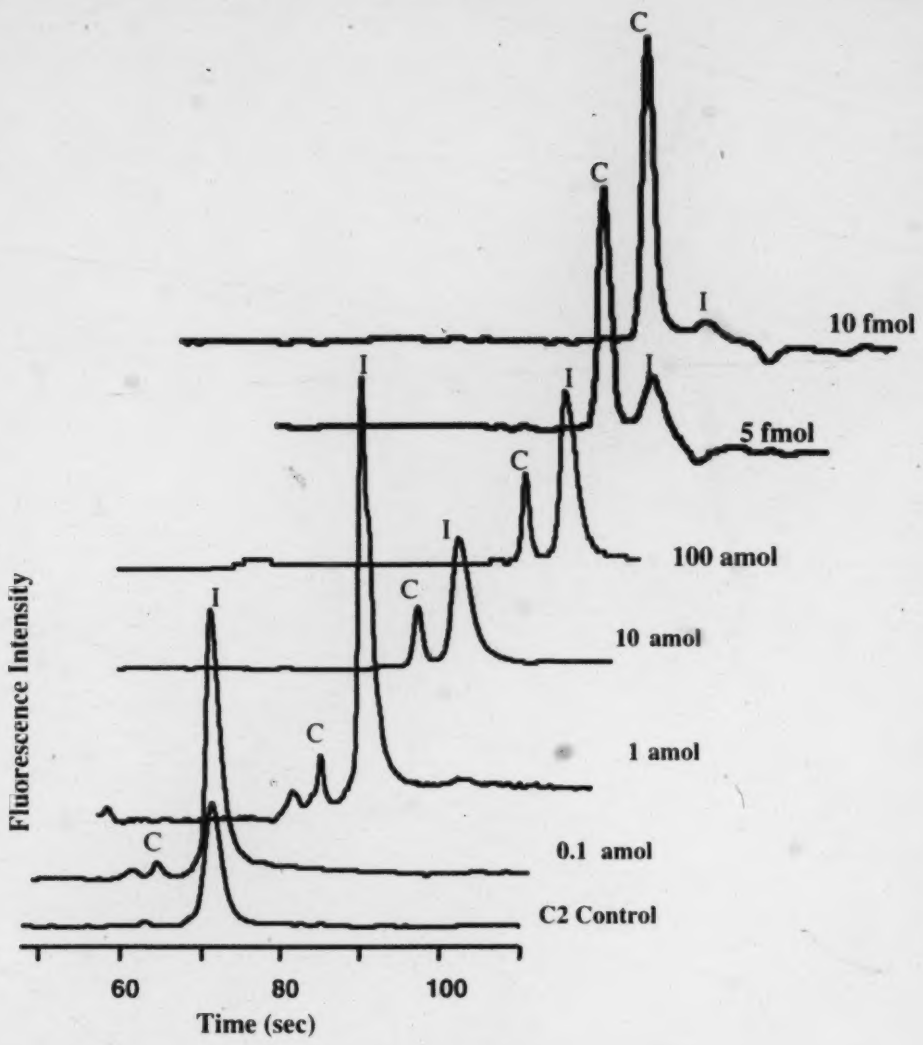

Figure 3.12: (a) Electropherograms of CPT reaction products in gel-free separation mode after cycling for 30 min in a 17.5 µl reaction volume and quenching with 17.5 µl of the quenching buffer . The separation was achieved in 10 mM phosphate buffer, 0.05% Triton X-100, 4 mM $MgCl_2$,0.2 mM spermine, 2.5 mM DTAB, 25 mM EDTA and 3.5 M urea. Injection was performed at 2kV for 5 s, and separation was at 3.5 kV (700 V/cm). Concentration of target varied from 0.1 amol to 10 fmol in 35 µl solution. C2 control was performed in absence of target. C is for cleaved probe and I for intact probe.

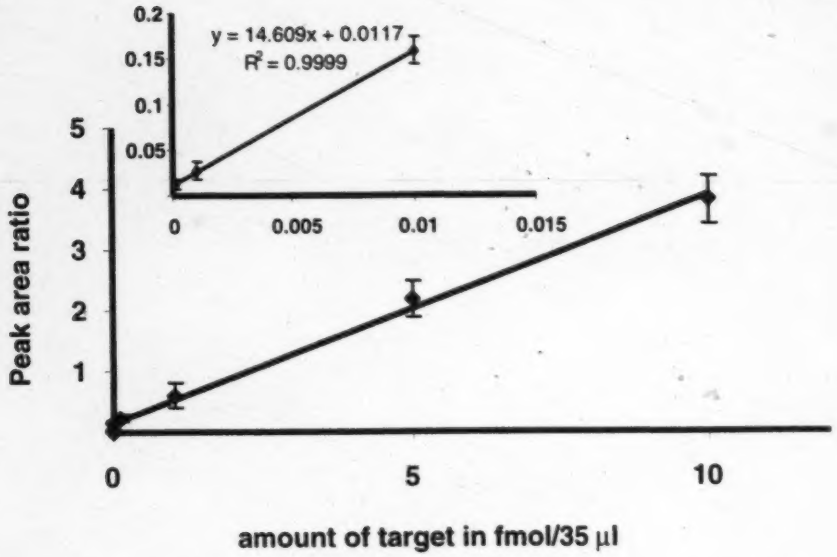

Figure 3.12:(b) Linear plot obtained for off-chip cycling and on-chip separation of the CPT products. The amount of target ranged from 0.1 amol of target to 10 fmol in a 35 µl volume. The inset shows the plot at lower range of target from 0.1 to 10 amol which reflects better linearity with an R^2 value of 0.9999. Error bars are the s.d. of 3 replicates

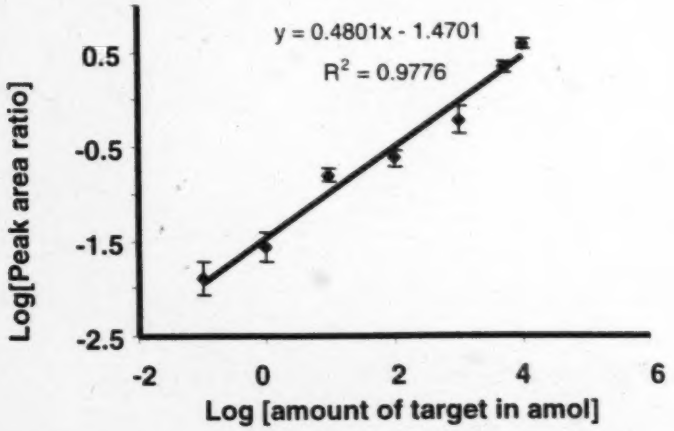

Figure 3.12: (c) Represents a log-log plot of the data in Figure 3.12b. The amount of target is amol/35 µl.

the fluorescent fragment above background with a S/N = 10, RSD in migration time of 1.8% and a 9% RSD for the peak area ratio of cleaved and intact probe. At 10 femtomoles, the predominant peak was the fluorescent fragment, followed by a minor peak due to residual intact probe with an amplification factor of 32.

Table 3.4: The percent probe cleavage and amplification factors of data in Figure 3.12a .

Amount of target in amol/35 µl *	% probe cleavage	Amplification Factor
0.1	2.4	85000
1	10.7	35000
10	24.8	8750
100	46.1	1575
5000	73.7	52
10000	90.0	32

* Probe and enzyme concentrations were 10 nM and 0.02 µg/µl.

The ratio of the peak area of fluorescent fragment to intact probe for each electropherogram in Figure 3.12a was plotted versus concentration of added target as shown in Figure 3.12b. We did not expect the data to reflect a true linear dependence between concentration of target and amount of fluorescent fragment produced during the 30 min incubations over the total concentration range. At low target concentrations, where overall consumption of intact probe was low during the 30 min period (in effect, where the concentration of intact probe remained relatively constant), the reaction kinetics can be described as pseudo-first order (see inset Figure 3.12b) [34]. However, in the higher concentration target regime, the concentration of intact probe decreased

appreciably, almost to zero as indicated by the electropherograms. Consequently, any approximation to first order kinetics was not reasonable. The data in Figure 3.12a are plotted as peak area ratio of cleaved to intact probe versus amount target (Figure 3.12b) to normalize for intensity changes caused by moving the chip for sample loading. The slope was higher at the low concentration regime (inset Figure 3.12b). A log-log plot of the data in Figure 3.12a plotted as log (peak area ratio) versus log (amount of target) was linear as shown in Figure 3.12c, however the slope was ~ ½. Indicating a non-linear kinetics over the whole range. Nevertheless the data could be constructed to provide calibration. Also it did not seem that DTAB improved the migration time of the CPT products, because there was no significant change in migration time.

The results presented in Figures 3.11 and 3.12a demonstrated that we could perform an on-chip CE analysis of the CPT reaction and that it was possible to formulate a common buffering system suitable for both reaction and separation. The work allowed us to proceed to the next stage of the development, combining the CPT reaction and CE analysis on-chip.

3.3.2 On-Chip mixing, Reaction, Separation and LIF Detection Using the GOCPTTT Device

In order to perform complete on-chip analysis, that is, mixing of sample and reagents, reaction, injection and separation, fluidic control of the microchip must be achieved after the channel walls have been coated with polyacrylamide. Initial characterization of mixing in these devices was performed by T. Tang. However, for performance of quantitative analysis, it was important to determine the best operating conditions for mixing. Three of the input channels on the GOCPTTT device, shown in

Figure 3.13b, were of the same length. The fourth one was slightly longer than the other three, in order to mate with the pattern of axis holes, which were spaced uniformly along two edges of the layout, separated by 16.7 mm. It was necessary to determine the voltage, required at the fourth reservoir to obtain reproducible loading and mixing. An experiment was performed where the voltage in the three reservoirs (containing buffer) interfaced to the input channels of the same length were kept at the same value of -3 kV, and the voltage on the fourth reservoir was varied. The fourth contained 10 nM fluorescein sample dissolved in buffer, as shown in Figure 3.13b. The voltage was varied from 3000V to 3800 V in steps of 100 V, and the resulting solutions were separated (step 8 and step 9, Table 3.3a). The change in fluorescence intensity shown in Figure 3.13a for various voltages, demonstrated fluidic control in the chip. The best reproducibility was achieved with 3500 V (% RSD in peak height ~8). Note each point on Figure 3.13 is averaged over five injections. The results show an extra 500 volts was needed on the fourth reservoir to ensure a symmetric flow in all four input channels to the reaction coil.

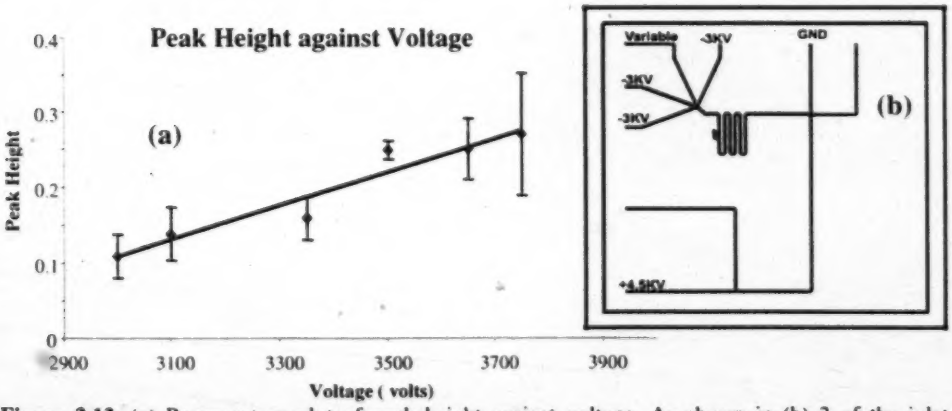

Figure 3.13: (a) Represents a plot of peak height against voltage. As shown in (b) 3 of the inlet reservoirs were at -3 kV (contained buffer) and the voltage on the fourth reservoir containing 10 nM fluorescein was varied from-3.0kV to -3.8 kV in increment of 100 V, during injection (20s). The best reproducibility in flow was achieved at -3.5 kV. The buffer used was 10 mM phosphate buffer, 0.05% Triton X-100, 4 mM $MgCl_2$. Separation voltage was 5.5kV (500 V/cm). Error bars are the s.d of 5 replicates.

3.3.2.1 Temperature Control On-chip

The CPT reaction requires an elevated temperature be held constant within ±1 °C. Variations in the reaction temperature can affect the hybridization of the intact probe and the cleaved fragments to the target DNA and thus alter the speed and specificity. High temperatures (in excess of 70 °C) would result in probe-target melting and enzyme denaturing. For the probe and target pair used in this work the optimum temperature for the CPT reaction was 60 °C [35].

For the GOCPTTT device depicted in Figure 3.13b and Figure 3.5, there was a need to control and maintain a steady temperature in the reactor coil region and to remove heat from outside the heated area. A two-stage Peltier element was used to provide heating. A water-cooled aluminum block served as the constant temperature reference for the Peltier heater and as the heat sink for the unheated area.

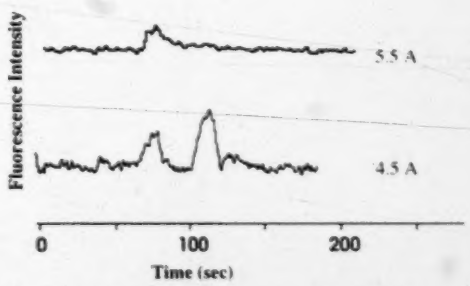

Figure 3.14: Electropherograms obtained for 100 amol of MRSA target in 100µl. Peltier currents were at 4.5 and 5.5 A respectively. Separation was performed in 10 mM phosphate buffer, 0.05% Triton X-100, 4 mM $MgCl_2$, 0.2 mM spermine. Injection was at 3.0 kV for 20 s and separation voltage was at 5.5 kV (500 V/cm).

T. Tang did an early temperature characterization and showed problems with performing CPT unless the heating was correctly adjusted. He showed that the Peltier current needed for optimum probe cleavage and fluorescence signal was 4.5 A. Later experiments I performed confirmed those results. At 4.5 A the inside of the reactor coil seemed to be close to the required 60 °C, based on the fact that this current produced stable, reproducible results with good sensitivity. The electropherograms

obtained in Figure 3.14 were obtained using the sequence of mixed vacuum and electrokinetic driven flow as shown in Table 3.3b. The concentration of MRSA DNA target, in the reaction coil, was 100 amol in 100µl. The two peaks confirmed the occurrence of CPT in the reaction coil at 4.5 A. Experiments done at 5.5 A Peltier current gave very poor injections with low intensity signal, as shown in Figure 3.14. Two explanations could be given for this phenomenon: (1) the coating was not stable at higher temperatures (i.e. loss of the acrylamide coating in the reaction zone resulted in ineffective electrokinetic pumping in the reaction zone) and (2) denaturing of the CPT components, the enzyme and the probe. From the data in Figure 3.14 either or both of (1) and (2) might be occurring. When a chip heated at 5.5 A was flushed with fresh reagents, (step 1, Table 3.3b), and operated at 4.5 A the original quality of data was not recovered. This suggested that the coating was damaged at the higher temperatures. Hence, the need to re-coat the device was necessary.

At 4.5 A, the probe cleavage and electrophoresis was reproducible on the chip, with about 8% RSD in the peak area ratio of cleaved to intact probe over five injections of a single reaction run. The results presented in Figure 3.14 indicate that temperature control could be incorporated into the chip-carriage design and that the temperature sensitive CPT reaction could be run reproducibly on-chip.

3.3.2.2 On-chip CPT process: Mixing, Reaction and Separation

We were able to demonstrate successfully the individual components of the CPT assay, namely, fluidic and temperature control, and CE separation of the reaction products. For the complete on-chip CPT process, the on-chip reagent reservoirs were filled as indicated in Figure 3.7 and Table 3.3a. Two of the "fingers" were loaded with

target DNA solution and two were loaded with probe and enzyme. Initially when the chips were fabricated we anticipated needing four independent reservoirs for reactants. However, subsequent work indicated that a two-component set of reactants would suffice. Therefore we used all four reservoirs, filling two with target and two with probe/enzyme mixture. The probe concentration was 100 nM and the enzyme concentration was 0.02 µg/µl. Each reservoir received 50 µl of solution. After mixing in the reaction coil the two components are essentially diluted by a factor of two giving a concentration of 50 nM for the probe and 0.01 µg/µl for the enzyme. The target was prepared in 100 µl of phosphate buffer, and 50 µl aliquots were delivered to each reservoir. The stated amount of target are for the concentration in the reaction coil.

The voltage and relay control for the chip is shown in Table 3.3a. The reactor coil was loaded with reactants by applying voltage at the various reservoirs, (Step 1, Table 3.3a for 600 sec). The total volume of the reactor coil was 160 nl. The separation channel was cleaned by flushing with buffer (step 2, 180 sec) and the on-chip control experiments were run as mentioned in the experimental section 3.2.14, prior to reaction. After running the control, high voltage to the chip reservoirs was terminated, and the temperature was raised by applying current (4.5 A) to the Peltier element for 30 min to complete the CPT reaction (step 5). The CPT products were then mobilized (step 6, 60 sec) to the channel arm connected to the double injector for injections and separations.

3.3.2.2.1 Diffusional Mixing

The reaction time was long enough to allow effective mixing by diffusion in the 130 µm wide channels of the reaction zone (step 5, Table 3.3a and b). Crank [36] provides a solution to the initial-boundary value problem of diffusion for a finite system,

where a species is initially confined to half the width of the channel and then is allowed to diffuse across the full channel. The numerical solution to the differential equation that defines the diffusion dispersion is,

$$C(x,t) = \frac{1}{2} C_o \sum_{n=-\infty}^{\infty} \left\{ erf\left[\frac{h + 2nw - x}{2\sqrt{(Dt)}} \right] + erf\left[\frac{h - 2nw + x}{2\sqrt{(Dt)}} \right] \right\} \qquad (3.1)$$

where x is the location across the channel of width w (130 μm), t is the diffusion time, C(x,t) is the concentration of any given x and t, C_o is the initial or maximum concentration before diffusion (t=0), n is an integer, h is the portion of the channel width that the species was initially confined to, and D is the diffusion coefficient. This expression was numerically evaluated, using a program written in HiQ script language (National Instrument, Austin, TX). The enzyme was chosen as the limiting reagent for diffusion calculation. This is because the probe is smaller compared to the enzyme and will diffuse quickly across the channel, while the DNA target is the biggest molecule among the three and will diffuse very slowly. Diffusion of the RNase H was calculated using Equation 3.1, and the result obtained are shown in the 3 dimensional plots, Figure 3.15a and b. The plot in Figure 3.15a and b illustrates the diffusion profile expressed as the ratio of concentration at time t and position x across the 130 μm wide reaction channel, relative to initial concentration C_o. Based on a molecular weight of 13.7 kDa and a diffusion coefficient of 1.2 x 10^{-6} cm^2/sec for similar enzyme Ribonuclease [37], nearly complete dispersion of the enzyme occurred within 55 sec, at room temperature (Figure 3.15a). The concentration profile, C(x,t)/Co varied by ~ 5 % between the two ends of the channel at t = 55 sec. Application of heat to the coil may have further promoted mixing by convection. The molecular weight of the RNase H used for the CPT experiments was

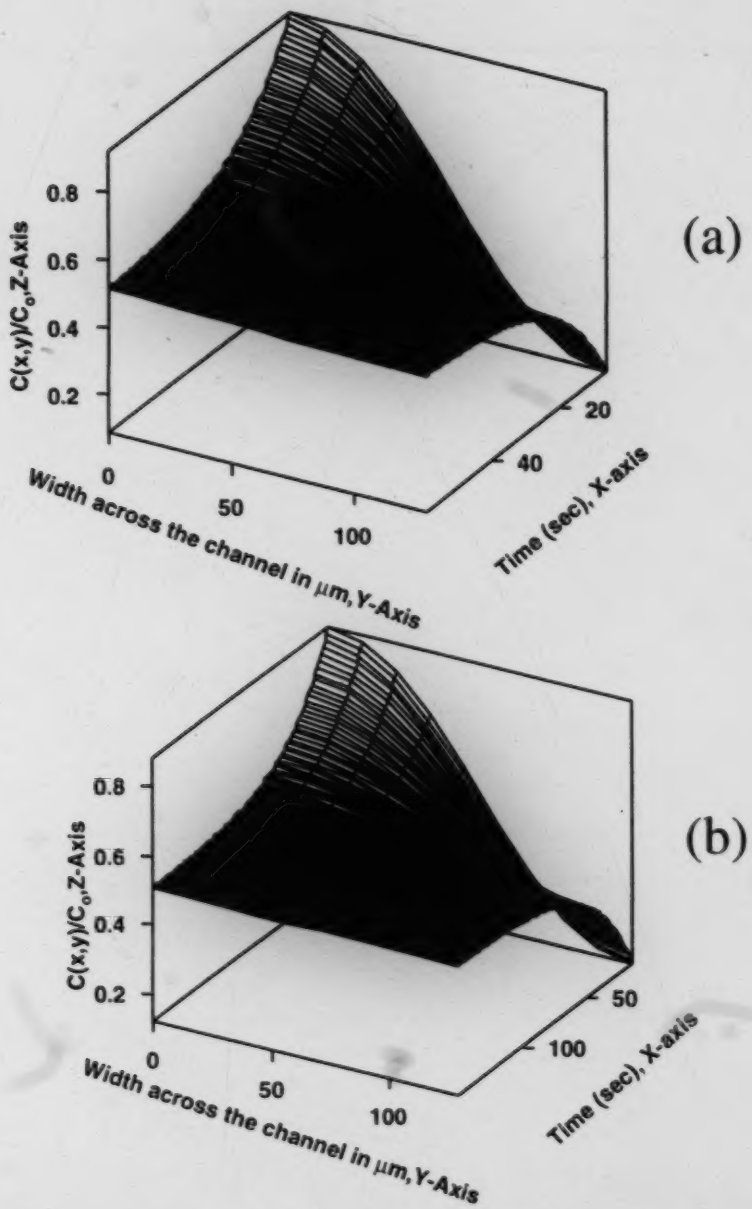

Figure 3.15: Diffusion plots across across a 130 μm wide channel: (a) for ribonuclease (M.W. 13.7 kDa and D = 1.2 x 10^{-6} cm^2/sec) and (b) for serum albumin (M.W. 6.5 kDa. D = 5.9 x 10^{-7} cm^2/sec) calculated using Equation 3.1. The X-axis represents the time axis in sec. The Y-axis represents the length across the channel in μm. The Z-axis represents the ratio of concentration C(x,y) at t=t to the initial concentration C_o at t=0. Sample is taken to initially occupy 50% of the channel.

17.6 kDa, so a similar value of D should apply, but a specific value is not available. Serum albumin, with a molecular weight of 65.0 kDa has a diffusion coefficient of 5.9 x 10^{-7} cm^2/sec and so would take 110 sec to diffuse across the 130 µm wide channels (Figure 3.15b) where C(x,t)/Co varied by ~ 5 % between the two ends of the channel at t = 110 sec. Thus, mixing of the RNase H would take between 55 to 110 seconds.

3.3.2.2.2: CZE Separation

For each sample, the process of on-chip analysis began by filling the reactor coil. Prior to heating, a control sample of the reactants was delivered to the injector and separated by CE, in step 1, 2, 3 and 4 in Table 3.3a.

In order to perform the CE separations, the CPT products (fluorescent fragment and intact probe) had to be transported from the reactor coil to the double T injector at the head of the separation channel. Voltage was applied to the corresponding reservoirs, for 60 sec, as shown with step 6 in Table 3.3a, for mobilization of the CPT products to the injector and to exclude any of the CPT reagents that diffused during the heating process. Since EOF in the channel network was eliminated by the acrylamide coating, the fluorescent fragment and intact probe molecules moved from the coil to the injector by electrophoretic migration alone. Even though the channel that connected the coil to the injector was wide (130 µm) and not actually designed for electrophoresis, some electrophoresis of the fluorescent fragment and the intact probe occurred nonetheless. Thus at the leading edge of the products, there was an enrichment of the faster migrating molecules, namely the fluorescent fragment. The timing sequence for this step (Step 6, Table 3.3a) was sufficiently long to pull the leading edge into the channel arm in the double T injector region and so into the separation channel. In the migrating "bulk

stream" behind the leading edge, molecular ratio was the same as it was in the reactor coil [21]. After flushing the separation channel (step 7, 180 sec), single T injections were performed by applying voltage to the respective reservoirs as shown in step 8, Table 3.3a. After doing 20 sec single T injection, voltage was then applied to the reservoirs as in step 9 in Table 3.3a. This step caused the molecules in the injector to be subjected to capillary electrophoresis in the separation channel.

The results of complete on-chip CPT analysis is shown in Figure 3.16a, where the sample solution contained 100 attomoles of target DNA in 100 µL. The lower trace is the electropherogram of the DNA and reagents prior to incubation. Here the fluorescence intensity is mainly contained in the intact probe peak (95 s), although a fluorescent fragment was observed at 60 s due to nonspecific reaction. CE analysis of the intact probe alone indicated that only trace amounts of the fluorescent fragment were present. The upper trace is the reaction mixture after heating for 30 min at 4.5 A and shows major peaks for both intact probe (95 s) and fluorescent fragment (60 s). The amount of probe cleavage was ~ 40% and the peak area ratio of cleaved to intact probe was 0.73 with a RSD of ~ 9%, for 5 replicates.

Figure 3.16b shows five consecutive injections of an incubated reaction mixture derived from the sample solution containing 25 attomoles target in 100 µL. The % RSD for migration time, area of intact probe and peak area ratio was, 0.78, 9 and 8.1 respectively. The amplification factor was in the order of 4.2×10^4 where the amount of target molecules in the 160 nl volume reaction coil was calculated to be ~25000. The amount of probe cleavage was ~20%. We expect the ratio of cleaved to intact probe to be relatively stable even if the peak heights varied due to movement of the chip during

(a)

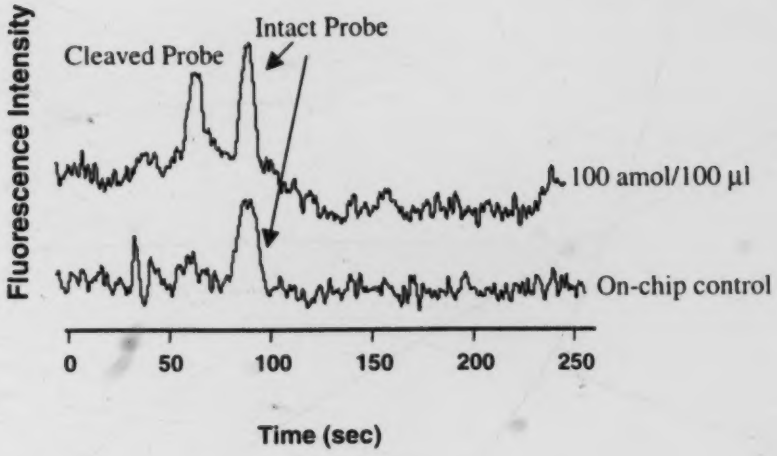

Figure 3.16: (a) Results of an on-chip amplification of 100 amol of MRSA DNA in 100 µl (30 min incubation at 60 °C). The bottom trace shows the CPT probe prior to cycling (On-chip control), the upper trace shows the generation of cleaved probe following incubation. Separation was performed in 10 mM phosphate buffer, 0.05% Triton X-100, 4 mM $MgCl_2$, 0.2 mM spermine. Injection was at 3 kV for 20 s and separation voltage was at 5.5 kV (500 V/cm). The cleaved to intact probe area ratios varied by less than 8% over 5 repeated injections.

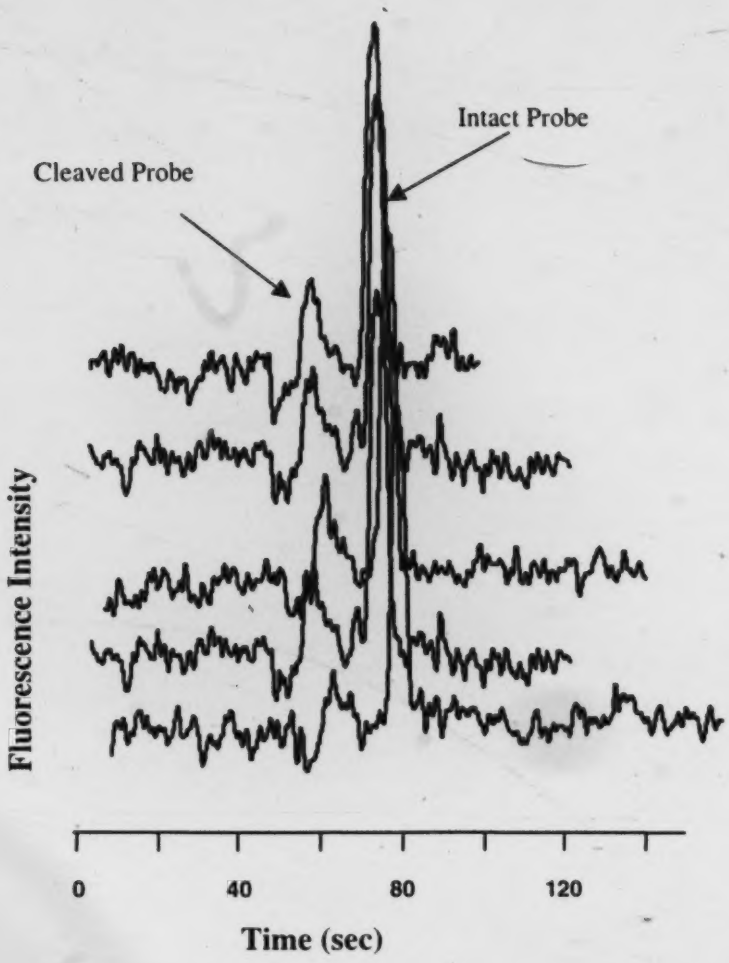

Figure 3.16 : (b) Electropherograms illustrating reproducibility between 5 repeated injections (~92%) for 25 amol of MRSA DNA in 100 µl cycled on-chip. The % RSD for area of intact probe was 9, % RSD for the migration time was 0.78 and the % RSD for peak area ratio was 8.1. S/N= 20 for the cleaved probe. The amplification factor = 4.2 x 10^4. Electropherograms were obtained after cycling was performed on chip for 30 min. Separation was achieved in 10 mM phosphate buffer, 0.05% Triton X-100, 4 mM $MgCl_2$, 0.2 mM spermine, using an injection voltage of 3.0kV for 20s and a separation voltage of 5.5 kV (500 V/cm) .

sample exchange. However, the peak heights were also stable (RSD ~ 8%), so the results are in fact better than just a stable ratio.

The material in the reactor coil should in theory provide more than 50 repeated injections. However, this was not tested. Instead, after five repeated injections the reaction coil was loaded with fresh sample using either step 1 in Table 3.3a.

The reproducibility of peak heights in Figure 3.16b demonstrates that the injector can be loaded reproducibly with solution from the reactor coil. Thus the device is stable with respect to electrokinetic effects and the performance of the polyacrylamide coating.

3.3.2.2.3: Calibration with On-chip CPT Reaction

Knowing that the CPT process was stable and reproducible on chip, an attempt was made to try CPT reactions for different amounts of target to show that a calibration curve could be constructed. The results shown in Figure 3.17a represent electropherograms for target concentrations ranging from 25 amol to 10000 amol in a 100 µl reaction volume (concentration in the reaction coil). The amplification factor varied from 4.2×10^4 to 425 for the data in Figure 3.17a as shown in Table 3.5.

Table 3.5: the percent probe cleavage and amplification factors of data in Figure 3.17a.

Amount of target in 100 µl*	% probe cleavage	Amplification factor
25	20.4	41500
100	40.1	22500
1000	60.0	3000
5000	72.2	720
10000	85.0	425

* Probe and enzyme concentrations were 50 nM and 0.01 µg/µl.

A calibration curve for the data in Figure 3.17a was constructed as shown in Figure 3.17b, with the peak area ratio of cleaved and intact probe plotted versus the amount of target DNA in a 100 µl volume. The calibration curve did not reflect good linearity in the target concentration range studied but, nevertheless, calibration with the reaction performed on chip was possible. Also in a log-log plot format a linear calibration curve of peak area ratio versus amount of target was obtained with a slope ~1/2, as shown in Figure 3.17c. The results were consistent with previously obtained data (from section 3.3.1) even though the GOCPTTT device did not incorporate a method of introducing quenching agents after incubation. As mentioned earlier in the experimental section 3.2.12, the GOCPTTT device sat on an aluminum cooling block. With cold water running in the aluminum block, the device was always at a temperature of about ~ 12 ^{o}C, which was enough to slow down the CPT reaction kinetics, so that any probe cleavage after the incubation period, should have been rather insignificant.

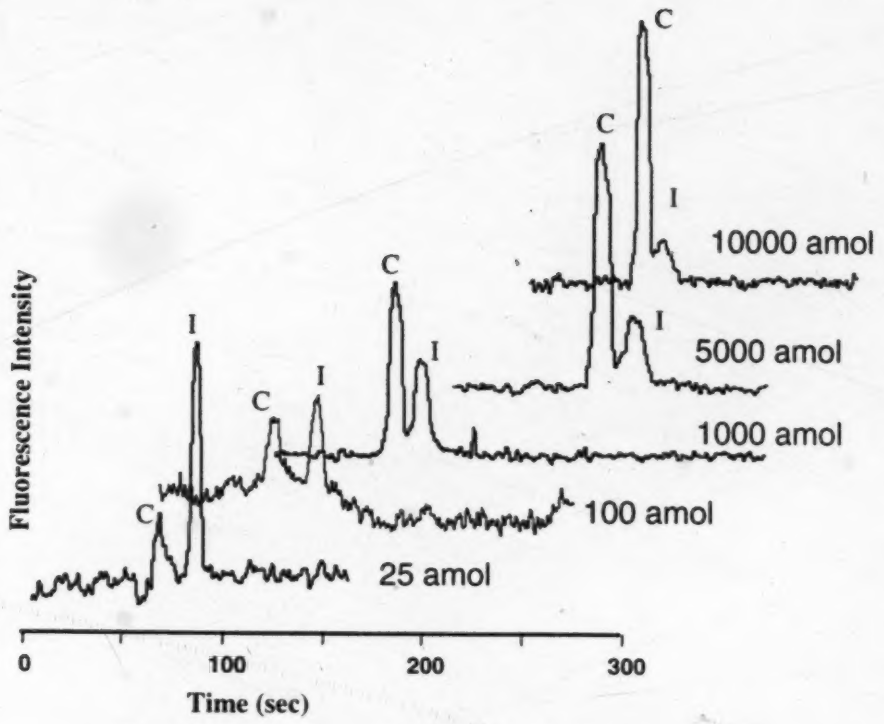

Figure 3.17 : (a) Electropherograms obtained with cycling performed on-chip for 30 min. The separation was achieved in 10 mM phosphate buffer, 0.05% Triton X-100, 4 mM $MgCl_2$, 0.2 mM spermine. Injection was at 3 kV for 20s and separation was at 5.5 kV (500 V/cm). Amount of target ranged from 25 amol to 10000 amol in 100 µl volume. C stands for cleaved probe and I for intact probe.

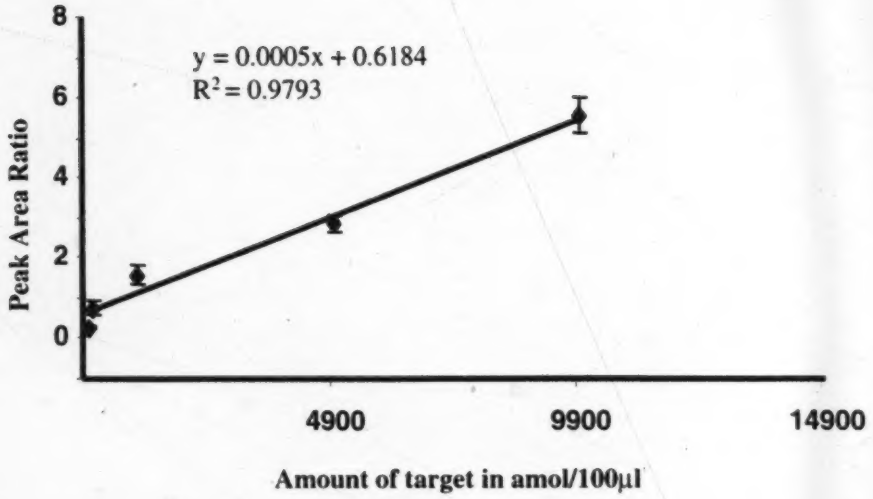

Figure 3.17: (b) Linear plot obtained for on-chip cycling and on-chip separation of the CPT products, with amount of target ranging from 25 to 10000 amol in 100 µl volume. Error bars are s.d. of 5 replicates.

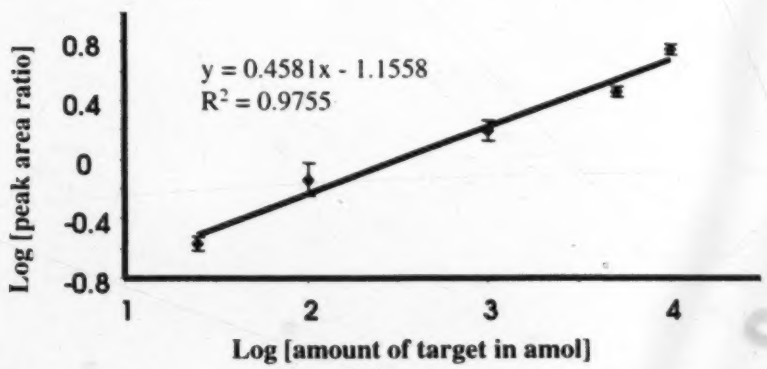

Figure 3.17: (c) Log-log plot of the data in Figure 3.17b.

3.4: Conclusion

In the first part of the study we showed the separation of DNA fragments in free flow electrophoresis mode. The reproducibility obtained allowed the generation of data sets and hence quantitative analysis. The lowest amount of MRSA target detected with CPT was 0.1 attomoles in 35 µl volume. The amplification factor was close to 10^5 not very far from other more advanced DNA amplification techniques such as PCR. Also CPT although not as sensitive as PCR, has a major advantage over the latter in that CPT involves signal amplification hence, no target DNA is being amplified. There is minimal carry-over effect, making integration of reaction and separation on a single wafer an easier process.

Knowing that the fragments could be separated in the CZE mode after being cycled or incubated in a thermalcycler, the next challenge was to integrate the mixing, reaction (CPT), separation and on-line detection on one single device, which we named the GOCPTTT device. The data presented in the study showed the system performed in a very reproducible way.

The calibration part, however, did not adequately reflect linearity for most of the study, but the data presented in Figure 3.12 showed that in low target concentration with respect to probe concentration, linearity can be approached with a pseudo first order kinetics.

In essence, the study demonstrated a complete integration of an isothermal DNA signal amplification reaction with a following separation step. The MRSA sample analyzed is representative of typical clinical assays. The results demonstrate the potential

of electrokinetic devices for an automated performance of a sequence of mixing, enzymatic reaction for DNA amplification, separation and detection.

3.4 References

1. (i) Jorgenson, J. W., Lukacs, K., *Anal Chem.*, 53, 1298-1302, 1981.
   (ii) Jorgenson, J. W., Lukacs, K., *Science*, 222, 266-272, 1983.
2. Harrison, D. J.; Fluri, K.; Seiler, K.; Fan, Z.; Effenhauser, C. S.; Manz, A., *Science*, 261, 895, 1993.
3. Chiem, N., and Harrison, D.J., *Anal. Chem.*, 69, 373-378, 1997.
4. Duck, P., Alvarado-Urbina, G., Burdick, B., and Collier, B., *Biotechniques*, 9, 142-147, 1990.
5. Bekkaoui, F., Poisson, I., Crosby, W., Cloney, L., Duck, P., *Biotechniques*, 20, 240-248, 1996.
6. Nakaruma, H.,Oda, Y., Iwai, S., Inoue, H., Ohtsuka, E., Kanaya, S., Kimura, S., Katsuda, C., Katayanagi., K., Morikawa, K., Miyashiro, H., Ikehara, M. , *Proc, Natl. Acad. Sci. USA*, 88, 11535-11539, 1991.
7. Uchiyama, Y., Shigenori, I., Uena Y., Ikehara, M., Ohtsuka Eika., *J. Biochem.* 116, 1322-1329, 1994.
8. Katayanagi, K., Miyagawa, M., Matsushima, M., Ishikawa, S., Kanaya, S., Ikehara, M., Matsuzaki, T., Morikawa, K., *Nature (London)*, 347, 1398-1405, 1990.
9. Woolley, A. T., Hadley, D., Landre, P., deMello, A. J, Mathies, R. A., Northrup, A. M., *Anal Chem.*, 68 4081-4086,1996.
10. Cheng, J., Shoffner, M. A., Hvichia, G. E., Kricka, J. L., Wilding P., *Nucleic Acid Res.*, 24, 381-385, 1996.

11. Kopp, M. U., deMello, A. J., Manz, A., *Science*, 280, 1046-1048, 1998.

12. Khandurina, J., McKnight, T. E., Jacobson, S. C,. Waters, L. C,. Foote, R. S, Ramsey, J. M., *Anal Chem.*, 72; 2995-3000, 2000.

13. Pourahmadi et al, Cepheid , *μTAS proc'd 2000*, pp 243-248, 2000.

14. Heller et al, Nanogen, *μTAS proc'd 98*, pp 221-224, 1998.

15. Beggs, M. L., Cave, M. D., Cloney, L., Marlowe, C., Duck, P., Eisenach, K. D., *J. Clin. Microbiol.*, 34, 2985-9, 1996.

16. Modrusan, Z., Bekhaoui, F., and Duck, P., *Mol. and Cell. Probes*, 12, 107-116, 1998.

17. Z. Modrusan, F. Bekhaoui, and P. Duck, *Mol. and Cell. Probes*, 12, 107-116, 1998.

18. (i) Persing, D. H., Smith, T. F., Tenover, F. C., White, T. J., " Diagnostics Molecular Microbiology, *Principles and Applications*", 1993.

(ii) Bergey D. H., Holt, J. G., "Bergey's Manual of Determinative Bacteriology" 9th ed., Baltimore, Williams and Wilkins, 1994.

19. Eisenach, K. D., Sifford, M. D., Cave, M. D., Bates, J. H., *Am. Rev. Respir. Dis.*, 144, 1160-1163, 1991.

20. Heller, C., Slater, G.W., Mayer, P., Dovichi, N.J., Pinto, D., Voivy, J., Drouin, G., *J. Chromatogr.*, 806, 113-121, 1998.

21. Harrison, D. J., Fan, Z., Fluri, K., Seiler, K., *Technical Digest*; Hilton Head Sensor and Actuator Workshop, June 13-16,; pp 21-24, 1994.

22. Harrison, D. J., Fluri, K., Chiem, N., Tang, T., Fan, Z., *Technical Digest*; Transducers 95, 8th Int. Conf. Solid-State Sensors and Actuators, Stockholm, June 25-29, pp 752-755, 1995.

23. Fluri, K., Fitzpatrick, G., Chiem, N., Harrison, D. J., *Anal. Chem.*, 68, 4285-4290, 1996.

24. Hjerten S., *J.Chromatogr.*, 347, 191-198, 1985.

25. Ocvirk, G., Tang, T., Harrison, D. J., *Analyst*, 123, 1429-1434, 1998.

26. Wetmur J. G., Davidson, N., *J. Mol. Biol.*, 31, 349-370,1968.

27. Thrower, K. J., Peacocke, A. R., *Biochem. J.*, 109, 543-557,1968.

28. Subirana, J. A., Doty, P., *Biopolymers*, 4, 171-187, 1966.

29. Chang, C. T., Hain, T. C., Hutton, J. R., Wetmur, J. G., *Biopolymers*, 13, 1847-1858, 1974.

30. Bloomfield, D. H., Benevides, Jr. G. J., *Nucleic Acids Res.*, 28, 3379-85, 2000.

31. Hamel, K. J., Crosson, P., Lee, J. S., *Biochemistry*, 30, 4455-9, 1991.

32. Panagiotis, C. A., Artandi, S., Calame, K., Silverstein, S. J., *Nucleic Acids Res.*, 23, 1800-1809, 1995.

33. Pingoud, A., Urbanke, C., Alves, J., Ehbrecht, H. J., Zabeau, M., Gualerzi, C., *Biochemistry*, 23, 5697-703, 1984.

34. Hogrefe, H. H., Hongrefe, R. I., Walder, R.Y., Walder, J A., *J. Biol. Chem.*, 265, 5561-5566, 1990.

35. Bekkaoui, F., McNevin, J., Leung, C., Peterson, G., Bhatt, R. and Bryan, R. Development of a colorimetric cycling probe technology assay for the identification of methicillin resistant *Staphylococcus aureus* cultures. Presented at the Cambridge Healthtech Institute Conference: Advances in labels, signaling and detection. June 5-6, San Diego, CA, 1997.

36. Crank, J. The Mathematics of Diffusion 2nd Edition. Oxford: Clarendon Press., pp 14-16. 1975.

37. Harris, D. C., "Quantitative Chemical Analysis" 5th Edition, pp 656, Freeman Press, 1998.

CHAPTER 4: A μ-TAS for Detection of Pathogens in the Environment Using Cycling Probe Technology for DNA Amplification

4.1 Introduction

The field of medical diagnostics and biodetection is about to undergo significant changes in terms of high throughput and speed with the advent of "lab on chip" technology [1-3]. The 90's has brought about many changes in how experiments are conceived in traditional chemistry, biology and other scientific and engineering laboratories. Chemical and biochemical reactions can be performed on microchip-based devices, followed by capillary electrophoresis (CE) based separation and detection [4-11]. The efficiency, speed and ease of automation these devices offer provides a convenient option in the near future for small, rugged and portable instrumentation.

The work presented in this chapter further explores the ideas presented in Chapter 3, using cycling probe technology (CPT) [12-14] as a DNA amplification technique for detecting bacterial pathogens in the environment. CPT, which utilizes the hybridization of a tagged DNA-RNA-DNA probe (~29 bases long) with target DNA in the presence of a nuclease enzyme, RNase H, has been reviewed in Chapter 1 and Chapter 3. The integrated DNA analysis system described in Chapter 3 is not equipped to isolate the DNA from bacterial spores, but it is feasible to connect our system to a sample delivery system such as the minisonicator for disruption of bacterial spore reported by Northrup et al [15].

In this chapter we show that the system described in Chapter 3 is suitable for detection of bacterial pathogens that may be present in the environment. Using different

concentrations of the genomic DNA target which was from the simulant, E*rwinia herbicola*, a calibration curve could be constructed to provide quantitation. *Erwinia herbicola* (EH) is Gram-negative bacteria. It is common in the environment and breaks down vegetative material found in ditch water. It has been used as field trial organism for developing new methods and apparatus for environmental monitoring. Since it is common in the outdoors, it poses little risk to the environment flora or fauna, nor to people conducting field trials.

The rapid and accurate detection and identification of bacterial pathogens in the environment is of high priority to avoid further contamination. The most sensitive method available to biologist for detecting bacterial pathogens is culture growth, which requires at least an 8 h incubation of the sample in culture medium, followed by biochemical and/or immunological tests to identify the bacteria [16,17]. Rapid immunological tests are available, but are less sensitive, with reliable results seen only in samples with over 10^5 CFU/ml [17]. Hence these tests are not adequately sensitive. In addition, the specificity of these tests is often inadequate. PCR has been applied to the detection and identification of a number of specific bacterial pathogens [17]. However, as reported in the literature [4-7] most of the micro-chip based systems incorporated two modules, one for doing PCR and the second for doing CE. In the present work CPT, being an isothermal reaction, allows for easier integration on a single wafer. The design described in Chapter 3 should lead towards full automation.

4.2 Experimental

4.2.1 Materials and Methods

4.2.1.1 Target DNA

All the work involved in the development of the probe and target for the *Erwinia herbicola* CPT assay was done at CW Bios Inc. (Calgary, AB, Canada) and the Defence Research Establishment Suffield (DRES) (Medicine Hat, AB, Canada).

Erwinia herbicola (ATCC # 33243) was obtained from the American Type Culture Collection (Rockville MD). Bacteria were grown overnight in Luria-Bertani broth at 27 °C. Genomic DNA was isolated by standard methods [18], phenol-extracted, sheared by 10 passages through a 21-gauge needle and resuspended in sterile nuclease-free water. Genomic DNA was sonicated to lengths of 0.5-2 kb and the concentration adjusted to 0.1 µg/µL. Sample dilutions were made in nuclease-free water (autoclaved diethylpyrocarbonate treated Millipores water (Milli, QUV plus)) from these stock concentrations.

4.2.1.2 CPT Reagents

The EH probe (Fluorescein- 5' acg cgg ggc gg (aaaa) cct gct ctc gca g3'-$(Biotin)_3$) and target DNA were obtained from CW Bios Inc. The enzyme RNase H from *thermus thermophilus* was from ID Biomedical, (Vancouver, BC, Canada). The 28 bases long chimeric probe was engineered and synthesized to complement the EH target (see section 4.3 for the probe, design strategy and assessment). The probe that was used for most of the study had three biotin labels at the 3' end and fluorescein at the 5' end and is referred to as the EH8 probe.

4.2.1.3 Chemical Reagents

All materials used when performing CPT (pipette tips, PCR tubes) were from Rose Scientific (Edmonton, AB, Canada) and were certified RNase and DNase free. Other chemicals used were all Molecular Biology grade from Sigma Chemicals, including phosphate buffer (K_2HPO_4 and KH_2PO_4), acrylamide, [γ-(methacryloyoxy)propyl]- trimethoxysilane, potassium persulfate, N,N,N,N'-tetramethylethylenediamine (TEMED), Triton-X 100, $MgCl_2$, urea and spermine hydrochloride.

4.2.2 Devices

Microchannels were etched in 4 inch square 0211 glass (Corning, NY, USA) as described and in Chapter 3 and Section 3.2.4 (see also refs 19, 20). Also, 1.9 mm diameter access holes were drilled in the cover plates which were then thermally bonded to the etched plates to form the microfluidic devices, as described in Chapter 3. The chip used was the GOCPTTT device shown in Figure 4.1 and the instrumentation has been described in detail in Chapter 3, Section 3.2.12 to 3.2.15. The CPT chip layout was designed with a four inlet mixer, in order to allow separate delivery of sample (target DNA) and reagents (namely the CPT probe, enzyme, Mg^{2+} and flushing buffer). Two of the inlet ports were loaded with EH DNA target and the other two with enzyme and probe, respectively. As illustrated in Figure 4.1, four channels intersected to mix the sample and reagents and were directed towards a reaction coil. A single exit channel from the reaction coil allowed delivery of the incubated CPT mixture to an injector and a separation channel. The reaction coil sits on a heating element, which can be raised to around 60 ^{o} C, the temperature at which the CPT reaction operates.

4.2.3 Channel Derivatization

Channel walls were coated with polyacrylamide with minor modification to Hjerten's procedure [21], see Chapter 3, Section 3.2.8 for details.

4.2.4 Instrumentation

Details on the instrumental setup are given in Chapter 3. The device in Figure 4.2 was run by previously described [19,20] in house built computer controlled power supply system (-15 KV, MJ series, Glass high voltage, Whitehouse station, NJ, USA) with high voltage relays (30 kV, kilovac, Santa Barbara, CA, USA). The optical detection used was based on an epifluorescent confocal microscope, described earlier by Ocvirk et al [22] and also in Chapter 3. All equipment and data acquisition was computer controlled (Macintosh, PowerPc 7100/80) and run by a program written in labview (National Instrument, Austin, TX, USA)

4.2.5 On-chip Cycling and Separation

The buffer used through the process of mixing, cycling (incubation) and separation was 10 mM phosphate (pH 6.8), 0.05 % Triton X-100, 4 mM $MgCl_2$ and 0.2 mM spermine. The probe concentration was 50 nM and the enzyme concentration was 0.02 µg/µl. Each reservoir received 50 µl of solution. After mixing in the reaction coil all reagents were essentially diluted by a factor of two giving concentration 25 nM for the probe and 0.01 µg/µl for the enzyme.

The voltage sequences used for EH analysis are all given in Table 4.1. The device consist of 4 inlet ports to drive reagents by electrokinectic pumping (step 1, 600 sec) to the reaction coil which sits on a heating element (Peltier operated at reversed mode). After flushing the excess reagents in the separation channel (step 2, 180 sec), 5

repeated injections and separations were performed (step 3, 20 sec and step 4, 300 sec) to obtained electropherograms prior to the CPT reaction, which were to be used as control experiments. Cycling (incubating) was then performed at 60 °C for 30 min (step 5). The CPT products were driven to the double T junction of the device (step 6, 60 sec). The leading edge of the reaction mixture was flushed away to Buffer Waste (step 7, 120 sec) prior to the injection (step 8, 20 sec). The separation (step 9, 300 sec) was then performed with detection by LIF. Five injections and separations were performed for each set of data. After 5 injections, the reaction coil was loaded with fresh reagents as in step 1 followed by a subsequent control run as in step 2 and 3 and so on.

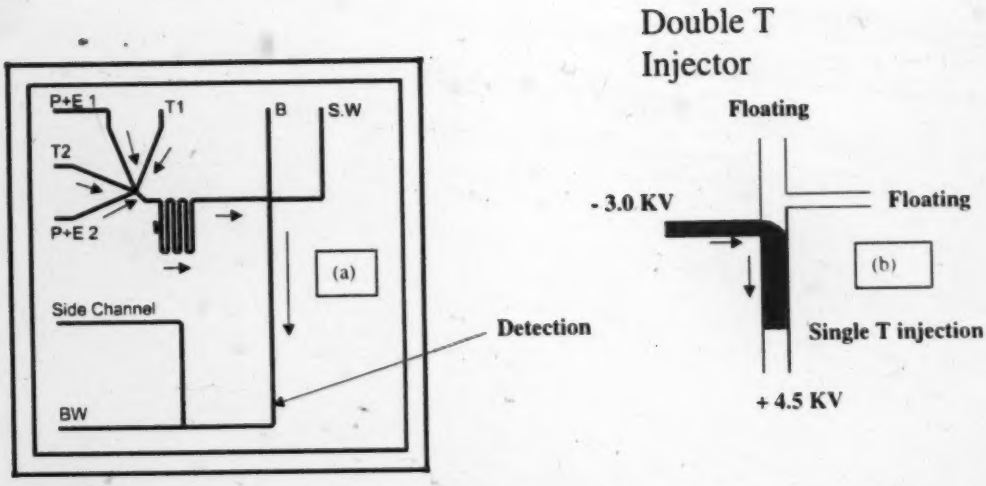

Figure 4.1: (a) CPT Chip layout, where P+E1and P+E2 represent probe and enzyme reservoirs and T1 and T2 represent target reservoir respectively. B, BW and SW are Buffer Inlet, Buffer Waste and Sample Waste reservoirs. (b) Illustrates a single T injection scheme.

Table 4.1: Voltage and Relays Switching Matrix for Fluidic Control of Microchip

		Reservoir voltage (kV)								
Step	**Reservoirs**	**P+E[1]**	**P+E[2]**	**T1**	**T2**	**B**	**BW**	**SW**	**Side**	**Time (sec)**
1	Fill Reactor	-3.5	-3.0	-3.0	-3.0		+ 4.5	-	-	600
2	Flushing					GND	+5.0	-	-	180
3	Injection	-3.5	-3.0	-3.0	-3.0		+4.5	-	-	20
4	Separation	-	-	-	-	GND	+5.0	-	-	300
5	Reaction	-	-	-	-	-	-	-	-	1800
6	Mobilization	-3.5	-3.0	-3.0	-3.0	-	-	+ 4.5	-	60
7	Flushing					GND	+5.0	-	-	120
8	Injection	-3.5	-3.0	-3.0	-3.0	-	+ 4.5	-	-	20
9	Separation	-	-	-	-	GND	+ 5.0	-	-	300

4.3 Results and discussion

4.3.1 Earlier Work

The integrated device presented in Chapter 3 worked successfully with the synthetic CPT reagents derived from methicilin resistant *Staphylococcus aureus* (MRSA) genes obtained from ID Biomedical. The lowest target concentration obtained on the device was in the order of attomoles in 100 µl. The next goal was to evaluate the system for detection and quantitation of genomic target derived from *Erwinia herbicola*, a simulant for anthrax contamination and bacterial pathogens in the environment.

A CPT assay has also been successfully developed, with sufficient sensitivity in a radioisotopic format to identify as few as 250 organisms of *Mycobacterium tuberculosis* [23]. Such an assay, when done by traditional bacteriological methods, is slow and expensive [16,17]. CPT has also been used to successfully identify vancomycin-resistant enterococci [24,25] and methicillin-resistant *Staphylococcus aureus* [26-29] in clinical samples using radioisotope and colorimetric enzyme immunoassay (EIA)-based detection in microtitre plates. Our aim was to evaluate the microchip-based system for detecting enviromental pathogens, using CPT.

4.3.2 Development of CPT Probes to Detect for *Erwinia herbicola* Target DNA

The development and the assesment of the probe was done by CW Bios Inc. and DRES in collaboration with ID Biomedical. Candidate sequences for CPT gene probe design were selected from published *Erwinia herbicola* (EH) gene sequences listed in the Genbank sequence database (National Center for Biotechnology Information, National Institutes of Health, Bethesda, MD, USA).

The design strategy included selecting sequences of 26-31 nucleotides containing four consecutive adenosine residues. Candidate sequences were analyzed for secondary structure formation and melting temperatures (T_m) using the OLIGO Program Version 5.1 for Macintosh (NBI/Genovus Inc. Plymouth, MN, USA). Sequences that exhibited low secondary structure formation (both intra- and inter-strand formation) and sequences in which the two cleaved product sequences had T_m that were similar, but lower than their intact parent probe, were screened against the Genbank database using either Internet BLAST searches [30] or FINDPATTERNS searches (GCG Wisconsin Package Release 9.1, July 1997, Genetics Computer Group, Madison, WI, USA). Sequences that exhibited unique homology to EH sequences were synthesized and assessed in CPT reactions. Using this approach, nine probe sequences representing three separate genes (beta-glucosidase, dimethylallyltransferase and tyrosine phenol-lyase) were synthesized by Integrated DNA Technologies (Coralville, IA, USA) with a 5' fluorescein label and three-3' biotin labels. Probes were analyzed by CE-UV and CE-LIF and ranged in purity from 95-100%. The 3' terminus of the 5' fluoresceinated probe was biotinylated with terminal deoxynucleotide transferase (Amersham Pharmacia following product directions) by reacting 1000 pmol of biotin-16-ddUTP (Sigma Chemical Co., St. Louis, MO, USA) with 100 pmol of 5' fluoresceinated probe (10:1 mole ratio). Labeled probes were purified on NICK® columns and eluted in a volume of 400 µL nuclease-free water to a final concentration of 250 nM. Biotinylated fluorescein probes showed greater than 90% biotin-labeling efficiency when analyzed by CE-LIF. These probes were subsequently used without further purification and were stored at –20 °C.

4.3.2.1 Assesment of CPT Probes

The nine probe sequences were characterized by CW Bios Inc. for C2 activity (probe cleavage in the absence of target DNA) and for producing cleaved products in the presence of synthetic and genomic target DNA using radioisotopic CPT. All probes were initially predicted to have a low probability of intra-strand and inter-strand interactions using the OLIGO™ program. However, experimentally, several probes exhibited C2 activities greater than 10%. The addition of EDTA to the C2 sample for these probes showed that the observed C2 activity was due to the enzymatic cleavage of the probe in the absence of target. Probe sequences that exhibited high C2 activity were subsequently re-analysed by computer, using temperatures and sodium ion concentrations closer to the actual reaction conditions. Re-analysis suggested the probes formed stable secondary structures that promoted non-specific cleavage of the ribonucleotide region by RNase H. One probe sequence that exhibited acceptably low background C2 activity, as well as good target recognition for both synthetic and genomic target DNA in isotopic assays, as shown in Figure 4.2, was EH8, a probe for the tyrosine phenol-lyase gene. The data shown in Figure 4.2 was obtained from ^{32}P CPT products separated by slab gel electrophoresis. The EH system performed well in the cycling probe reaction when using the EH8 probe for target detection. With 10^7 to 10^4 EH target copies, 53.7 to 13.7 % cleavage of the probe were observed. The data in Figure 4.2 also include a C1 control where only probe was incubated in cycling buffer. This was done to measure the integrity of the probe to resist heat without undergoing DNA-RNA bond cleavage.

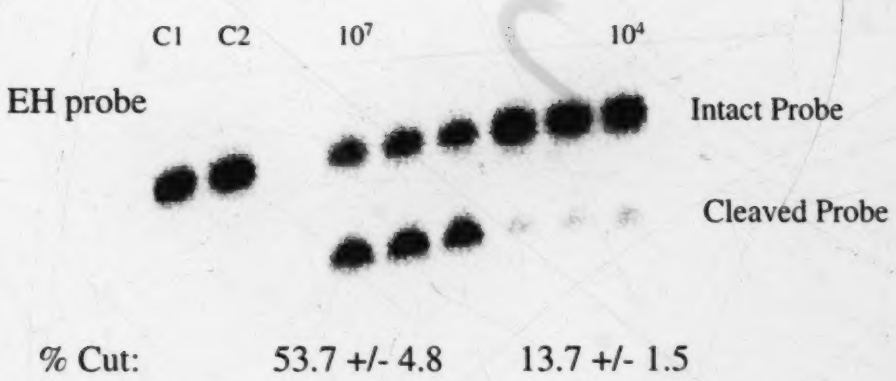

Figure 4.2: Representative isotopic CPT assays with sonicated *Erwinia herbicola* genomic DNA. Assays were performed using 2 fmol probe/reaction. Samples used $10^7$and 10^4 copies of chromosomal DNA as indicated. Values beneath autoradiograms indicate corrected % cuts EH8. Courtesy of CW Bios Inc. (Calgary, AB, Canada) and DRES (Suffield, AB, Canada).

The fluorescent labeled probe was then tested in LIF capillary gel electrophoresis (CGE) format. The successful results obtained (data not shown), indicated performing the assay in a chip format was possible.

4.3.3 CPT Assay for *Erwinia herbicola* in a Chip Format

The next challenge, which is the main focus of this chapter, was to test whether the experimental conditions optimized for earlier work with MRSA DNA system would work for the EH analysis. The probe used was again an asymmetric probe, with the 3' end labeled with three biotins and the 5' end labeled with fluorescein for LIF detection. After the CPT reaction, the products obtained were excess (unreacted) intact probe and two classes of probe fragments, one containing fluorescein and the other biotin. Three biotin labels on the 3' end of the probe helped in the separation by providing a moiety of the DNA mer with a perturbed charge to friction ratio [31]. Since the fluorescein labeled fragmented DNA probe did not have the biotin, separation of the two was readily achieved.

The complete assay on-chip for EH is shown in Figure 4.3. The electropherograms shown in Figure 4.3 were obtained using the same optimized conditions as for earlier work with an MRSA sample. These conditions are described in Chapter 3 (10 mM phosphate buffer, 0.01% Triton X-100, 4 mM $MgCl_2$ and 0.2 mM spermine). The amount of EH target DNA was prepared in 100 µl of phosphate buffer and 50 µl aliquots were delivered to each reservoir. The stated amount of target are for the concentrations in the reaction coil, which was 1.6 attomoles in 100 µl. The three traces shown in Figure 4.3, from bottom to top are electropherograms, (i) prior to

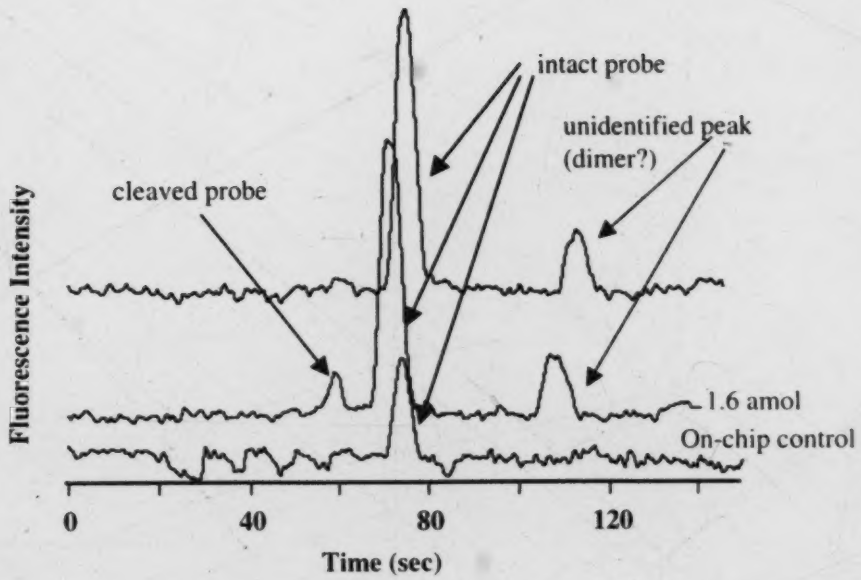

Figure 4.3: On-chip CPT reaction for 1.6 attomoles (10^6 copies) followed separation of EH target DNA in 100 µl reaction volume in a 10 mM phosphate buffer, 0.05% Triton-X-100, 4 mM $MgCl_2$, and 0.2 mM spermine. Reaction time was 30 min. The bottom trace is the On-chip control before incubation, the central trace is after cycling and the upper trace is after flushing with unreacted probe. 20 s single T injections were performed at 3.0 kV, followed by 5.5 kV separation voltage. The ratio of cleaved to intact probe is 0.1 with % RSD of 9. The amount of cleaved probe is ~10 % corresponding to an to amplification factor of about 10^5.

incubation (cycling), (ii) after cycling for 30 min, (iii) after flushing out the reaction zone and running in new sample from the reservoir. The various time periods and sequence of voltages used in loading, flushing, cycling and separation for any of the on-chip experiments dealing with EH analysis are found in Table 4.1. The first trace from the bottom shows the electropherogram prior to reaction, where only the intact probe was observed. The second trace shows the emergence of the peak from the cleaved probe before the intact probe. The third trace confirms that the cleaved probe was due to cycling. The % RSD for the peak area ratio of cleaved to intact probe was ~ 9%. The amount of cleaved probe was ~ 10%, which led to an amplification factor, calculated from the ratio of cleaved probe and amount of target used of $\approx 10^5$. One point to note, though, is the occasional appearance of a third peak, which may be a dimer artifact for either the probe-probe hybrid or probe-target hybrid. For the purpose of detecting the target DNA, dimerization is not really a concern. However, such artifacts can be a significant issue in quantitation. Usually dimers appear because of the absence of a quenching or denaturing reagent such as urea. During the design of the GOCPTTT device, it was decided not to deliver CPT quenching reagents or additional buffers to adjust the solution composition for separation. A y-shaped mixing intersection could be added in future designs to allow for composition adjustments downstream of the reactor. In essence, for the present work, the goal was focused on the detection rather than the exact quantitation of the EH target using CPT on a chip.

The lowest amount of target detected i.e. 1.6 amol/100µl shows the technology's sensitivity towards the detection of biological pathogens in the environment.

4.3.3.1 Calibration

The experiment was also run for different concentrations of target cycled for 30 min on-chip. Figure 4.4a shows the electropherograms from 1.6 to 16 amol of target in a 100 µl volume. The calibration curve of the peak area ratio for cleaved to intact probe versus target concentration is shown in Figure 4.4b, covering the range from 1.6 to 64 amol in 100 µl volume. At 64 amol the graph in Figure 4.4b reaches a plateau at which the probe has been mostly consumed. The calibration curve has good linearity in the range 1.6 to 16 amol of target where a log–log plot of the data in Figure 4.4a was linear and had a gradient of 1.17 as shown in Figure 4.4c. The amplification factor was on the order of 10^5, as shown in Table 4.2. The results also reflect the same phenomenon observed in the case of MRSA sample where linear kinetics [32] were observed only in a range of low target probe consumption. Nevertheless, the data illustrate that quantitative calibration is feasible.

Table 4.2: The percent probe cleavage and amplification factors for data in Figure 4.5a.

Amount of EH Target amol /100 µl*	% Probe Cleavage	Amplification Factor
1.6	10	1.56×10^5
6.4	37	1.44×10^5
9.6	50	1.30×10^5
16	64	1.00×10^5
64	95	3.70×10^4

* Probe and enzyme concentration were 25 nM and 0.01 µg/µl.

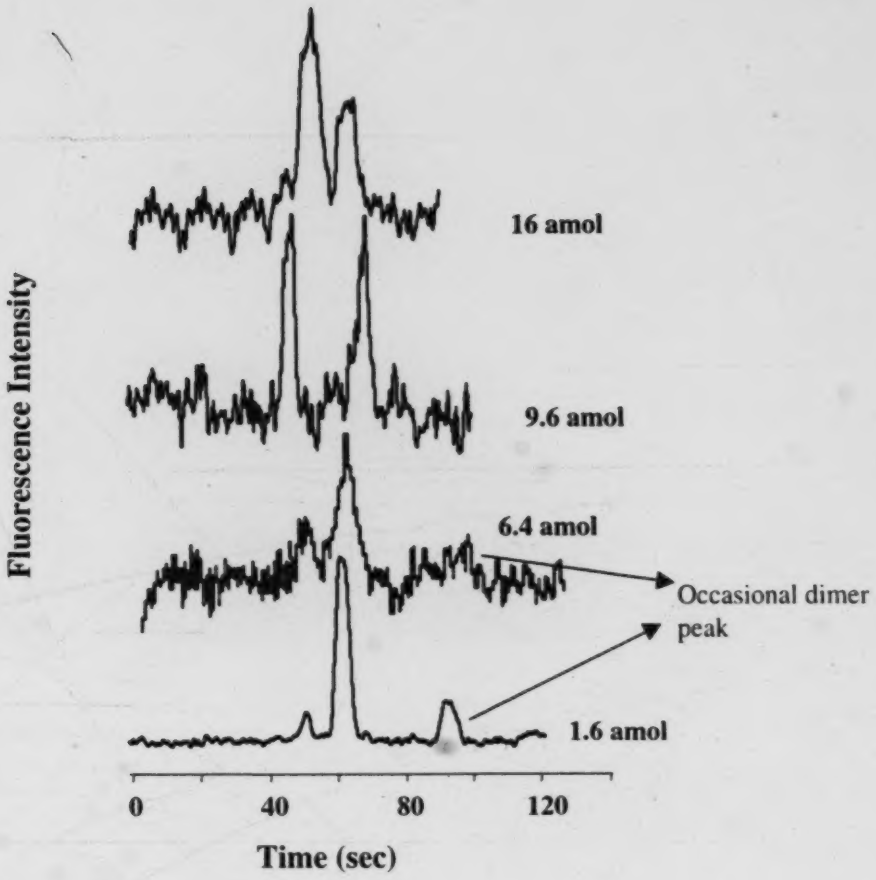

Figure 4.4: (a) Electropherograms of on-chip CPT reaction products for 1.6 to 16 amol of EH target DNA in 100 µl CPT buffer: 10 mM phosphate buffer, 0.05% Triton-X-100, 4 mM $MgCl_2$, and 0.2 mM spermine. 20 s single T injections at 3 kV. Separation voltage of 5.5 kV.

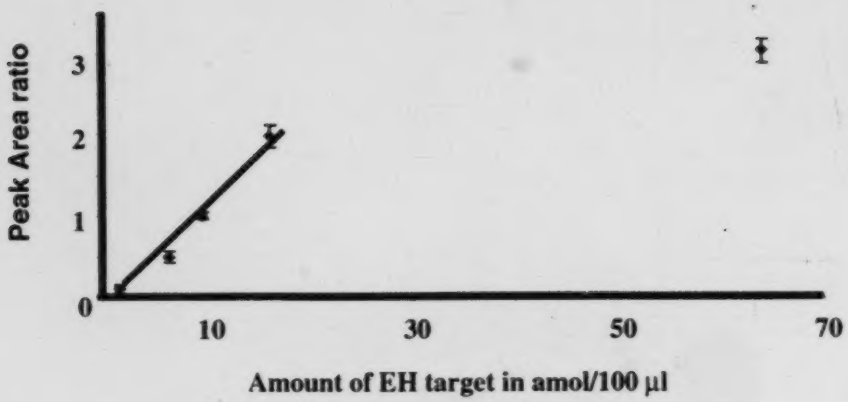

Figure 4.4: (b) On-chip calibration curve for EH samples between 1.6 to 64 amol of target in 100 µl. Error bars represent s.d. for 5 replicates

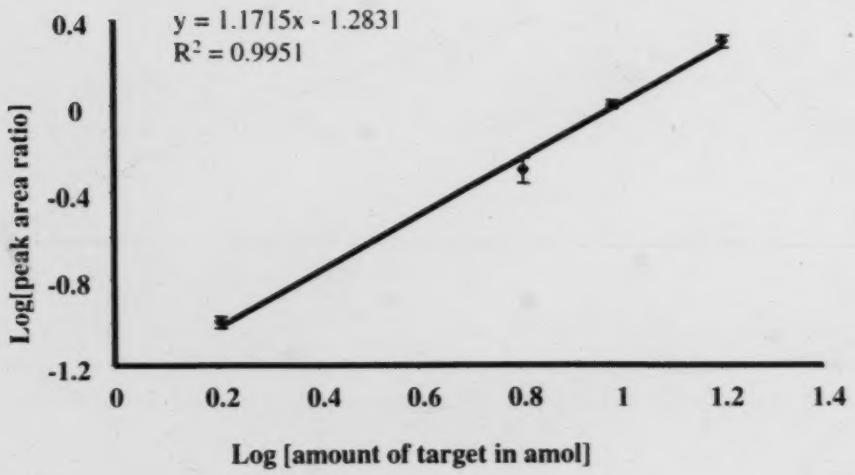

Figure 4.4: (c) On-chip calibration curve for EH sample from 1.6 to 16 amol of target in 100 µl in a log-log plot format.

4.3.3.2 On-chip Reaction using 15 min Incubation Time

When compared to the earlier work with MRSA, the assay for the EH sample showed faster kinetics. For 30 min incubation time and 25 amol/100µl of MRSA target DNA, 18 % probe cleavage was observed. However, with 16 amol/100µl EH target DNA, 64 % probe cleavage was observed. The greater reactivity for EH suggested the reaction required a shorter incubation period. An assay with 16 amol of EH target DNA in 100 µl volume was allowed to incubate for only 15 instead of 30 min. The electropherogram in Figure 4.5 shows the resulting CPT products.

The peak area ratio for cleaved and intact probe was 0.47, with a 10 % RSD. The amount of cleaved probe was ~35 %, as compared to 64 % probe cleavage observed with a 30 min incubation time. The experiment shows that the analysis time can be reduced.

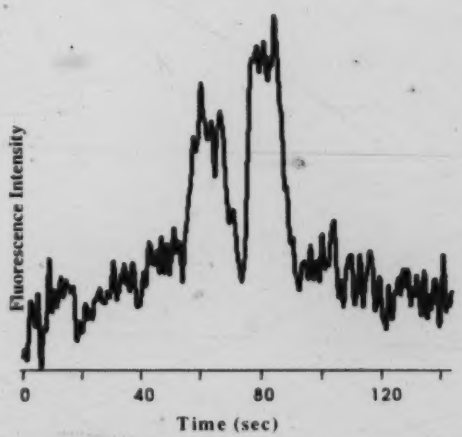

Figure 4.5: Electropherogram following 15 min incubation of 16 amol of EH in 100 µl solution. The same buffer conditions were used as in Figure 4.4a.

4.4 Conclusion

The traditional method for detection of bacterial pathogens uses culture formation requiring several hours as a minimium analysis time [16,17]. For field measurements such methods are inadequate when results are needed in matters of minutes. This chapter explores the idea of a rapid method that detects nucleic acid on a chip using cycling probe technology. The results show promise for detection of pathogens in the environment

offering a faster analysis, with potentially greater reliability of identification of a specific organism. Detection limits in the attomole range have been demonstrated, indicating good sensitivity. Quantitation can be linear in the attomole range. However, the occasional presence of an artifact peak may require further improvements to optimize quantitative measurements.

4.5 Reference

1. Manz, A., Graber, M., Widmer, H. M., *Sens. Actuators*, B, 1, 244-248, 1990.
2. Harrison, D. J.; Manz, A.; Fan, Z.; Lüdi, H.; Widmer, H. M., *Anal. Chem.*, 64, 1926-1932, 1992.
3. Harrison, D. J.; Fluri, K.; Seiler, K.; Fan, Z.; Effenhauser, C. S.; Manz, A., *Science*, 261, 895-897, 1993.
4. Woolley, A. T., Hadley, D., Landre, P., deMello, A. J, Mathies, R. A., Northrup, A. M., *Anal Chem.*, 68 4081-4086,1996.
5. Cheng, J., Shoffner, M. A., Hvichia, G. E., Kricka, J. L., Wilding P., *Nucleic Acids Res.*, 24, 381-385, 1996.
6. Kopp, M. U., deMello, A. J., Manz, A., *Science*, 280, 1046-1048, 1998.
7. Waters, L. C., Jacobson, S. C., Kroutchinina, N., Khandurina, J., Foote, R. S., Ramsey, J. M., *Anal. Chem.*, 70, 158-162, 1998.
8. Jacobson, S. C., Ramsey, J. M., *Anal. Chem.*, 68, 720-723, 1996.
9. Khandurina, J., McKnight, T. E., Jacobson, S. C., Waters, L. C., Foote, R. S., Ramsey, J. M., *Anal Chem.*, 72, 2995-3000, 2000.
10. Taylor, T. B., Winn-Dawn, E. S., Picozza, E., Wodenberg T. M., Albin, M., *Nucleic Acids Res.*, 25, 3164-3168, 1997.

11. Colyer, C. L., Tang, T., Chiem, N., Harrison, D. J., *Electrophoresis*, 18, 1733-1741, 1997.

12. Duck, P., Alvarado-Urbina, G., Burdick, B., Collier, B., *Biotechniques*, 9, 142-147, 1990.

13. Bekkaoui, F., Poisson, I., Crosby, W., Cloney, L., Duck, P., *Biotechniques*, 20, 240-248, 1996.

14. Z. Modrusan, F. Bekhaoui, and P. Duck, *Mol. and Cell. Probes*, 12, 107-116, 1998.

15. Belgrader P., Hansford, D., Kovacs, G. T. A., Venkateswaran, K., Mariella, R., Milanovich, Jr., F., Nasarabadi, S., Okuzumi, M., Pourahmadi, F., Northrup, M. A., *Anal. Chem.*, 71 , 4232 -4236, 1999.

16. Bergey D. H., Holt, J. G., "Bergey's Manual of Determinative Bacteriology" 9th ed., Baltimore, Williams and Wilkins, 1994.

17. Persing, D. H., Smith, T. F., Tenover, F. C., White, T. J., " Diagnostics Molecular Microbiology, *Principles and Applications*", 1993.

18. Sambrook, J., Fritsch, E. F., and Maniatis, T., Molecular cloning: A Laboratory Manual. Cold Spring Harbor Laboratory Press: Cold Spring Harbor, NY, 1989.

19. Chiem, N., Harrison, D. J., *Anal. Chem.* 69, 373-378. 1997.

20. (i) Harrison, D. J., Fan, Z., Fluri, K., Seiler, K., *Technical Digest*; Hilton Head Sensor and Actuator Workshop, June 13-16,; pp 21-24, 1994. (ii) Harrison, D. J., Fluri, K., Chiem, N., Tang, T., Fan, Z., *Technical Digest*; Transducers 95, 8th Int. Conf. Solid-State Sensors and Actuators, Stockholm, June 25-29,; pp 752-755, 1995.

21. Hjerten, S., *J .Chromatogr.*, 347, 191-198, 1985.

22. Ocvirk, G., Tang, T., Harrison, D. J, *Analyst*, 123, 1429-1434, 1998.

23. Beggs, M. L., Cave, M. D., Cloney, L, Marlowe, C., Duck, P., Eisenach, K. D., *J. Clin. Microbiol.*, 34, 2985-2989, 1996.

24. Modrusan, Z., Hedberg, B.J., Marlowe, C.B., Pirseyedi, D., Wheeler, D and Bryan, R., Detection of vancomycin resistant enterococci (VRE) in clinical isolates by cycling probe technology (CPT). Paper presented at ASM Conference on Molecular Diagnostics and Therapeutics, August 15-19, 1997, Kananaskis, Alberta, Canada.

25. Modrusan, Z., Marlowe, C., Wheeler, D., Pirseyedi, M., Bryan, R. N., *Mol. Cell. Probes*, 13, 223-231, 1999.

26. Cloney, L., Marlowe, C., Wong, A., Chow, R., Legasse, H., Dawson, T. and Bryan, R. 1997. Rapid detection of the *mecA* gene in clinical isolates using a novel DNA-probe assay. Presented at the ASM 97th General Meeting, May 4-8, 1997, Miami Beach, Florida.

27. Bekkaoui, F., McNevin, J., Leung, C., Peterson, G., Bhatt, R. and Bryan, R. Development of a colorimetric cycling probe technology assay for the identification of methicillin resistant *Staphylococcus aureus* cultures. Presented at the Cambridge Healthtech Institute Conference: Advances in labels, signaling and detection. June 5-6, 1997, San Diego, CA.

28. Bekkaoui, F., McNevin, J. P., Leung, C. H., Peterson, G. J., Patel, A., Bhatt, R. S., Bryan, R. N., *Diagn. Microbiol. Infect. Dis.*, 34, 83-90, 1999.

29. Cloney, L., Marlowe, C., Wong, A., Chow, R., Bryan, *R. Mol. Cell. Probe.*, 13, 191-197, 1999.

30. Altschul, S. F., Gish W., Miller, W., Myers, E. W., Lipman, D. J., *J. Mol Biol.*, 215, 403-410, 1990.

31. Heller, C., Slater, G.W., Mayer, P., Dovichi, N.J., Pinto, D., Voivy, J., Drouin, G., *J. Chromatogr.*, 806, 113-121, 1998.

32. Hogrefe H. H., Hongrefe, R.I., Walder, R.Y., Walder, J. A., *J. Biol.Chem.*, 265, 5561-5566, 1990.

CHAPTER 5: Conclusion and Future Suggestions

5.1 Conclusion from the Thesis Work

The thesis work focuses on integrating an isothermal DNA amplification reaction to detect for specific DNA strains, being representative of typical clinical and biological assays. In the first chapter I overviewed most of the "lab on chip" technology related to DNA assays, reported in the literature. I explained why cycling probe technology (CPT) was chosen, instead of renowned methods such as PCR, to be implemented on a chip for DNA amplification and quantitation. The first reason was the isothermal nature of CPT and the second reason was CPT was developed as a linear amplification reaction as compared to PCR, hence making quantitation on-chip a much easier process. In essence this thesis work demonstrates two important aspects of CPT. First, quantitation of DNA is possible on-chip using CPT, and secondly, to get a linear calibration, we need to operate in a region where target concentration is small relative to probe concentration. This was shown in Chapter 3 where the plot of peak area ratio of the cleaved to intact probe versus amount of target in the low concentration regime gives a rectalinear calibration curve, Figure 3.12b.

This thesis work started with the development of a CE system based on poly(dimethylsiloxane) PDMS coated capillaries. Previous group members found that PDMS coating worked well for protein separation. However, further experiments we performed to study the flow behavior showed that to get predictable and near zero EOF in PDMS coated capillaries, the addition of ionic surfactants was needed. The reason for choosing the PDMS coating was mainly because the coating is cured at high temperature (see experimental section Chapter 2). Hence it was expected that the PDMS coating

would be highly stable at 60 °C, temperature at which CPT operates. However, the need to add surfactants such as CTAB, to get near zero EOF, deterred its use for further work on the CPT project.

On the other hand, the conclusion from Chapter 2 demonstrates the potential of using PDMS coated capillaries for protein separation. Also, addition of surfactant created a subsequent dynamic coating that can work simultaneously with the permanent PDMS coating to enhance the latter's performance for preventing analyte-wall interaction. It can be anticipated that the addition of surfactant can also act as a pump to induce flow in whichever direction is required in the PDMS coated capillaries.

For the subsequent CPT work, Hjerten's procedure [1] for coating was used, where acrylamide is polymerized inside the channels. The coating worked perfectly, in the preliminary stage of the CPT work, when a free-flow (i.e., CZE mode) separation technique was being developed. In the early stage of the work, the CPT was performed off-chip and separation on chip, where no heating was done on the chip, hence the reason for the good performance of the coating, to produce reproducible results. However, problems started with the on-chip work in the GOCPTTT device. The coating was not stable at high temperature and successive heating cycles (incubation) damaged the polyacrylamide coating. This problem was alleviated by using fresh coating chemicals. The chemicals that played an important role to improve surface modification was the radical initiator for the polymerization of acrylamide, namely TEMED and potassium persulfate. The degree of purity of TEMED and the persulfate dictated the quality of the coating. With the improved coated surface, the number of heating cycles that could be performed on the chip was considerably increased. Hence, enough samples could be run

to effectively construct a calibration curve before any deterioration of the coating was observed. With improved surface modification, on-chip CPT was reproducibly performed, which eventually led to calibration.

Two distinctive DNA assays were shown to work on-chip, where the synthetic MRSA and genomic EH samples analyzed (from Chapter 3 and 4 respectively), are representative of typical clinical assays for the former and simulants of bacterial pathogen in the environment for the latter. The results demonstrate the potential of electrokinetic devices for the integration of the sequence of mixing, enzymatic DNA reactions to provide signal amplification, separation of the reaction products and finally detection.

5.2 Surface Modification and Suggestions for Further Work with Preliminary Data

5.2.1 Surface Modification

Obviously, there were problems with the acrylamide coating, and even though we made it work, research should still be done on finding new coatings which are stable at high temperatures. Such coatings should also be easily implemented on devices with complicated geometry such as the GOCPTTT device. Two coatings mentioned in the literature seemed well suited for high temperature work on chip. The first one is a coating reported by Dovichi and co-workers [2] based on surface modification with Si-C sublayers (Grignard coating) and a series of *N*-substituted acrylamide top-layers. With the Si-C based coating excellent performance after 300 runs was claimed by the authors. Performing the anhydrous Si-C bond formation steps within a network of flow channels, while maintaining rigorously dry conditions was too complicated, and was not used in the present thesis work. Such coating can in essence be tried in our lab, with a proper set-up

to flush the coating reagents in the chip in an inert atmosphere, because of the Grignard reaction. The second coating was reported by Kuhr and co-workers [3], which uses an epoxy resin to coat the surface of the capillary walls. The author claims optimal resolution of single and double stranded DNA fragments was obtained, using buffers containing 0.5% HEC at pH 11 with plate numbers exceeding 3×10^6 plates/m. Coating the microchips with the epoxy reagents was tried and preliminary results were obtained. In the next section a brief experimental detail of the coating procedures will be outlined.

5.2.2 Epoxy Coating

5.2.2.1 Epoxy Coating Procedure

The epoxy resin (Epoxy Technology, Bellirica, MA, USA) consists of two components A and B with mixing ratio A:B of 100:6. The epoxy components were mixed in acetone (analar grade) according to mixing ratio mentioned before and flushed in the "COPI" device (Figure 3.3a) using vacuum. The reagents were allowed to sit for 2 min in the channels and subsequently flushed out using nitrogen. The chips were then introduced in a programmable oven, for coating curing. The curing schedule was, 102 °C for 3h, followed by 150 °C for 1h , 180 °C for 30 min and natural cooling to room temperature.

5.2.2.2 Separation of a Synthetic Mixture of DNA Fragment and the MRSA Probe in Epoxy Coated Channels

The eletropherogram in Figure 5.1 shows the separation 10 nM synthetic mixture of fluorescein labeled 9 mer DNA fragment and the MRSA probe (concentration ratio of 4:1) on the "COPI" device. The buffer was the same as used for the on-chip experiments in Chapter 3 and 4, with 10 mM phosphate (pH 6.8) buffer, 0.05 % Triton X-100, 4 mM

$MgCl_2$ and 0.2 mM spermine. The separation, even though not optimized for the epoxy coating, gave markedly resolved Guassian peaks.

5.2.3 Conclusion

The epoxy coating, if further optimized, can be used as a potential generic coating, in the analysis of DNA on a chip. Such a coating should in essence be more stable than the polyacrylamide coating used in this thesis work.

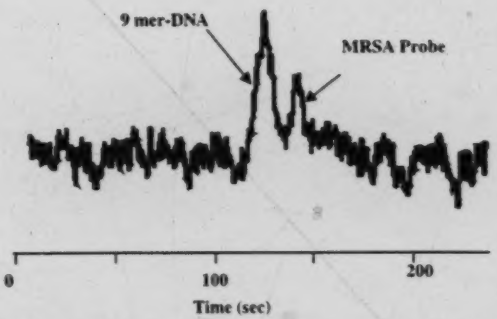

Figure 5.1: Electropherogram for the gel-free separation of , 9 mer-DNA and MRSA probe (concentration ratio of 4:1, 8 nM : 2 nM), in 10 mM phosphate (pH 6.8), 0.05 % Triton X-100, 4 mM $MgCl_2$ and 0.2 mM spermine in the 'COPI' device. 5 s injections at 2.5 kV was performed with a separation voltage at 3.5 kV.

5.3 Future Design

5.3.1 A New Chip and New Set-up

In Chapter 3 and 4, we observed that the four inlet ports in the GOCPTTT design were not necessary, two inlet reservoirs would suffice. Also if better quantitative results are needed, the reactions would most probably need quenching, where more importantly, artifacts like dimers should be avoided. Such things can be avoided with a proper quenching channel after the reaction zone. A Y-shape intersection can be used and such an intersection has been used by former graduate students and post doctoral fellows in this group [4]. Mixing of the reagents occur within seconds for a 40 μm wide channels. In Figure 5.2a a new design of the GOCPTTT is shown. The design would have two inlet ports, A and B, to drive DNA reagents to the reaction zone. Online quenching can be achieved after the CPT reaction by driving the quenching reagents from the reservoir C as

shown in Figure 5.2, before injection and separation. A tentative design is shown in Figure 5.2b where 5 layouts are patterned in one single 4 ″ square wafer.

For future design, better heat controllers would be needed and also a better method to dissipate heat from the unheated area of the chip should be envisaged. The present system only cooled the bottom of the chip, which most probably created a temperature gradient inside the channels. Such problems can sometimes cause the baseline to drift. In future, a two way cooling system should be made that will cool both the top and bottom of the chip.

5.3.2 Ruggedness and Portability

For this apparatus to be really useful, it has to be portable and easy to operate. Our group recently developed with Dycor Technologies (Edmonton, AB) and Defence Research Establishment at Suffield (DRES) under the DARPA project [5], an automated microfluidic platform for immunoassays (DARPA BOX). The first prototype, as shown in Figure 5.3, has been tested in our Laboratory by A. Jemere and N. Chiem. The instrument performed remarkably, even in field trial experiments done at DRES. Such a prototype was designed to fit any type of experiment done on chip. Presently, the DARPA BOX does not incorporate a heating element to perform the CPT reaction, but such an element can be envisaged in a future generation microfluidic platform. Presently, a peristaltic pump which is mounted on the BOX, drives reagents from the outside world to the chip reservoir. This pump can be connected to a sample delivery system such as the minisonicator from Northrup and co-workers [6], hence making a completely portable field instrument for biodetection based on nucleic acid analysis.

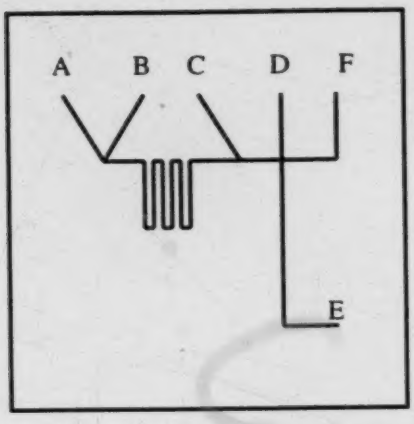

(a)

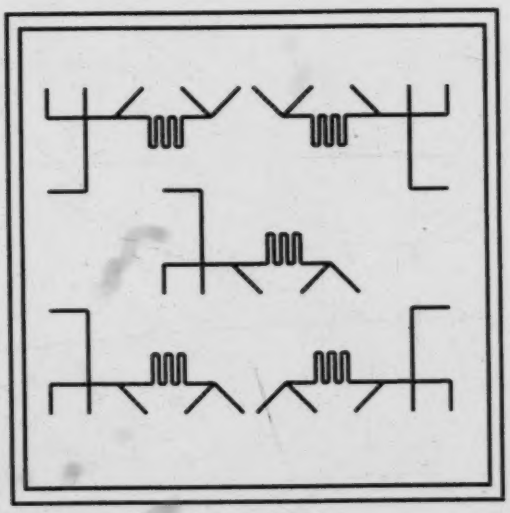

(b)

Figure 5.2: (a) Illustrates a possible future design of the GOCPTTT chip. The device will consist of two inlet ports, A an d B, to drive probe + enzyme and target through to the reaction coil. After incubation the reaction products can be quenched online before exiting to the double T junction (injector). The quenching will be a y-type intersection as shown in the figure and the quenching reagents are driven through from reservoir C. The reservoirs D and E are Buffer Inlet and Buffer Waste respectively. Resevoir F is the sample waste. (b) Illustrates 5 devices patterned on a 4″ wafer.

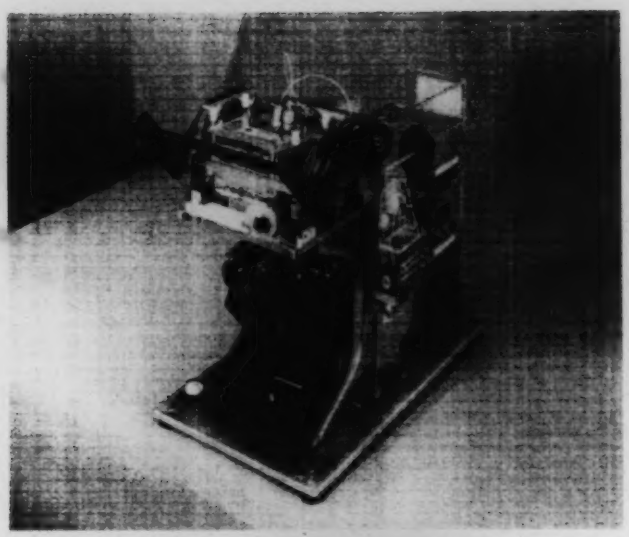

(a)

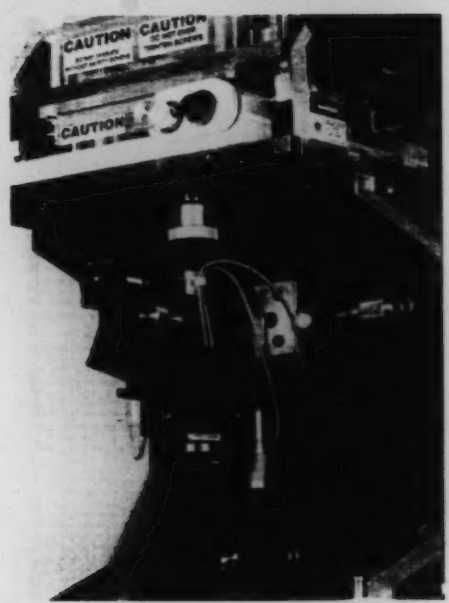

(b)

Figure 5.3: (a) Is the first prototype of a complete microfluidic platform, which incorporate the power the supply, chip holders, lid to provide electrical contact on the chip and also to avoid intrusion of light, pump (for sample introduction) and optical detection system based on the epifluorescence confocal design shown in (b).

5.4 FINAL CONCLUSION

In the DARPA project, we had to show that CPT could be used as a viable DNA amplification technique to detect for specific environmental pathogens on chip format. From the thesis work we show that the CPT assay is possible on-chip and the running of successive CPT assays of increasing target DNA concentrations did establish quantitative performance. Such a technology can be used in the medical and biodetection field.

5.5 Reference

1. Hjerten S., *J.Chromatogr.*, 347, 191-198, 1985.
2. Gelfi, C., Curcio, M., Righetti, P. G., Sebastiano, R., Citterio, A., Ahmadzadeh, H., Dovichi, N. J., *Electrophoresis*, 19, 1677-1682, 1998.
3. Liu, Y., Kuhr, W. G., *Anal. Chem.*, 71, 1668-1673, 1999.
4. (i) Fluri, K., Fitzpatrick, G., Chiem, N., Harrison, D. J., *Anal. Chem.*, 68, 4285-4290, 1996. (ii) Chiem, N., Harrison, D. J., *Anal. Chem.*, 69, 373-378, 1997.
5. Lee, W. E., Jemere, A. B., Attiya, S., Chiem N. H., Paulson, M., Ahrend, J., Burchett, G., Bader, D. E., Ning, Y., Harrison, D. J., *J. Cap. Elec. & Microchip Tech.*, 6, 51-59, 1999.
6. Belgrader P., Hansford, D., Kovacs, G. T. A., Venkateswaran, K., Mariella, R., Milanovich, Jr., F., Nasarabadi, S., Okuzumi, M., Pourahmadi, F., Northrup, M. A., *Anal. Chem.*, 71 , 4232 -4236, 1999.